APPLICATION OF TUBULAR CERAMIC NANOFILTRATION MEMBRANES FOR TEXTILE WASTEWATER DESALINATION

A Thesis Submitted to
the Graduate School of Engineering and Sciences of
İzmir Institute of Technology
in Partial Fulfillment of the Requirements for the Degree of

MASTER OF SCIENCE

in Chemical Engineering

by
Safiye YALDIZ

July 2017

İZMİR

We approve the thesis of **Safiye YALDIZ**

Examining Committee members:

Prof. Dr. Muhsin ÇİFTÇİOĞLU
Department of Chemical Engineering, İzmir Institute of Technology

Assoc. Prof. Dr. Yaşar AKDOĞAN
Department of Material Science and Engineering, İzmir Institute of Technology

Assist. Prof. Dr. Canan URAZ
Department of Chemical Engineering, Ege University

24 July 2017

Prof. Dr. Muhsin ÇİFTÇİOĞLU
Supervisor, Department of Chemical Engineering,
İzmir Institute of Technology

Prof. Dr. Fehime ÇAKICIOĞLU ÖZKAN
Head of the Department of
Chemical Engineering

Prof. Dr. Aysun SOFUOĞLU
Dean of the Graduate School of
Engineering and Sciences

ACKNOWLEDGMENTS

Firstly, I would like to express my sincere gratitude to my advisor Prof. Dr. Muhsin ÇİFTÇİOĞLU for the continuous support of my Master Degree study and for his patience, motivation, enthusiasm and immense knowledge. His guidance helped me in all the time of research and writing of this thesis.

I would like to express my gratitude to Burcu ALP, Rukiye ÇİFTÇİOĞLU and Ali Emrah ÇETİN for the useful comments, remarks and engagement through the learning process of this master thesis.

I thank my labmates Iklima ODABAŞI, Kaan YALTRIK and Pınar ÇETİN in for the stimulating discussions, and for all the fun we have had in the last three years.

I must express my very profound gratitude to my parents; Mehmet Ali YALDIZ, Gülizar YALDIZ and Muharrem YALDIZ for providing me with unfailing support and continuous encouragement throughout my years of study and through the process of researching and writing this thesis. This accomplishment would not have been possible without them.

Finally, I would like to thank my husband, Mehmet Salih KOÇAK. He was always there cheering me up and stood by me through the good times and bad.

This study was supported by The Scientific and Technological Research Council of Turkey (TUBITAK) within the context of ÇAYDAG 113Y344 project.

ABSTRACT

APPLICATION OF TUBULAR CERAMIC NANOFILTRATION MEMBRANES FOR TEXTILE WASTEWATER DESALINATION

Textile industry generates coloured wastewater containing a significant level of dye/inorganic salts. Environmental concerns and efficient energy use make the recovery of reusable water and salts from textile wastewater vital globally. Ceramic nanofiltration (NF) membranes are becoming increasingly important for the recovery and purification of dyes and salts (e.g., NaCl) in high salinity waste streams. They have superior chemical/mechanical/thermal properties compared to their polymeric counterparts. Desalination performances of the ceramic NF membranes depend on the concentration and chemical structure of the target ions, pH of feed and the wastewater stream along with the chemical/surface/nanostructural properties of the selective NF layer. Metal oxides are generally used as NF layer materials due to their amphoteric behaviour.

Repulsive/attractive forces between the ionic species in the solution and the NF layer may make the separation of ionic species possible. In this work, zirconia doped titania based NF layers were designed. Desalination experiments were conducted with 10^{-3} M Na_2SO_4 and $MgSO_4$ salts at different pH values. Salt retention capacities of 5 different membranes were determined. Percent retention was calculated using ion concentrations in permeate and retentate streams. The Mg^{2+} and SO_4^{-2} ion concentrations were determined by titration with 0.01 M EDTA and by spectrophotometer at 420 nm, respectively. A clear pH dependency of the salt retention was found in filtration tests. The highest SO_4^{-2} and Mg^{+2} ion retentions were obtained with using MF+disperel (boehmite)+P2 (600 ^{0}C)+TTIP hydrosol+Ti/Zr polymeric (double layer) membrane as 95% and 91%, respectively.

ÖZET

TEKSTİL ATIK SULARINDAN TUZ GİDERİMİNE YÖNELİK TÜBÜLER SERAMİK NANOFİLTRASYON MEMBRANLARININ KULLANIMI

Tekstil endüstrisi, büyük miktarda boya/inorganik tuz içeren renkli atık su üretmektedir. Çevresel kaygılar ve verimli enerji kullanımı, tekstil atıksuyundan gelen yeniden kullanılabilir su ve tuzların hayati bir önem taşımasını sağlamıştır. Seramik nanofiltrasyon (NF) membranları, yüksek derecede tuz içeren atıksularda, boyalar ve tuzların (örn., NaCl) geri kazanılması ve saflaştırılması için gittikçe önem kazanmaktadır. Seramik membranlar polimerik membranlara kıyasla üstün kimyasal/mekanik/termal özelliklere sahiptirler. Seramik NF membranlarının tuzdan arındırma performansları, hedef iyonların konsantrasyonuna ve kimyasal yapısına, beslenen atıksuyun pH'ına, atık su akışına ve seçici NF tabakasının kimyasal/yüzey/nano-yapısal özelliklerine bağlıdır. Amfoterik davranışlarından dolayı metal oksitler NF tabakası malzemesi olarak kullanılırlar. NF tabakasının yüzey yükü, büyük oranda beslenen atıksuyun pH'ına bağlıdır. Çözeltideki iyonik tuzlar ile NF tabakası arasındaki itici/çekici kuvvetler, iyonik tuzların ayrılmasını mümkün kılar. Bu çalışmada, zirkonya katkılı titanyum esaslı NF tabakaları tasarlandı. Desalinasyon deneyleri, farklı pH değerlerinde 10^{-3}M Na_2SO_4 ve $MgSO_4$ tuzları şle gerçekleştirilmiştir. 5 farklı membranın tuz tutma kapasiteleri belirlendi. Membranların tuz tutma yüzdeleri süzüntü ve kalıntı örneklerinin iyon konsantrasyonları kullanılarak hesaplanmıştır. Mg^{2+} iyon konsantrasyonu, 0.01 M EDTA titrasyonuyla, SO_4^{-2} iyon konsantrasyonu ise 420 nm dalga boyunda spektrofotometre ile tespit edilmiştir. Filtrasyon testleri sonucunda tuz tutulumunun pH'a bağlı olduğu açıkça görülmüştür. En yüksek SO_4^{-2} ve Mg^{2+} iyon tutulmaları sırasıyla % 95 ve% 91 olarak MF+disperal (böhmit)+P2 (600 0C)+TTIP hidrosol+Ti/Zr polimerik (çift katmanlı) membran kullanılarak elde edilmiştir.

TABLE OF CONTENTS

LIST OF FIGURES IX

LIST OF TABLES……...…….XIII

LIST OF SYMBOLS……..……..XIV

CHAPTER 1. INTRODUCTION 1

CHAPTER 2. MEMBRANE TECHNOLOGY 6

2.1. Historical Overview of Membranes 6

2.2. Membrane Processes 9

2.3. Classification of Ceramic Membrane Processes 10

2.3.1. Microfiltration 11

2.3.2. Ultrafiltration 12

2.3.3. Nanofiltration 14

2.4. Membrane Filtration Operation Modes 16

2.5. Membrane Configurations 17

2.6. Symmetric and Asymmetric Membrane Structures 20

2.7. Material Used in Membrane Technology 22

2.7.1. Polymeric Membranes 22

2.7.2. Ceramic Membranes 23

CHAPTER 3. CHALLENGES OF MEMBRANE TECHNOLOGY 25

3.1. Membrane Fouling 26

3.2. Concentration Polarization 28

CHAPTER 4. TEXTILE WASTEWATER DESALINATION WITH CERAMIC MEMBRANES…….…..…29

4.1. Literature review 30

4.2. Retention Mechanism 33

4.3. DSPM 34
4.3.1. Theory 36
4.3.2. Extended Nernst-Planck Equation 37

CHAPTER 5. EXPERIMENTAL 40
5.1. Materials 40
5.2 Methods 41
5.2.1 Colloidal and Polymeric Sol-gel Processes 41
5.2.2. Preparation of Support Materials 41
5.2.3 Preparation of the Membrane Interlayers by the Colloidal Sol-gel Process 42
5.2.3.1. MF Layer Preparation 42
5.2.3.2. UF1 Layers Preparation 43
5.2.3.3. UF2 Layers Preparation 45
5.2.4 Preparation of the Membrane Top Layer by the Polymeric Sol-gel Process 47
5.2.4.1 NF Layer Preparation 47
5.3. Membrane Characterization 48
5.3.1. Structural Characterization 48
5.4. Filtration Procedure 48
5.4.1. Pure Water Flux 49
5.4.2. Desalination Experiments with Model Salts 49
5.5. Ion Determination Techniques 50
5.5.1. SO_4^{-2} Ion Determination 50
5.5.2. Mg^{+2} Ion Determination 51

CHAPTER 6. RESULTS AND DISCUSSION 53
6.1. Preparation of Support Materials 53
6.2. Preparation of Selective Membrane Layers 53
6.2.1.Characterization of Particle Sizes of Selective Membrane Layer Sols ... 54
6.2.2.Characterization of Membrane Layers with Scanning Electron Microscope 58
6.3.Membrane Performance 60
6.3.1.Pure Water Flux 60

6.3.2.Salt Retention for Model Salts 62
6.3.2.1. Na_2SO_4 63
6.3.2.2. MgSO4 70

CHAPTER 7. CONCLUSION 78

REFERENCES 80

LIST OF FIGURES

Figure **Page**

Figure 2. 1. Schematic of membrane separation principle (Source: Lee, 2013).....9

Figure 2. 2. Schematic of separation process through a semi-permeable membrane.....10

Figure 2. 3. Schematic of asymmetric UF membrane structure with SEM micrograph 900X magnification. (Source: Lee, 2013).....14

Figure 2. 4.Separation mechanisms of dead-end and cross-flow filtrations (Source: Lee, 2013) 16

Figure 2.5. Schematic of tubular type membrane.....18

Figure 2.6. Schematic of hollow fiber membrane 18

Figure 2.7. Schematic of flat sheet membrane.....19

Figure 2.8. Schematic of spiral wound membrane 19

Figure 2.9. Asymmetric porous membrane structure. 21

Figure 3.1. The schematic presentation of membrane fouling and corresponding membrane resistance components (Source: Erkmen, 2013). 26

Figure 5.1. Schematic presentation of MF layer preparation 43

Figure 5.2. Schematic presentation of UF-1 disperal (boehmite) layer preparation.....44

Figure 5.3. Schematic of Preparation of colloidal TiO_2 (TTIP) hydrosols.....45

Figure 5.4. Schematic of Preparation of colloidal TiO2 (TTB) hydrosols (titanium tetrabutoxide: glycerol: water: nitric acid=1:1:556:3.2) 46

Figure 5.5. Preparation of zirconium-doped polymeric sols 47

Figure 5.6. Image of membrane filtration system.....49

Figure 5.7. The SO_4^{-2} ion concentration determination scheme 50

Figure 5.8. Absorbance vs. SO_4^{-2} ion concentration (mg/L) calibration curve.....51

Figure 5.9. Mg^{+2} ion concentration determination scheme.....52

Figure 6.1. Tubular alumina ceramic membrane supports 53

Figure 6.2 The volume based particle size distribution of the 0.5 μm α-alumina colloidal sol (wt 7% α-alumina, 0.8% PVA) 54

Figure 6.3 The volume based particle size distribution of the AKP-50 colloidal sol (wt 7% AKP-50).....55

Figure 6.4 The volume based particle size distribution of disperal (boehmite) colloidal sol (0.6 wt % boehmite, 0.8 wt % PVA).....55

Figure 6.5. The volume based average particle size distribution of the P2 (boehmite) colloidal sol (0.6 wt % P2).....56

Figure 6.6. The volume based average particle size distribution of the TTIP hydrosol (TTIP: DEA:HNO_3:H_2O:2-Propanol=1:0.8:2.4:1000:10) 57

Figure 6.7. The volume based average particle size distribution of the TTB hydrosol (TTB: Glycerol: H_2O: HNO_3= 1:1:556:3.2) 57

Figure 6.8. The volume based average particle size distribution of the titanium tetraisopropoxide (TTIP)/ zirconium tetrapropoxide (ZTP) polymeric sol 58

Figure 6.9. SEM micrograph of the surface (a) and cross-sectional area of microfiltration layer (b).....59

Figure 6.10. SEM micrograph of the surface of UF-1 layer.....59

Figure 6.11. SEM micrograph of the surface and cross-sectional areas of TTIP (UF-2) layer.....60

Figure 6.12. Clean water flux as a function of time at TMP 2 (support, α-alumina, AKP-50, boehmite and P2) 61

Figure 6.13. Clean water flux as a function of time at TMP 2 (TTIP, TTB, NF (one, two and three layer)) 61

Figure 6.14. Permeate flux as a function of time at different pH values of 10^{-3} M Na_2SO_4 salt solution using MF (double layer) +AKP-50 membrane 63

Figure 6.15. Salt retention vs. pH for 10^{-3} M Na_2SO_4 salt solution using MF(double layer) +AKP-50 membrane.....64

Figure 6.16. Permeate flux as a function of time at different pH values of 10^{-3} M Na_2SO_4 salt solution using MF + boehmite + P2 (400 ^{0}C) membrane 65

Figure 6.17. Salt retention vs. pH for 10^{-3} M Na_2SO_4 salt solution using MF + boehmite + P2 (400 ^{0}C) membrane.....66

Figure 6.18. Permeate flux as a function of time at different pH values of 10^{-3} M Na_2SO_4 salt solution using MF + boehmite + P2 (400 ^{0}C) + Ti/Zr polymeric (double layer) membrane.....66

Figure 6.19. Salt retention vs. pH for 10^{-3} M Na_2SO_4 salt solution using MF + boehmite + P2 (400 ^{0}C) + Ti/Zr polymeric (double layer) membrane.....67

Figure 6.20. Permeate flux as a function of time at different pH values of 10^{-3} M Na_2SO_4 salt solution using MF + boehmite + P2 (600 ^{0}C) + TTIP hydrosol + Ti/Zr polymeric (double layer) membrane.....68

Figure 6.21. Salt retention vs. pH for 10^{-3} M Na_2SO_4 salt solution using MF + boehmite + P2 (600 ^{0}C) + TTIP hydrosol + Ti/Zr polymeric (double layer) membrane ..69

Figure 6.22. Permeate flux as a function of time at different pH values of 10^{-3} M Na_2SO_4 salt solution using MF + boehmite + P2 (400 ^{0}C) + Ti/Zr polymeric (triple layer) membrane.....69

Figure 6.23. Salt retention vs. pH for 10^{-3} M Na_2SO_4 salt solution using MF + boehmite + P2 (400 ^{0}C) + Ti/Zr polymeric (triple layer) membrane.....70

Figure 6.24. Permeate flux as a function of time at different pH values of 10^{-3} M $MgSO_4$ salt solution using MF (double layer) +AKP-50 membrane.....71

Figure 6.25. Salt retention vs. pH for 10^{-3} M $MgSO_4$ salt solution using MF (double layer) +AKP-50 membrane.....72

Figure 6.26. Permeate flux as a function of time at different pH values of 10^{-3} M $MgSO_4$ salt solution using MF + boehmite + P2 (400 ^{0}C) membrane 73

Figure 6.27. Salt retention vs. pH for 10^{-3} M $MgSO_4$ salt solution using MF + boehmite + P2 (400 ^{0}C) membrane.....74

Figure 6.28. Permeate flux as a function of time at different pH values of 10^{-3} M $MgSO_4$ salt solution using MF + boehmite + P2 (400 ^{0}C) + Ti/Zr polymeric (double layer) membrane 74

Figure 6.29. Salt retention vs. pH for 10^{-3} M $MgSO_4$ salt solution using MF + boehmite + P2 (400 ^{0}C) + Ti/Zr polymeric (double layer) membrane 75

Figure 6.30. Permeate flux as a function of time at different pH values of 10^{-3} M $MgSO_4$ salt solution using MF + boehmite + P2 (600 ^{0}C) + TTIP hydrosol + Ti/Zr polymeric (double layer) membrane 76

Figure 6.31. Salt retention vs. pH for 10^{-3} M $MgSO_4$ salt solution using MF + boehmite + P2 (600 ^{0}C) + TTIP hydrosol + Ti/Zr polymeric (double layer) membrane .. 77

LIST OF TABLES

Table **Page**

Table 1.1. Reference values for water reuse in textile industry (Source: Alcaina-Miranda et al., 2009) 2

Table 2.1. Chronologically milestone developments of membrane science (Source: Lee, 2013) 8

Table 2.2. Pressure-driven membrane comparison (Source: Cheremisinoff, 2002; Friedrich, 2003; Hajarat, 2010; Meyn, 2011). 11

Table 2.3.Membrane module properties (Source: Lee, 2013) 20

Table 2.4. Ceramic membrane preparation methods (Source: Lee, 2013) 24

Table 2.5. Comparison of the features for polymeric, inorganic and mixed-matrix membranes (Source: Lee, 2013) 24

Table 5.1. The used materials and characteristics 40

Table 6.1. Properties of related cations and anions 62

Table 6.2. Isoelectric Point (IEP) of Membrane Layer Materials 63

LIST OF SYMBOLS

c_i: concentration in membrane (mol/m^3)

C_i: concentration in solution (mol/m^3)

$C_{i,f}$: concentration on feed side of membrane (mol/m^3)

$C_{i,p}$: concentration in permeate (mol/m^3)

$D_{i,p}$: hindered diffusivity (m^2/s)

$D_{i,\infty}$: hindered diffusivity (m^2/s)

F: Faraday constant (C/mol)

G: lag coefficient

I: current density (A/m^2)

J_i: ion flux (based on membrane area) (mol/m^{2}s)

J_v: volume flux (based on membrane area) (m/s)

k: Boltzmann's constant (1.38x10^{-23} J/K)

K: enhanced drag coefficient

$K_{i,c}$: hindrance factor for convection

$K_{i,d}$: hindrance factor for diffusion

r_p: effective pore radius (m)

rs: solute Stokes radius (m)

R: real rejection

R: gas constant (8.3143 J/molK)

T: absolute temperature (K)

x: distance normal to membrane (m)

Δx: effective membrane thickness (m)

X: effective membrane charge (mol/m^3)

z_i: valence of ion

λ: ionic radius to pore radius ratio

ψ: electric potential (V)

$\Delta\psi_D$: Donnan potential (V)

η: dynamic viscosity of the electrolyte (0.65x10^{-3} kg/ms)

π: standard dimensionless constant

ϕ: steric partitioning term

CHAPTER 1

INTRODUCTION

The stress created on the environment is expanding continually in an accelerating rate and mainly originates from industrial activities. Water is vital for the continuation of human existence and activities. It is also essential for the industrial production necessary to maintain the desired human living conditions. Moreover, climate changes cause water shortage. This circumstance reveals the water scarcity and requires the legislation, water reformation and industrial water reuse. Treatment of wastewater, brackish water and seawater are sensible solutions as a source of fresh water (Condom, Larbot, Alami Younssi, & Persin, 2004). Regulations constrain the fresh water utilization and sludge release into main sewage network. At the present time, half of the water is used by household and the other half is used for agricultural and industrial applications (Tang & Chen, 2002). Textile industry is the most contaminating industry because of high volume and composition effluents among all industries. Textile industry spends extremely high amounts of water. Generally, 0.2–0.5 m^3 of raw water is expended per kg of finished product (Barredo-Damas et al., 2010). Besides, wastewater of textile includes variance and complexity because of the utilization of a few receptive specialists, frequently included high fixations and dyes. Also, inorganic salts, for example, NaCl (6.0 wt%) or Na_2SO_4 (5.6 wt%), are added to upgrade the color take-up by the texture when the dyeing procedure happens (Lin et al., 2015). Along these lines, textile effluents are described by solid shading and high chemical oxygen demand (COD), concentration of salts and pH.

Table 1.1 demonstrates some reference criteria found in literature concerning the breaking point values set up for the reutilization of the treated textile wastewater.

The most used techniques in wastewater treatment are physicochemical and biological treatments by activated sludge. These techniques are viewed as adequate keeping up with legislative requirements but not with a specific end goal to permit water reuse in textile procedures. Tertiary methods, for example photo catalysis, advanced oxidation or membrane filtration methods can be used to obtain water with enough quality to be utilized as process water. Developing advanced techniques in order

to reduce waste fractions (including zero release) is necessary for the continuity of sustainable improvement in industry as well as economic interest (Majewska-Nowak & Kawiecka-Skowron, 2011). Membrane technologies have been demonstrated as a reasonable option for water recovery from textile effluents and desalination. The utilization of membranes are increasing since they are one of the suggested treatment strategies for textile effluents recovery in the BAT reference archive (Barredo-Damas et al., 2010).

Table 1.1. Reference values for water reuse in textile industry (Source: Alcaina-Miranda et al., 2009)

Parameter	**Criteria**
COD (mg/L)	60-80
Conductivity (µS/cm)	1000
pH	6-8
Turbidity (NTU)	1
Color (Pt-Co)	None
Suspended solids (mg/L)	5
Dissolved solids (mg/L)	500
Total hardness (mg/L as $CaCO_3$)	25-50

In the last decade, membrane technology has turned into a minimal cost and high productivity separation method for industrial procedures (Chen et al., 2015). Membrane based partition procedures have step by step turned into an attractive other option to the traditional separation processes in the treatment of wastewater because of the large amounts of fresh water consumption. Membrane separation process provides high removal efficiencies and allows reuse of water and valuable waste constituents (Fersi, Gzara, & Dhahbi, 2005). Specifically, nanofiltration (NF) is a great choice, since their application involves important reductions in the previously mentioned parameters (Alcaina-Miranda et al., 2009). Pressure-driven membrane processes are attracting increasing interest among all the methods available for desalination.

NF is a pressure-driven membrane process for the specific separation of solvents from solvent-solute mixtures and the molecular weight cut-off varies from 200 to 1000 Da (Chen et al., 2015). This membrane process is in between between

ultrafiltration (UF) and reverse osmosis (RO). NF membranes are generally used for petrochemical, food, environmental, and other industries for separation processes. Moreover, NF membrane process is thought to be energy efficient and environment-friendly. NF has significantly higher small molecules retentions than UF and higher fluxes than reverse osmosis (RO). The interest to NF applications in water treatment such as wastewater reutilization and desalination of seawater have been increased especially in the last two decades (Luo & Wan, 2013). The presence of ions in solutions causes positive or negative charging of the NF membranes in contact with an aqueous solution. Consequently, small ionic components or inorganic salts can be eliminated with NF membranes (Van Gestel et al., 2002b). NF and even UF can also be used for desalination if membranes with pore diameters lower than 10 nm can be prepared (Condom et al., 2004). UF and MF are not appropriate for reutilization purposes since the pore size of the membrane is too large to reject salt molecules. MF and UF can be used as pretreatment processes to NF due to this reason (Uzal, Yilmaz, & Yetis, 2009).

There are two main groups in NF membranes according to material properties: organic polymeric membranes and inorganic ceramic membranes (Van Gestel et al., 2002a). Commercially accessible polymeric membrane materials are polysulfone, cellulose acetic acid derivation, polyamide etc. Polymeric NF-membranes are used for different industrial applications such as waste and drinking water treatment. Nonetheless, the major drawbacks of the polymeric membranes are poor mechanical, chemical and thermal stabilities (Majewska-Nowak & Kawiecka-Skowron, 2011). Ceramics membranes have superior thermal, chemical and mechanical stabilities when compared with the polymeric membranes possessing the possibility of regeneration and long life, high separation efficiency and high-pressure resistance (Alventosa-deLara, Barredo-Damas, Zuriaga-Agustí, Alcaina-Miranda, & Iborra-Clar, 2014; Majewska-Nowak & Kawiecka-Skowron, 2011; S. Sarkar, Bandyopadhyay, Larbot, & Cerneaux, 2012). These properties make ceramic membranes important for the high stability requiring conditions. Consequently, many researchers concentrate on the improvement of ceramic nanofiltration membranes. A number of producers manufacture industrial-scale ceramic membranes currently. Their molecular weight cut-off values are about 1000 Da (Weber, Chmiel, & Mavrov, 2003) which are appropriate for use in NF applications.

MF ceramic membrane use in separations involving liquids started in the mid-1980s. Introduction of UF ceramic membranes followed in the late 1980s (Sondhi R.,

2003). The relatively high initial cost however is the most important disadvantage of ceramic membranes. This situation can be compensated with long lifetime and higher fluxes. Continuous reduction has been observed in the cost of ceramic membranes during the recent years. Ceramic membrane technology is gaining importance in industrial wastewater treatment and this have been reported by many researchers (Barredo-Damas, Alcaina-Miranda, Iborra-Clar, & Mendoza-Roca, 2012). The most commonly used ceramic materials are γ-Al_2O_3 as well as TiO_2 and ZrO_2 due to their high stability in a wide range of temperatures and pH (Mazzoni, Orlandini, & Bandini, 2009). These materials are also hydrophilic due to the presence of surface hydroxyl groups (Ren, Fang, Gu, Winnubst, & Chen, 2015).

Superior performance (high fluxes and low molecular weight cut-off values) in ceramic NF membranes can be achieved by an asymmetric multilayer structure. The objective of the multilayered structure is gradually reducing pore size (S. Sarkar et al., 2012). A multi-step synthesis procedure is applied to develop multilayer membrane structure based on the sol-gel process. The first step is forming of a suitable support material. Generally, high purity alumina is used as a strong macroporous tubular support material and sintered at temperature above 1500^0C (Sandeep Sarkar et al., 2014). The second step is mesoporous interlayers generation to straighten the surface roughness. The last layer is microporous top-layer. It is the thinnest layer. The molecular weight cut-off value of this layer is lower than 1000 Da. The most commonly used ceramic membrane materials are Al_2O_3, ZrO_2, TiO_2 and silica (Van Gestel et al., 2002a, 2002b). Commercialization of ceramic NF membranes formed from a macroporous γ-Al_2O_3 support with a TiO_2 top thin layer and cut-off values of 1000 Da were reported by Soria and Cominotti (Van Gestel et al., 2002b).

Despite the advantages of membranes, there are two main obstacles in membrane technologies, which are the reduction of the membrane performance because of fouling and concentration polarization and managing of the retentate effluent (Barredo-Damas et al., 2010). Concentration polarization is defined as an aggregation of organic matter, suspended solid, salts etc. on the thin top layer of the membrane during the operation. Accumulation on the membrane surface enhances the osmotic pressure close to the interface of the membrane solution. A reduction in the permeation volume is thus observed due to the decreasing driving force. Membrane fouling also arises from the deposition of the constituents present in treated liquid phases in the pores or onto the membrane surface due to the interaction of the membrane with the solutes/particles

(Alventosa-deLara et al., 2014). Implemention of the proper pretreatment technique is quite significant for flux decline control and achieving an effective membrane separation with high fluxes. MF and UF are mostly preferred pretreatment techniques for wastewater treatment over the sand filtration and ozonation techniques (Capar, Yetis, & Yilmaz, 2007). Reuse criteria of the water can be obtained by applying NF membrane technology after a proper pretreatment process.

Asymmetric ceramic membranes (MF-UF-NF) with a decreasing pore size sequence were prepared in the first stage of this work. Selective layer sols were prepared by two different sol-gel techniques. Prefabricated strong α-alumina tubular supports were coated with these layer sols by using dip-coating method. The aim of this work was to investigate the effectiveness of the thin top layers of the asymmetric membranes in the separation of salts from solutions by determining compositions and fluxes of the permeate streams. Different aqueous salt solutions were fed as feed solutions to a cross-flow pilot scale membrane filtration set-up. Pure water fluxes were determined initially to determine the membrane performance. The Mg^{+2} and SO_4^{-2} ion separation capacities of a series of membranes as a function of pH were determined by using Na_2SO_4 and $MgSO_4$ model salt solutions.

CHAPTER 2

MEMBRANE TECHNOLOGY

There are many synthetic membrane application areas currently in use such as generating drinkable water from seawater, industrial wastewater treatment, regaining valuable components, concentrating mixtures of macromolecules in the food and drug industries and separation vapors and gases. Membrane processes were initially presented as a scientific apparatus in chemical and biomedical research facilities, however they evolved quickly into mechanical items and procedures with critical specialized and business affects. The expansive scale industrial utilization of membranes started around 1970 with water desalination and purification to create valuable industrial water (Strathmann, 2000). From that point forward membranes have turned into a broadly utilized device as a part of process designing with noteworthy specialized and business affect.

Membrane process applications can be classified in three main categories. The first one contains desalination of seawater and refining of wastewater. The utilization of membranes is sensible but there are different alternative procedures like biological treatment and distillation. Membrane processes must compete with alternative methods in terms of economic feasibility. The second category involves the molecular mixture separation in the drug and food industry and the generation of ultrapure water. Membrane processes have environmental (cleaner), technical and commercial advantages when compared with other methods. Therapeutic systems and artificial organ applications constitute the third category. There is no sensible alternative to membrane processes in this area (Strathmann, 2000).

2.1. Historical Overview of Membranes

Synthetic membranes nowadays are generally utilized as a part of numerous technical and commercial separation methods. Desalination of sea and brackish water, bioproducts and food stuff purification, gas and vapor separation are the common usage areas (Strathmann, 2000). The pioneering studies on membranee were conducted at the

center of the eighteenth century by Nollet (1748). He used a system which was mainly a pig's bladder. Water passed the bladder when it was brought into contact with a water-ethanol mixture on one side and the water on the other side. The relation between osmotic pressure and a semipermeable membrane was thus detected (Strathmann, 2000).

The important development of synthetic membranes began in the 1960s. As stated in Table 2.1, the underlying improvement from the eighteenth to mid twentieth century is the finding of different mass transport phenomena across membranes. One of the most important developments in membrane technology was the discovery of the cellulose acetate reverse osmosis membranes by Loeb and Sourirajan in 1962 (Lee, 2013). This membrane supplied a high salt refuse and high fluxes at moderate pressures. This was a noteworthy progress toward the use of reverse osmosis membranes as a viable apparatus for the creation of consumable water from the sea. Loeb and Sourirajan developed a membrane which an asymmetric structure. This membrane included a dense skin at the surface. Skin layer determines the selectivity of the membrane and flux. The highly porous body with large pores supports the dense skin layer and increases the mechanical toughness of the membrane (Lee, 2013).

The research and development on asymmetric membranes in the 1960s improved the perm-selectivity of the membranes significantly. Membranes were also able to compete with other separation methods. The progress in the viable packing of membranes into components was a critical step for bringing membrane separation into large scale industrial applications. Different membrane based application areas were rapidly developed such as purification of dairy and water, desalination of sea and brackish water, manufacturing food and drinks, separation of vapor and gas, hemodialysis, etc. (Strathmann, 2000). Innovations on membranes have significantly improved the abilities to rebuild production processes, conserve the nature, and additionally give new advances to maintainable development.

Table 2.1. Chronological milestone developments in membrane science (Lee, 2013).

Year	Development/Discovery	Scientist(s)
1748	Discovery of osmosis phenomenon	A. Nollet
1833	The law of gaseous diffusion	T. Graham
1855	Phenomenological laws of diffusion	A. Fick
1860-1880s	Semipermeable membranes:osmotic pressure	M. Traube, W. Pfeffer, J.W. Gibbs, J.H. van't Hoff
1907-1920	Porous membrane filters	R. Zsigmondy
1920s	Research on reverse osmosis	L. Michaelis, E. Manegod, J.W. McBain
1930s	Electrodialysis membranes	T. Teorell, K.H. Meyer, J.F. Sievers
1950s	Electrodialysis, micro- and ultra-filtration, hemodialysis and ion-exchange membranes	Many
1963	Defect-free, high flux, asymmetric reverse osmosis membranes	S. Loeb, S. Sourirajan
1968	Spiral wound RO membranes	J. Westmorland
1977	Thin film composite membranes	J. Cadotte
1970-1980	Membrane and process improvements	Many
1980s	Industrial membrane gas separation process	J.M.S. Henis, M.K. Tripodi
1990s	Hybrid and novel membrane processes	Many

2.2. Membrane Processes

The origin of the word ‘membrane’ comes from Latin word ‘membrana’. It has various meanings in different areas. Membrane can be explained as a semi-permeable thin barrier between two phases (Lee, 2013). Membranes specifically prevent the transfer of one or more components. They control not only matter but also energy and information exchange between different regions (Strathmann, 2000). The membrane working principle as demonstrated schematically in Figure 2.1. Membrane technology is a specific discipline since it involves a quite comprehensive theoretical background (Boncukoğlu, 2013). A membrane can transport one component more easily than other elements due to the physical or chemical differences between the permeating components and the membrane. As shown in Figure 2.1 a mixture of substances is defined as a feed. The easily passing filtrate stream through the membrane is commonly called as permeate which symbolizes the refined phase. The untreated or retained stream is called the concentrate or retentate (Friedrich, 2003).

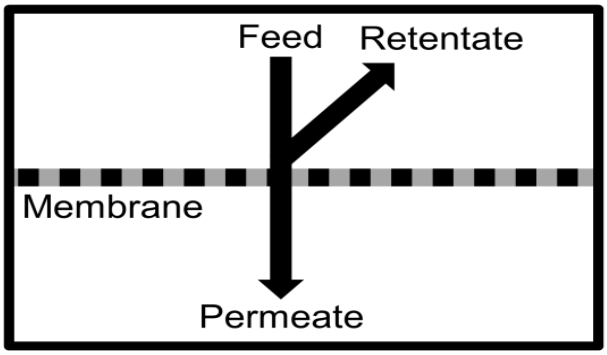

Figure 2. 1. Schematic of membrane separation (Lee, 2013).

The membrane selectivity and the flux of the solvent control the membrane performance. High selectivity and permeability along with high thermal/chemical stability is required for high separation performance. Dissimilarity in chemical and physical structures and size between the different constituents in the mixture provide the separation in membrane mechanism. Membrane based separation processes are more effective, faster and economical when compared with the currently applied separation

processes (Hajarat, 2010). The most important benefits of membrane based separation processes can be listed as follows:

1. Continuous separation.
2. Low energy consumption.
3. Combination of other separation techniques.
4. It is suitable for scale-up.
5. Membranes can have various properties with the adjustment.
6. No additives are required.

In waste water treatment applications, when waste water is forced towards the semipermeable membrane, waste stream and product stream are generated. Mechanism is shown in Figure 2.2. Concentration, temperature and electric potential are examples of the driving forces in membrane system. Separation takes place due to the driving forces. Numerous membranes used in water treatment are pressure driven. Some of the constituents move across the membrane and the other constituents are rejected. Therefore, product stream contains impermeable constituents and retentate stream includes rejected constituents (Meyn, 2011).

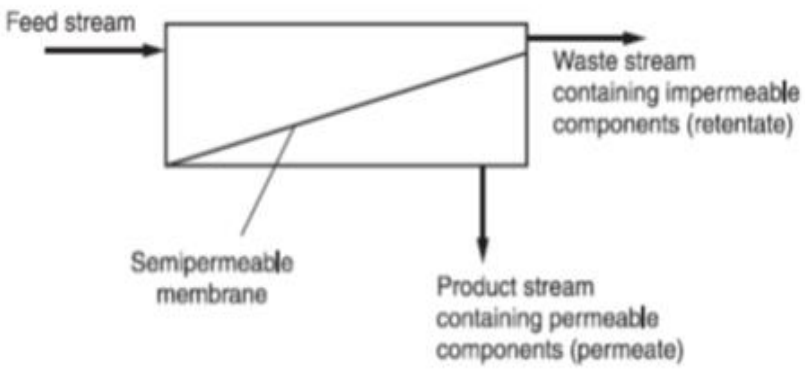

Figure 2. 2. Schematic of separation process through a semi-permeable membrane.

2.3. Classification of Ceramic Membrane Processes

Commonly used membrane processes in waste water treatment can be categorized in four major groups: MF, UF, NF and RO. These types of membranes use pressure as the driving force. Membranes are separated from each other in terms of retained material type, working pressures, pore sizes and separation mechanisms. There

is decreasing sequence in the pore size from microfiltration to reverse osmosis. Additionally, membrane resistance and the pressure increases. The comparison of the different types of pressure driven membrane processes is outlined in Table 2.2. This table includes structure of the membranes, driving force, separation mechanisms, membrane pore sizes, and removed components (Cheremisinoff, 2002; Friedrich, 2003; Hajarat, 2010; Meyn, 2011).

Table 2.2. Pressure-driven membrane comparison
(Cheremisinoff, 2002; Friedrich, 2003; Hajarat, 2010; Meyn, 2011).

Membrane Process	Driving Force	Separation Size	Structure	Mechanism	Applications
Microfiltration	Pressure 0.1-3 bar	0.08-1.4 μm	Symmetric	Sieving	Separation of solid matter from suspensions
Ultrafiltration	Pressure 0.5-10 bar	5 nm- 0.1μm	Asymmetric	Sieving	Separation of macromolecules or colloids
Nanofiltration	Pressure 2-40 bar	0.5-8 nm	Asymmetric	Solution/diffusion	Separation of dissolved organic molecules, salts
Reverse Osmosis	Pressure 5-70 bar	< 2 nm	Asymmetric	Solution/diffusion	Separation of organic molecules, all salts

2.3.1. Microfiltration

Microfiltration membranes have pore sizes between 0.08 to 1.4 μm and they are used to reject emulsions and suspensions (Hajarat, 2010). Porous membrane structure is observed in microfiltration membranes. Sieving mechanism ensures the separation. High porosity and narrow pore size distribution are the most important structural parameters to optimize MF membrane. Polymeric and ceramic materials can be used for the preparation of MF membranes.

Pressure difference is the driving force in the MF membranes and applied pressure is less than 3 bar (Hajarat, 2010). Sieving mechanism separates the molecules according to their shape and size. Large and wide molecules are rejected by the membrane and small and narrow molecules pass. The rejection of molecules depends on not only pore size but also another factor that some molecules smaller than the pore size can be absorbed by the membrane. Moreover, the retention of positive or negative charged molecules can be affected by the zeta potential of the membrane environment. Small particles will be captured by the membrane when the molecules are smaller than the pore size but diffuse with the feed when they are large. This is called as inertial-impaction (Hajarat, 2010).

MF membranes are commonly prepared from inorganic materials. This is due to their high mechanical/chemical/thermal stabilities along with the ease in the control of the pore size and its narrow distribution. Sintering, anodic oxidation and solution/gel techniques are utilized in ceramic MF preparation (Hajarat, 2010).

Flux decline is the major weakness in MF membrane processes. Fouling and the concentration polarization are the two major factors in flux deceases. Accumulation of the solute on the membrane pore or surface causes membrane fouling. Another parameter in fouling is the membrane operation mode. Dead-end or cross-flow modes are adjusted in order to reduce concentration polarization and fouling.

Separation of particulates from water based suspensions and biomass recovery are the lab-scale MF membrane applications. Furthermore, clarification and sterilization of beverages in food and pharmaceutical industry are other application areas. Cell harvesting can be carried out by the MF membranes in biotechnology. Wastewater treatment, separation of oil-water emulsions, vapor and gas filtration, and continuous fermentation can all be listed as MF membranes applications (Hajarat, 2010).

2.3.2. Ultrafiltration

The driving force of UF membrane processes is also a pressure difference. UF membranes basically retain the dissolved macromolecules and suspended solid particles. UF membranes have pore sizes between 5 to 100 nm (Lee, 2013). Pore sizes of UF membranes can also be specified by the size of the rejected molecules. UF membranes have molecular weight cut-off values (MWCO) in between 1000 and

10,000 g/mol (Dalton) (Meyn, 2011). Separation occurs via molecular sieving and chemical affinity of the solute molecules also affect the separation mechanism (Hajarat, 2010). Separation not only depends on the pore size and pore size distribution, but also on the chemical affinities of the solute molecules.

Porous membrane structure is observed in UF membranes. Organic (polymeric) and inorganic (ceramic) materials are used in UF membrane preparation. Phase inversion technique is preferred in polymeric UF membrane preparation (Hajarat, 2010). The mostly used polymers are polysulfone (PS), cellulose acetate (CA), polyvinylidene fluoride (PVDF), polyethersulfone (PES), polyacrylonitrile (PAN), etc. Polymeric UF membranes have low cost, good selectivity and high permeability. On the other hand, they have fouling and swelling problems. Concentration polarization and membrane fouling greatly affect the UF membrane performance and consequently design of the membrane structure must be adjusted to reduce fouling (Hajarat, 2010). They cannot be used in high temperature applications, acidic and alkaline environments (Lee, 2013). The commercial UF membrane which has asymmetric membrane structure is shown in Figure 2.3.

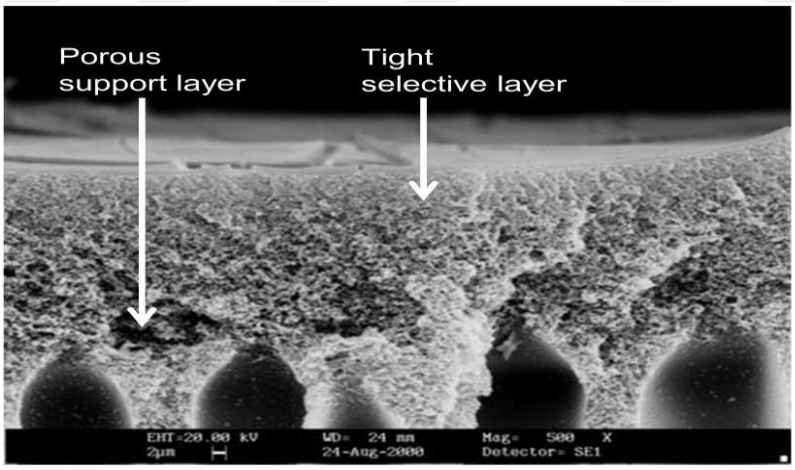

Figure 2. 3. SEM picture of asymmetric UF membrane structure at 900X magnification (Lee, 2013).

The different application areas of the UF membranes can be listed as drinking water production, biochemical process, pharmaceutical, chemical, sewage treatment, textile, paper and leather industry and food industry (Hajarat, 2010; Lee, 2013). The efficiency of UF membranes is quite high and they are preferred in purification, fractionation, purification and removing of macromolecules from suspensions. The

membrane resistance in MF membranes is determined by the whole membrane. However, in UF membranes, active thin top layer determines the membrane resistance due to the asymmetric structure (Hajarat, 2010). The thin active layer provides the high selectivity on top of support layer. Also, it has small pore sizes and mechanical resistance is increased by thin layer. Asymmetric structure increases separation efficiency and permeability.

2.3.3. NF

The driving force of NF membrane is pressure difference. NF membranes are obtained from derivation of RO membranes. They are located between RO and UF according to molecule removal range (Hajarat, 2010; Meyn, 2011). High quality permeate can be obtained by using RO membrane but it consumes high energy. However, NF membranes have less energy demand. In 1986, the first NF membranes are launched to the market (Jonathan, 2012). NF membranes are characterized with high density, high surface charge and nanometer size pore. Generally, NF membranes need low transmembrane pressures than reverse osmosis. The structure of the NF membranes consists of composite asymmetrical multilayers. The active thin top layer is about 1 μm thick and inner layer thickness is 30 nm. NF membranes have pore sizes between 0.5 to 8 nm. NF membranes have molecular weight cut-off value (MWCO) between the range of 200 to 2000 g/mol (Dalton) (Meyn, 2011).

There are two main groups in NF membranes according to their materials: polymeric and ceramic membranes. Duo to the low cost and easy production procedure, polymeric nanofiltration membranes have been extensively preferred. The major drawbacks are low mechanical, chemical and thermal stability. Even though ceramic NF membranes have high production cost and complex production steps yet they can overcome high temperature and extreme pH values and they have longer lifetime. Another benefit is the easy cleaning (Hajarat, 2010). Phase inversion technique is the mostly used in NF membrane preparation.

The application areas of NF membranes are listed as water softening process, removing hardness, natural organic matter, heavy metals, viruses and bacteria, and concentrating organic dyes (Hajarat, 2010). The small particles which have molecular

size of 200 Da or more will be removed by NF membranes. NF is suitable for removing of color from surface water and organic pollutants (Jonathan, 2012).

Different membrane materials show different membrane surface charge which affects the fouling behavior of the membrane filtration. The consisted charge between the membrane surface and the feed creates the electric potential called the “Donnan potential”. Ions, which have smaller size than the membrane pore can be removed from the water by the help of this electrical (Jonathan, 2012).

Specific salts can be separated from water by using NF membranes. Monovalent salt ions easily get through the membrane. In contrast to monovalent salt ions, multivalent salt ions are rejected at some point. Permeability of the salts is highly affected by the valence of anion (Meyn, 2011).

Understanding the separation behavior and development of separation mechanism in NF membrane is the vital for desalination of brackish and seawater. Even though NF membrane has a higher permeate flux than RO, the rejection ratio is lower. Steric (sieving), convection, diffusion and electrostatic (Donnan) effects are the mechanism which provide the separation with NF membranes. Non-ionised organics and monovalent salt ions have molecular weight less than 150 Da which is low for the rejection. However, organics and multivalent ion salts which have molecular weight higher than 300 Da is suitable for rejection (Hajarat, 2010). Positive or negative charge is observed in most NF membrane surface depending on the material used. One of the important benefits of nanofiltration membrane is requiring lower operating pressure than RO. Fouling is the major drawback of the NF membranes. The reasons of fouling are listed as pore blockage, foulant adsorption on the pore walls and surface fouling which can be cake and gel layer formation.

Charged and uncharged solutes are separated from the solution by using NF membranes. The mechanisms in separation of uncharged molecule are diffusion rate difference or size exclusion. The mechanism in separation of charged (ion) molecule is membrane surface charge and the solute charge interaction. Another mechanism which plays important role in ion separation is size of the ions. Charged molecules will be rejected in case the ion size is bigger than the membrane pore. Convection and diffusion are the two important mechanisms in solute permeation through the nanofiltration membrane. Physical parameters like conversion rate and pressure affects the conversion transfer. In contrast, chemical parameters like pH and concentration affects the diffusion transfer. Better result is obtained in case of high pressure in convection mechanism.

Additionally, larger ions are retained better because of physical parameter dependency of convection. However, chemical selectivity is higher at low pressures because diffusion depends on the chemical parameters. As a result, high selectivity is achieved at low pressure due to the diffusion and high retention is achieved ate high pressures due to the convection (Hajarat, 2010).

2.4. Membrane Filtration Operation Modes

Membrane filtration operation modes can be categorized as dead-end and cross-flow. The mechanism of the operation modes is shown in Figure 2.4. The working principle in dead-end filtration is that feed goes in the direction of membrane orthogonally. This direct flow causes the penetrating and deposition of the rejected constituents on the membrane surface. In contrast the dead-end operation, feed stream goes parallel to the membrane surface in cross-flow filtration. Small part of the feed passes the membrane due to the parallel flow by force of pressure. In cross-flow filtration, due to the tangentially feed flow on the surface of the membrane, high permeation flux is observed. The reason is the continuous rejected constituent removal (Lee, 2013).

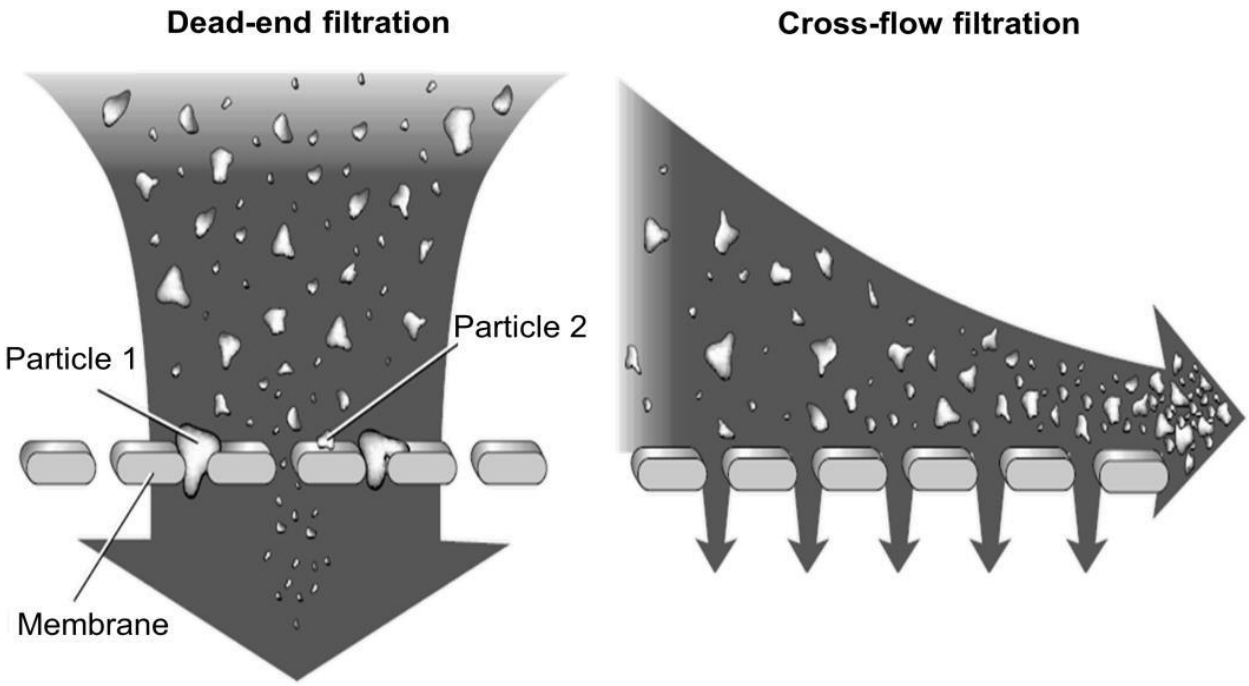

Figure 2. 4.Separation mechanisms of dead-end and cross-flow filtrations (Lee, 2013).

The dead-end filtration mode needs less energy than cross-flow filtration mode. The most important disadvantage of the dead-end filtration is being more tends to be fouling. Cross flow considerably avoids the generation of fouling. Shear and buoyancy forces are generated by the cross-flow at the membrane surface which can get rid of rejected constituents from the surface of membrane. So, it decreases the membrane fouling. However, sometimes fouling is observed on the membrane surface in cross-flow mode and performance of the membrane decreases. Consequently, the retained components accumulate on the membrane surface and create the fouling layer for both operational modes. The remarkable performance reducing occurs (Jonathan, 2012).

The dead-end filtration is preferred for common filtration processes, for example secondary effluents in waste water treatment and surface water purification. Rapid membrane fouling accelerates the solute/rejected material concentration increasing of the feed. The permeate qualities will thus be reduced in time. Cross-flow filtration gives huge structural benefits in comparison with dead-end filtration and it is extensively utilized as a part of most commercial pressure-driven membrane processes. The flux decline can be fixed by adjusting the parameters, for example shear rate and the transmembrane pressure (Lee, 2013).

2.5. Membrane Configurations

Membrane module selection is important parameter for effective membrane applications. Specific necessities, such as generation cost, packing density, utilization of energy, managing concentration polarization and membrane fouling must meet in membrane modules (Strathmann, 2000). Although, there are numerous different module types, the mostly used in industrial scale are tubular, flat sheet, hollow fiber and spiral wound (Lee, 2013). Schematics of module types are shown in Figures 2.5, 2.6, 2.7, 2.8. All type of membrane modules differs from each other in terms of design, cost, operation mode, energy necessity etc. As previously indicated, the most important characteristic is managing concentration polarization and membrane fouling. Property comparison of each membrane module is given in Table 2.3.

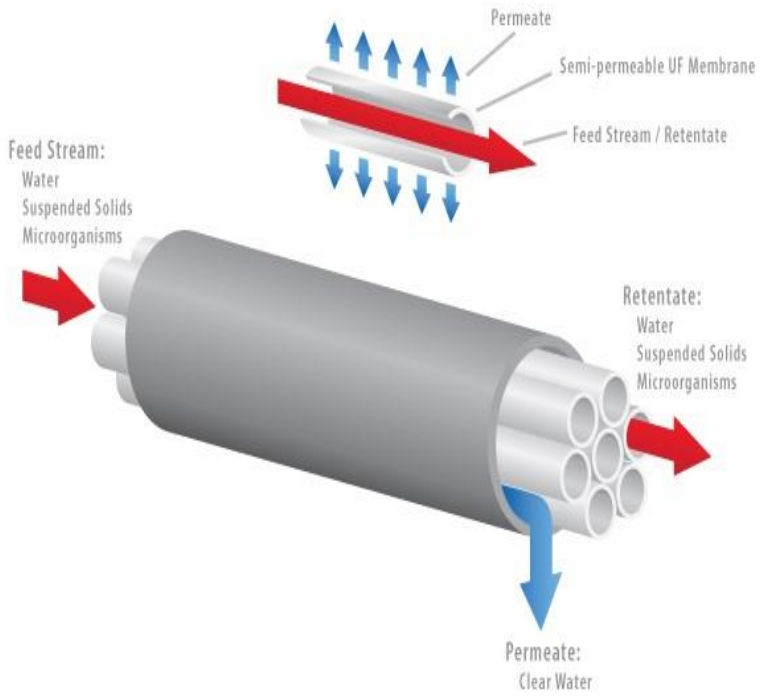

Figure 2.5. Schematic of tubular type membrane

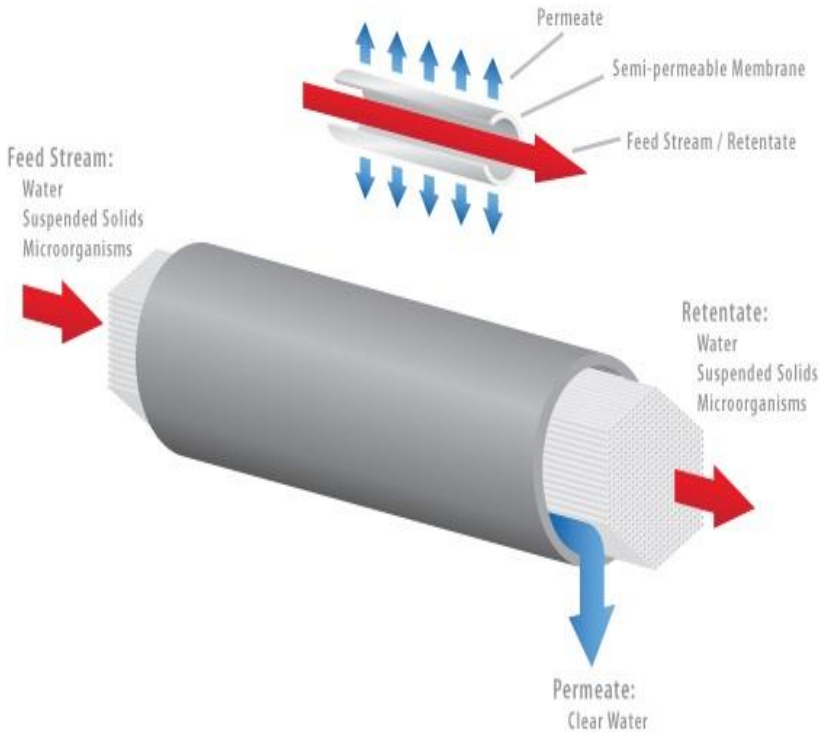

Figure 2.6. Schematic of hollow fiber membrane

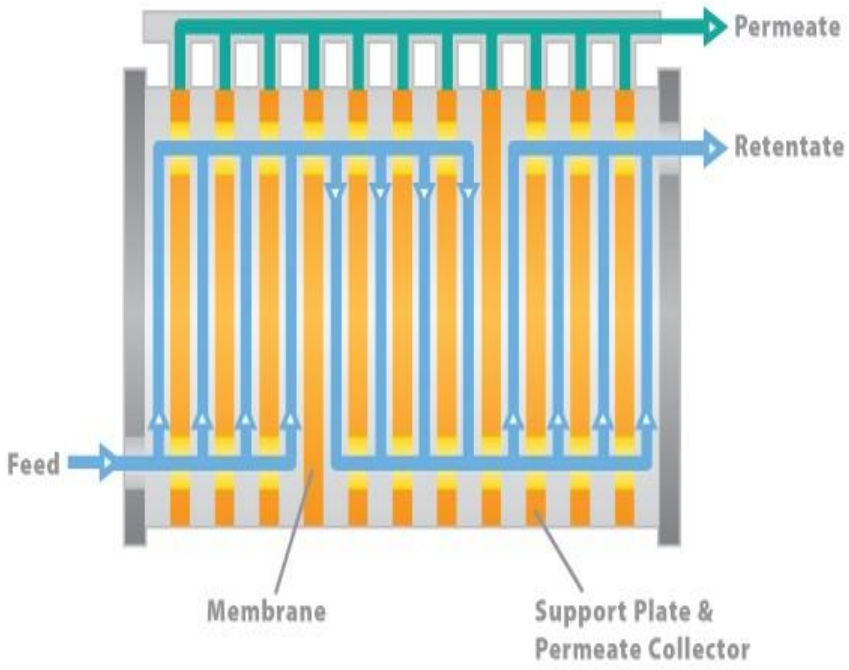

Figure 2.7. Schematic of flat sheet membrane

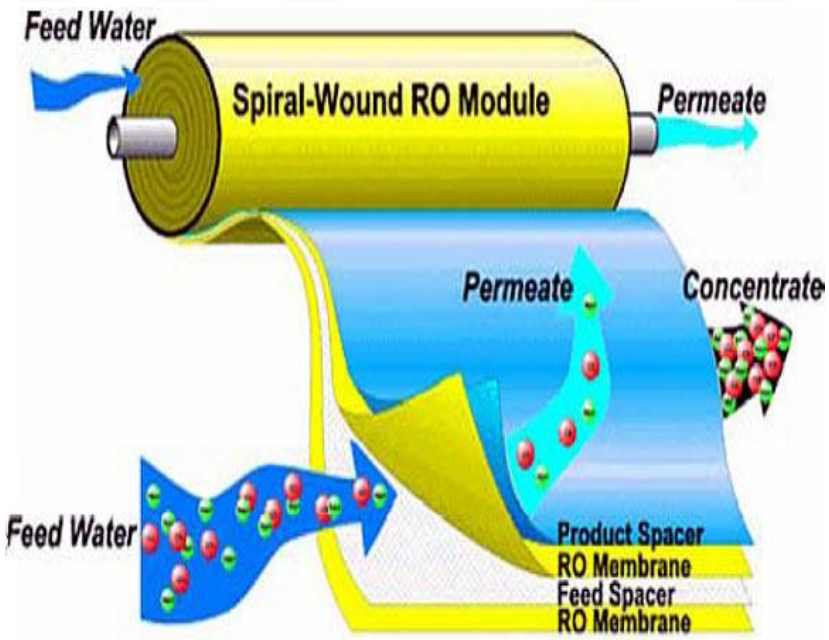

Figure 2.8. Schematic of spiral wound membrane

Table 2.3.Membrane module properties (Lee, 2013)

Property	Flate sheet	Tubular	Spiral wound	Hollow fibre
Packing density	Moderate (300-500 m^2m^{-3})	Low (<100 m^2m^{-3})	High (600-800 m^2m^{-3})	Very high (>600 m^2m^{-3})
Investment	High	Low-high	Low	Moderate
Energy	Moderate	High	Moderate	Low
Variable costs	Average	Low-high	Low	
Fouling tendency	Average	Low	Average	Low-high
Cleanability	Good	Good	Difficult	Good
Replacement	Sheet	Tubes	Element	Element
Manufacturing	Simple	Simple	Complex	Moderate

2.6. Symmetric and Asymmetric Membrane Structures

Membranes may have two types of structure: symmetric and asymmetric. The transport properties and the structure are same through the membrane cross-section. Flux property of symmetric membrane is determined with the membrane thickness. MF, electrodialysis and dialysis processes used symmetric membrane structure. In contrast the symmetric membranes, transport properties and structure changes along the membrane cross-section in asymmetric membrane structure. Today, many pressure-driven membranes use asymmetric membrane structures. Figure 2.9 shows the asymmetric porous membrane structure. Good mechanical resistance and high mass transfer rate are desired properties in asymmetric membrane structure and they provide high separation (Strathmann, 2000). Membrane thickness, pore size distribution and porosity are parameters which determine the mass transfer through a membrane. Small resistance of transport is desired property in porous ceramic membrane (Ren et al., 2015). Multilayer asymmetric structure provides high performance parameters like high permselectivity and permeability, in porous ceramic membrane.

- Support layer with large pores increases the mechanical strength.

- Intrinsic deficiencies on the support layer surface are reduced by applying one or more intermediate layers. Moreover, intermediate layers prevent the top layer material from leaking into the support pores.

- The last layer is a thin, microporous separation top layer that allows certain substances to be transported (Bayati et al., 2013).

The thickness of the support layer varies from 1 to 3 mm. The MF layer has 10-30 μm thickness. Zirconia (ZrO_2) and alumina (Al_2O_3) are the most used metal oxides in MF membrane. A few micrometer thickness is observed in ultrafiltration membranes. The most used metal oxides are titania (TiO_2), ceria (CeO_2) and zirconia in ultrafiltration layer. The thickness of the top skin layer, NF layer, is lower than 1 μm. The mostly used metal oxides are zirconia and titania (Zaiter, Belouatek, Chougui, Asli, & Szymczyk, 2013). The critical layer is the thin top layer because the material and pore size of this layer mainly determines the separation characteristics of the membrane. Thickness of skin layer specify the mass flux (Strathmann, 2000). Multiple coating steps are performed to create the asymmetric membrane structure. The classical ceramic membrane coating methods are used to make support and MF layer. The mostly applied technique for UF and NF layers is sol-gel method (Zaiter et al., 2013).

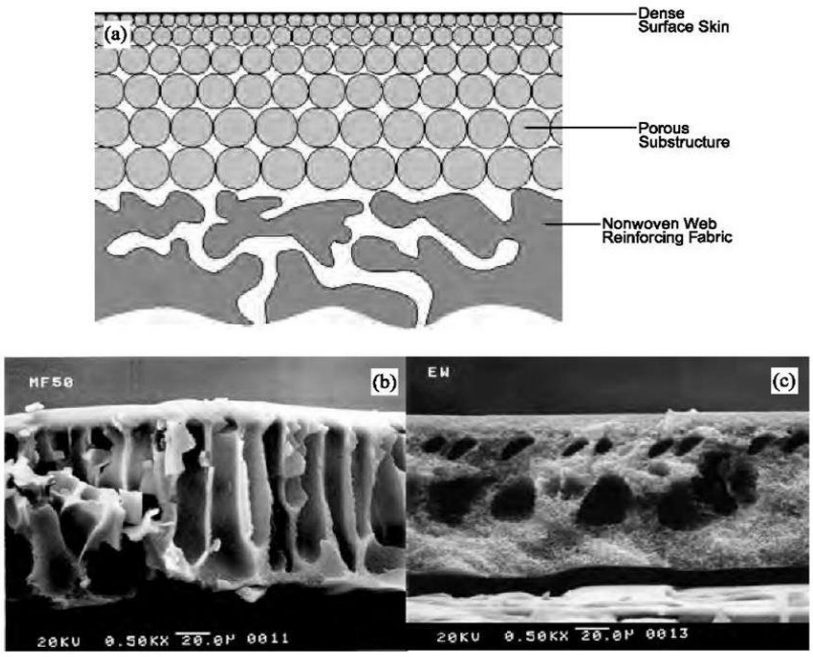

Figure 2.9. Asymmetric porous membrane structure.

2.7. Material Used in Membrane Technology

Different membrane materials have been created for various membrane applications. Various chemical and physical properties can be brought by using various membrane materials, such as perm-selectivity, burst pressure, chemical resistance, oxidant tolerance, fouling tendency, pH operating range, wettability, biocompatibility, and so on (Jonathan, 2012; Lee, 2013). Membrane materials can basically be divided into two main groups as organic (polymeric) and inorganic (ceramic). Choosing the most appropriate material in membrane applications is vital. Polymeric membranes are mostly preferred as a drinking water membrane material because of the low cost (Jonathan, 2012). Also, ceramic membranes are utilized in this application area. Being hydrophilic or hydrophobic is another fundamental property about membrane material. Hydrophilic membranes attract the water molecules. In contrast the hydrophilic, hydrophobic membranes push the water molecules. Attracting and repelling occur thanks to the surface tension. Membrane will attract the liquid when liquids have lower surface tension. This characteristic affects the wettability and applied pressure in the membrane system (Jonathan, 2012). At the point when fluids have brought down surface pressure than a film the layer will pull in the fluid and it will spread on the film material.

2.7.1. Polymeric Membranes

Polymeric membranes are started to use in the 1960s in industrial scale. Since then, it holds leading positions in the commercial membrane market because of the low cost and competitive performance. The mostly used polymers in membrane preparation are cellulose acetate, polyether sulfone, polyamide, polysulfone, polyacrylonitrile and polyvinylidene fluoride. Phase inversion or in other words immersion precipitation technique is used in most polymeric membrane fabrication. Mass transfer rate and the phase separation identify the ultimate membrane structure. Design of the membrane reveals the various separation characteristics. The desired separation properties are a narrow pore size range to provide good selectivity and high porosity to provide high fluxes (Lee, 2013).

2.7.2. Ceramic Membranes

Considering the fact of membrane filtration process being energy intensive it is good to have alternatives with less energy consumption and lower pressure. Energy demand is significantly affected by choosing appropriate membrane material. Ceramic membrane material is a good option for decreasing the energy demand. The most common ceramic membrane materials are alumina (γ-Al_2O_3 or α-Al_2O_3), titanium dioxide (TiO_2), zirconium dioxide (ZrO_2) and ceria (CeO_2) (Meyn, 2011). Ceramic membranes are mostly preferred over polymeric ones because of the high thermal, mechanical and chemical stability. Ceramic membranes have high tolerance under harsh operating conditions. Due to the high thermal stability, ceramic membranes can be utilized at high temperatures for long time. In industrial applications, ceramic membrane processes take place at a temperature above 1000^0C (Yelken, 2000). High chemical stability provides the wide pH working range. Many different chemicals can be used in membrane cleaning procedure due to the chemical tolerance of membrane. In this way, fouling problem in membrane will be dissolved by using chemicals and high membrane performance and life can be provided. This advantage allows the utilization of ceramic membrane in drinking water treatment (Jonathan, 2012). Moreover, easy cleanability is reduced the production cost (Yelken, 2000). Ceramic membranes show high mechanical stability under high pressures.

Different techniques to form ceramic membranes are shown in Table 2.4. The desired membrane structure and the application type specify the preparation method (Lee, 2013). The advantage and disadvantages of the ceramic, polymeric and mixed matrix membranes are summarized in Table 2.5.

Table 2.4. Ceramic membrane preparation methods (Lee, 2013).

Process	Materials
Thermal sintering	Alumina, Silica, Titania, Zirconia
Sol-gel	Alumina, Silica, Titania, Zirconia
Chemical vapour deposition	Silica
Prolysis	Silicon carbide, Silicon nitride
Hydrothermal treatment	Silicalite
Anodic oxidation	Alumina (amorphous)
Phase separation/leaching	Silica
Dynamic membranes	Zirconia (amorphous)

Table 2.5. Comparison of the features for polymeric, inorganic and mixed-matrix membranes (Lee, 2013)

Properties	Polymeric membranes	Ceramic membranes	Mixed matrix membranes
Permeability	High	Low	High
Separation performance	Moderate	Moderate	Enhanced
Cost	Economical	Expensive	Moderate
Packing density	High	Low	High
Chemical & thermal stability	Moderate	High	High
Mechanical strength	Good	Poor	Excellent
Compatibility to solvent	Limited	Wide range	Limited
Swelling	Frequent	Free of swelling	Free of swelling
Handling	Robust	Brittle	Robust

CHAPTER 3

CHALLENGES OF MEMBRANE TECHNOLOGY

Flux decline in membrane permeate and the decreasing selectivity are the most challenging problems in membrane technology (Hajarat, 2010; Lee, 2013). The reasons which cause the flux decline can be listed as fouling, concentration polarization and adsorption of molecules into membrane surface. All the listed reasons cause the resistance increasing through the membrane, thus decreasing in membrane rejection and decline in permeate flux are observed with time. Membrane and feed characteristics play an important role in permeate flux decline. Membrane resistance can be explained by transportation of one type molecules or rejected molecules. Concentration polarization resistance is the result of formation of particle layer in the membrane surface. Gel layer resistance arises when the concentration increases at some point. A pore-blocking resistance appears because of solute particle penetration through the pores. Adsorption resistance originated from the solute adsorption. A better understanding of concentration polarization and fouling significantly contributes to the prevention of the decreases in permeate flux and rejection (Hajarat, 2010).

The various resistances that may arise are shown in Figure 3.1. In the ideal case, the total resistance only includes the membrane resistance R_m. Because the membrane retains certain amounts of molecules and molecules which were accumulated near the membrane surface forms a deposit. Thus, the layer near the membrane becomes more concentrated, and this layer also forms a resistance against mass transfer. This is indicated by the concentration polarization R_{cp}. A gel layer is formed with a very high concentration of accumulated solute molecules, which is resistance R_g. Porous membranes and some solutes may leak into the membrane. This causes pore blockage which is associated with pore blockage resistance R_p. Finally, another resistance that may arise is the adsorption resistance R_a.

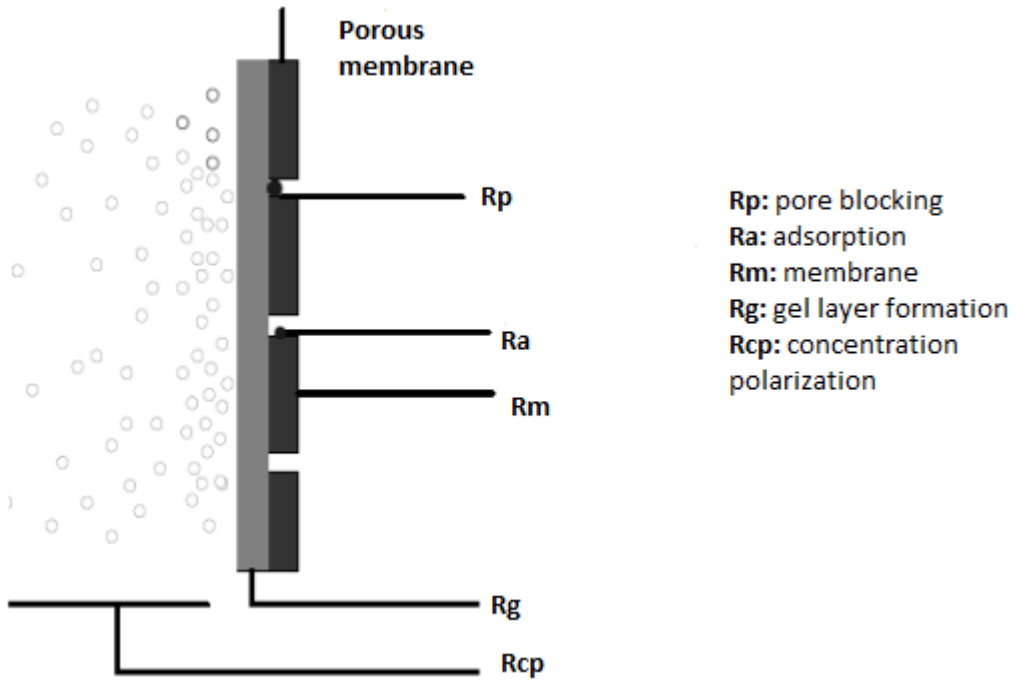

Figure 3.1. The schematic presentation of membrane fouling and corresponding membrane resistance components.

3.1. Membrane Fouling

The main challenges in membrane filtration process are the fouling which causes production reduction, energy consumption increasing, membrane changing, chemical usage. During the flux decline, feed concentration, flow rate and pressure remain constant (Meyn, 2011). Decrease in performance and flux of a membrane arises from suspended or dissolved molecule accumulation on external surfaces. This is called as fouling. The main factors affecting the fouling are solute and membrane property, which includes interaction of solute-membrane and hydrodynamic conditions. The primary fouling formations are explained in below:

1. ***Adsorption*** is the result of interrelation between the membrane and the solute. A particle and solute monolayer which is originated from adsorption operates as the hydraulic resistance. In case of concentration dependent adsorption, increasing in concentration polarization irritates the adsorption ratio. If the molecule size in feed is larger than the pore size of membrane, pore blockage appears. Pore closure leads to a decrease in permeate fluxes.

2. ***Deposition*** can be defined as an accumulation of particles at the membrane surface layer by layer. This is the cake resistance and leads to important hydraulic resistance.
3. High level of concentration polarization causes the existence of ***gel formation*** by macromolecules (Lee, 2013).

Fouling can be divided into two groups as reversible and irreversible fouling. If the composed membrane resistance can be removed by hydraulic backwash, this is called as reversible fouling. The deposited cake layer on the membrane surface is exposed to clean at certain time intervals by using backwashing technique. When the fouling reaches a certain level, chemical cleaning is applied to remove fouling. If fouling cannot be removed by chemical and backwashing techniques, this type of fouling named as irreversible fouling (Meyn, 2011). Transmembrane pressure difference between the first operating cycle and any next operating cycle correspond to irreversible fouling measurement. However, the estimation of the irreversible fouling may be difficult with short run time of filters (Jonathan, 2012).

There are a lot of process parameters and conditions which determine the degree of membrane fouling. They can be listed as membrane properties (morphology, roughness, structure, physical and chemical properties), cleaning procedures, operating conditions (pre-treatment, pH value, temperature, flux), the module configuration (hydraulic configuration, packing density, void zones, backwashability) and the properties of the treated fluid (constituents, origin) (Meyn, 2011). The main fouling elimination techniques are as follows:

1. Pretreatment can be applied on feed solution, such as pre-microfiltration, pre-filtration, pH adjustment and addition of complexing agents.
2. Altering the membrane properties.
3. If process conditions change, fouling degree changes. For example, fouling is related with concentration polarization ratio. When concentration polarization decreases, fouling decreases, also. In this situation, increasing mass transfer coefficient decreases the concentration polarization and increases the membrane flux.
4. Chemical cleaning, mechanical cleaning and hydraulic cleaning may be applied to remove fouling (Hajarat, 2010).

3.2. Concentration Polarization

Permeate has lower solute concentration than the feed bulk because membrane rejects the solute and permits the solvent to permeate through it. The concentration increases in rejected molecules is observed at the membrane surface with time. After the certain point, the membrane surface's concentration will higher than the bulk solution's concentration. This phenomenon is called as concentration polarization. The components in the feed have different permeating rates. This difference causes the concentration gradient at both sides of the membrane and thus, concentration polarization appears. Additionally, diffusion of rejected molecules back to the feed bulk will be seen. After stabilization is achieved, there will be balance between the solute convective flow toward the membrane surface and solute flux through the membrane. Flux of solutes will diffuse back to the feed bulk away from the membrane surface (Hajarat, 2010).

CHAPTER 4

TEXTILE WASTEWATER DESALINATION WITH CERAMIC MEMBRANES

Investment of NF membranes is the crucial improvement in membrane technology (Bowen & Mukhtar, 1996). NF name comes from the molecular weight cut-off values of uncharged molecules which indicate the diameter of pore size about one nanometer. A NF membrane is a member of pressure driven membrane. It has separation characteristics which are lying between UF and RO (Al-Zoubi & Omar, 2009; Bowen & Mukhtar, 1996; Hilal, Al-Zoubi, Mohammad, & Darwish, 2005; Schaep, Bruggen, Vandecasteele, & Wilms, 1998). When NF is compared with UF in terms of pore size, NF membranes can reject the small organic molecules which have relatively low molecular weight (MW) between 200 to 1000 g/mol (Al-Zoubi & Omar, 2009; Schaep et al., 1998). There is a wide range of industrial and environmental application areas of nanofiltration membrane usage. When separation of low molecular weight solute from a solvent is required, NF membrane is generally used (Schaep et al., 1998). Major applications of NF membranes are water treatment, wastewater reuse, production of drinking water, desalination and fractionation of small molecules and salts (Al-Zoubi & Omar, 2009; Bowen & Mukhtar, 1996; Schaep et al., 1998). The reason for worldwide interest of NF membrane is having the a lot of advantages, such as low operating pressure, high flux, high rejection of multivalent anion salts and dissolved organic matter, and low maintenance cost and investment (Al-Zoubi & Omar, 2009; Hilal et al., 2005). If NF process is compared with other processes, it presents many benefits like easy operation control, low energy consumption, reliability and high efficiency (De´on, Dutournie´, & Bourseau, 2007; Hilal et al., 2005). Steric, electric and electrostatic effects provide the salt retention of NF membranes. Thanks to these three force, small or weakly charged and bigger or more charged ions are separated (De´on et al., 2007). Using NF membranes in desalination process is feasible for this reason. In order to develop desalination process and decrease its unfavourable effect, a lot of improvement sprang. For example, using different source of energies and new material

development (Perez-Moreno, Bonilla-Suarez, & Rodriguez-Munoz, 2013). Up to now, the mostly used material in NF is polymer. Polymeric membranes have great potential for desalination process but they have some restrictions at the same time. Limited temperature range, chemical and stability problems and very low resistance to organic solvents are the major drawbacks of the polymeric NF (J. Schaep et al., 1999; Van Gestel et al., 2002a). In recent years, ceramic membranes attracted the attention for NF as a desalination process with new improvements. The advantages of the ceramic membranes can be listed as high mechanical strength, great chemical, biological and thermal stability, long lifetime and be convenient for structural and chemical modification (Perez-Moreno et al., 2013). Ceramic membranes can be used alone or in combination with other systems for desalination. Consequently, ceramic NF membranes are used many researchers in desalination process and it has full of promise (Van Gestel et al., 2002a).

4.1. Literature review

NF membranes have been recently attracted the attention of many researchers about the rejection of different particles, especially salt rejection. There are many researches for the rejection of different salts like NaCl, $MgCl_2$, Na_2SO_4, $CaSO_4$, $MgSO_4$ etc. In this context, commonly used membranes were polymeric ones. Type of the membranes effects the rejection results. Schaep et al. (1998) used NF40 and UTC 20 membranes at 10 bars for the rejection of NaCl salt. The rejection values were 45% and 55% for NF40 and UTC 20 polymeric membranes, respectively. Similar results were obtained for the rejection of divalent ions for both membranes which was about 95%. Afonso et al. (2001) used Desal G-10, Desal G-20 and PES5 polymeric NF membranes in their studies. PES5 membranes had 15% rejection of NaCl salt, while other membranes had similar results. Hilal et al. (2005) investigated the concentration and pressure effect on rejection. Three different polymeric NF membranes (NF90, NF270 and N30F) were used in the experiments. The results showed that 95% ion rejection was achieved with low concentrations. When concentration increased up to 25000 ppm, 41% rejection was observed. Moreover, not only decreasing concentration but also increasing pressure is enhanced the rejection. Al-Zoubi and Omar (2009) studied with polymeric membranes at high concentration of ionic compounds and rejection of different salts

ranged in between 15% to 60% as a function of pressure. The commonly preferred polymeric TAMI non-impregnated NF membranes were used by Mazzoni et al. (2009). When concentration of $CaCl_2$ salt was 5mol/m^3, rejection was about 50%. Rejection decreased to 5% with the increase of concentration to 10mol/m^3.

Studies in recent years focus on the ion removal with using ceramic NF membranes. Retention mechanism is provided by electrostatic interactions since the pores of the NF membranes are larger than the ionic radius of ions. Ceramic membrane studies can be categorized in three major sections. They are single-layer, modified and multi-layer ceramic membranes (Khalili, Sabbaghi, & Zerafat, 2015).

Alami-Younssi et al. (1995) coated the surface of the support with γ-alumina by using sol-gel dip-coating method and achieved the NF membranes. According to obtained results, charge of the membrane played important role in rejection. Moreover, if there are high-valence cation in solution, higher anion rejection exists. Hafnia NF membranes were prepared by Blanc et al. (1998). The results indicated that high NaCl rejection were obtained when membrane has positive charge. This result is valid for acidic and neutral pH, also. In contrast the acidic pH, low $CaCl_2$ rejection was observed for basic pH because membrane surface has negative charge. The rejection of NaCl, $MgCl_2$ and $LaCl_2$ salts were examined by Schaep et al. (1999). The membrane was the mesoporous γ-alumina coated and the experimental parameter was the different salt concentrations. The final result obtained at the end of the experiment was that solution pH has great effect on the rejection value. Moreover, in the case of increasing pressure and constant NaCl concentration, increase in rejection value was observed. Tsuru et al. (2001) studied with the titania NF membranes which were achieved by sol-gel method, for the separation of liquid phase. The results showed that the rejection and the flux were depended on the pressure, concentration of the feed and the membrane surface charge. Increasing the feed concentration decreases the rejection at a constant pH and pressure differential according to the results of these studies. The isoelectric point (IEP) of membrane for NaCl solution was pH=6.5. It means flux is as far as high and minimum rejection. The IEP is different for other salts. Different salts were removed with using titania NF membranes by Labbez et al. (2002a, 2002b). Once again, salt concentration, effective charge density and pH have great effect on the rejection. The IEP was found as pH=6.2. Minimum rejection values were obtained at the IEP point because of the amphoteric behavior. Furthermore, when results were examined carefully, reduction in rejection values was seen with the increasing flux at a constant

pH. Weber et al. (2003) examined the rejection of NaCl and Na_2SO_4 salts. The active top-layer of the used membrane was made from titania. The findings indicated that membrane charge controls the rejection. pH of the salt solution, type of the salt and concentration were the effective mechanism on the rejection, again. De Lint and Benes (2005) determined the NaCl-$CaCl_2$ double ionic solutions' rejection by using the NF membrane which was coated by γ-alumina sol. The experimental parameters in examination of rejection behavior were pH and pressure. When rejection values of divalent and monovalent ion were compared, results indicated the higher rejection value of Ca^{2+} than Cl^- and Na^+. Condom et al. (2004) examined the rejection performance of γ-alumina, $CoAl_2O_4$ and $TiO_2/ZnAl_2O_4$ membranes with different electrolyte solutions. The results showed that electrolyte concentration, salt nature and pH had great effect on salt rejection. Rejection of MA_2 salt relatively higher than M_2A salts. Interaction between membrane and ions caused this result. The γ-alumina membrane had positive charge on the surface at natural pH. Positive charge more repulsed M^{2+} divalent co-ions than M^+ monovalent co-ions.

To enhance performance of the NF membranes, a few researchers were focused on using additive on top layer. Separation behavior of sugars and salts were investigated by Combe at al. (1997). Tubular alumina-titania supports were coated with zirconia-MgO by the sol-gel technique and NF membranes were achieved. While high retention was observed in acidic and basic conditions, very low retention values were obtained in neutral conditions. Vacassy et al., tried to modify zirconia NF membranes with MgO. The rejection values were 31.5% and 66.6% for monovalent and divalent ions, respectively although membranes had high charge densities. Perez-Moreno et al. (2012) investigated the effect of modification of commercial ceramic TAMI NF membrane surface with platinum and silver on the salts rejection of seawater. The studied pressure was 6 bar. The results showed that salt rejection of modified membranes was about 30% in total dissolved solids (TDS). In the case of nonmodified membrane, rejection was about 5%. Electric charges between impregnated silver or platinum metal and ions provided the rejection. Moreover, determination of anion and cation rejection presented high cation removal with impregnated membranes. The last study about additives was examined by Skluzacek et al. (2006). He modified the NF membrane surfaces by using Fe.

Creating a multi-layer top-layer is another option for the rejection enhancement. Multilayer ceramic membrane structure was created on tubular substrates of micro-

porous titania membranes by Puhlfürβ et al. (2000). Polymeric sol-gel method was used while membranes were prepared. NaCl and Na_2SO_4 salts were used in the rejection experiments. Comparison of the titania top-layer results with and zirconia top-layer presented that there is no difference with γ-alumina. However, titania top-layer membranes showed relatively high rejection than zirconia membranes. Smaller pore size distribution of titani top-layer is the reason of this difference. Rejection depended on the pH and charge of membrane. Moreover, when concentration is decreased and pressure is increased, high rejection resulted. Van Gestel et al. (2002) determined the $LiCl_2$, NaCl, KCl, Na_2SO_4 and $CaCl_2$ salts' rejection with titania NF ceramic membranes. Again, multi-layer structure was used and substrate was made of α-alumina. Sol-gel method was used in the preparation of intermediate and titania top-layer. Isoelectric point was found at pH=6 by applying the zeta potential measurements. According to results, increasing NaCl salt concentration decreased the rejection at all pH values. While same rejection behavior was observed for Na_2SO_4, $CaCl_2$ salt had reverse rejection.

4.2.Retention Mechanism

The research conducted up to date shows that convection, diffusion and electromigration controls the mass transfer mechanism for NF (Schaep et al., 1998; J. Schaep et al., 1999; Tang & Chen, 2002). Pressure gradient, concentration gradient and electrical potential gradient across the membrane cause convection, diffusion and electromigration, respectively (J. Schaep et al., 1999). When uncharged solute is considered, only convention and diffusion are responsible for transport of uncharged solutes. A sieving mechanism provides the retention of uncharged solutes. In the case of charged molecules, electromigration takes place in addition to convection and diffusion. Electrostatic interaction exist between the membrane and the molecule (Schaep et al., 1998). The highest ion rejection of NF membrane is achieved at a pH which is far from isoelectric point (IEP). High membrane potential exist farther pH of IEP. Types of salt ions and their concentrations are responsible from the membrane charge and potential. (Samueldelint, Zivkovic, Benes, Bouwmeester, & Blank, 2006). At high pressure values, only electromigration and convection take place on the transport of charged solute. At low pressure values, diffusion becomes dominant. As a result of diffusion,

retention decreases or the concentration in the permeate increases (J. Schaep et al., 1999). Charged component transport is function of membrane charge and this relation was explained in the beginning of this century by Donnan. This is called as Donnan exclusion mechanism and used for explanation for the retention of ions (Schaep et al., 1998).

4.3.DSPM

When performance of NF with charged molecules is predicted, not only size but also charge effects are considered because of electrostatic interaction between charged molecules and membrane charge. In the case of salt solution, equilibrium exists between the membrane and the ions in the solution. Ionic concentration in the membrane is different from ionic solution because of the fixed membrane charge (Schaep et al., 1998). Co-ion has the same charge and counter-ion has the opposite charge with the membrane. When electrolyte solution interacts with charged membrane, co-ion concentration is lower in the membrane than in solution. The opposite conditions are valid for counter-ion. So, counter-ion concentration is higher in the membrane than in solution. Because of this concentration difference of the ions at the interphase, Donnan potential exists to keep electrochemical equilibrium between membrane and solution. If pressure difference is created across the membrane, transportation of water is achieved through the membrane. Co-ions are repelled from the membrane and counter-ions are attracted to provide the electoneutrality requirement (Peeters, Boom, Mulder, & Strathmann, 1998; Schaep et al., 1998). Salt concentration, fixed charge concentration in the membrane, co-ion valence and counter-ion valence are the four main factors which effecting the Donnan equilibrium. When fixed membrane charge decrease and salt concentration increase in the electrolyte solution, co-ion concentration increases in the membrane. In this case, low salt rejection is observed if salt rejection is determined with co-ion rejection. Decreasing co-ion valence and increasing counter-ion valence provide the co-ion concentration increase in the membrane (Peeters et al., 1998). The dominant mechanism is Donnan exclusion in separation but steric exclusion should be considered because it influences the rejection. The membrane which has negative charge, reject the higher valence anions. So, higher rejection of chloride salts is achieved. Strong steric hindrance comes into existence because the narrow pores in the

separating layer forces it. Counter-ions have larger hydrated radius because of steric hindrance. Higher magnesium salt rejection is obtained than sodium salt (Zaiter et al., 2013).

To understand the retention mechanism of NF membrane, many researchers tried for several years. Some models were developed the retention performance of NF membrane. The most known and appropriate one is Donnan-steric portioning pore model (DSPM). Detailed presentation of DSPM model was made by Bowen et al. (1997) and Schaep et al. (1999). Mass transfer of neutral and charged solutes is described in this model. This theory was improved based on the extended Nernst-Planck equation (Schaep, Vandecasteele, Mohammad, & Bowen, 1999). Nernst-Planck equation contains electromigration, ionic diffusion and convection in the membrane pores. Additionally, behavior of hindered diffusion and convection of the solutes in the membrane is taken in consideration. There are three main parameters in order to characterize membrane which are average pore radius, the volumetric charge density and the effective membrane thickness (Bandini & Vezzani, 2003). Three primary properties of the DSPM model are listed below.

1. The membrane is assumed like a charged porous layer. Average pore radius, effective membrane thickness and volumetric charge density can be arranged to determine characteristics of the membrane.

2. Steric hindrance and Donnan equilibrium describe the portioning effect between the external phase and the membrane at the interface.

3. Extended Nerns-Planck equation is used to predict mass transfer through the membrane and this equation takes in consideration hindered convection and diffusion (Bandini & Vezzani, 2003).

Many researchers suggested the theory to predict mechanism of ionic transfer until today. Existing electrical potential in the membrane pores responsible for ion movement in NF membrane. Surface charge and preferential adsorption of certain ions are related with electric potential. In addition, filtered solution and membrane pore size have great effect on the electric potential. Ceramic NF membranes generally have amphoteric behavior. Because of this reason, membrane material and the ions in electrolyte solution have interaction. Ionic and molecular compound separation can be performed due to this interaction (Baticle et al., 1997).

The mostly used ceramic membrane materials in desalination process are titania, zirconia, alumina, zeolite and modified zeolite. Most of the works were studied today

was performed with low salt concentration with NF membrane. In some instances, salt rejection is as high as RO rejection value. The adsorbed ions in the pores have an effect on retention mechanism and it causes not only size exclusion but also Donnan exclusion. Studied showed that the rejection value of divalent ions is higher than monovalent ion rejection (Perez-Moreno et al., 2013). The main reason of high rejection of divalent ions have bigger radius than monovalent ions, when hydrated. In case of metal impregnation of membrane surface, metals increase the electropositiveness. As a result, higher retention for cations than anions are obtained. Single salt retention experiments were performed on TiO_2 NF membrane in many works. According to result, divalent salt ions greatly impress the zeta potential of the membrane. In addition, selectivity of the TiO_2 membrane is changed. This situation is the result of divalent ion adsorption like Ca^{2+}, Mg^{2+} and $SO4^{2-}$. Finally, permeation flux and effective pores sizes reduce (Chevereau et al., 2010).

Chevereau et al. (2010) investigated the retention of single salt solution on commercial ceramic ultrafiltration TiO_2 membrane. The IEP point of TiO_2 powder in water was found as pH=4.1. The results showed that steric effects caused the higher divalent salt rejection than sodium chloride. The Stoke's radii of the sodium and magnesium ions were 0.184 and 0.348 nm, respectively. This retention difference was the result of surface charge of the membrane, also. Wang et al. (2016) examined the retention performance of γ-Al_2O_3/α-Al_2O_3 hollow fiber NF composite membranes. The used salts were $FeCl_3$, $AlCl_3$, $MgCl_2$, $CaCl_2$, NH_4Cl, NaCl, $MgSO_4$, and Na_2SO_4. The results showed that the retention of multivalent ions was higher than monovalent ions. The dominated mechanisms were Donnan and size exclusion. Hydrated radii of ion were responsible the retention when ions had the same valence. The higher the salt concentration the lower the salt retention becomes. Thickness of the electric double layer decreased due to the increasing ionic strength with the salt concentration increase. In the case of thinner electric double layer, electrostatic interaction decreased between charged membrane surface and electrolyte.

4.3.1. Theory

The transport of ionic components in NF membrane pores is developed around three main mathematical models in the literature (De´on et al., 2007). Donnan

exclusion, dielectric exclusion, solvation energy and steric hindrance are effective on NF membranes for retention of solutes (Bargeman, Westerink, Guerra Miguez, & Wessling, 2014). They can be listed as:

1. *The Extended Nernst-Planck Equation:* Convection, diffusion and electromigration are the three terms to provide salt transport mechanism.

2. *The Stefan-Maxwell Equation:* Electrochemical potential which is the balance between the driving force and the forces of the friction are responsible from transport of a solute.

3. *The Thermodynamics of Irreversible Process (TPI):* Concentration dependency of ions make difficult to estimation of paramaters (Bargeman et al., 2014). Membrane is considered as a black box when applying this model (Schaep et al., 1998).

The extended Nernst-Planck equation is the most widely used because they can be applied easily. This model is the simplest and needs a lower number of parameters than other models. In addition, extended Nernst-Planck equation is the simple form of Stefan-Maxwell equation (Bargeman et al., 2014; De´on et al., 2007).

4.3.2. Extended Nernst-Planck Equation

The extended Nernst-Planck equation contains different possibilities of approach to describe the NF. Diffusion, electromigration and convection terms were used to describe ion transport across the membrane. The Nernst-Planck equation is the restricted form of reverse osmosis. The average pore radius, the volumetric charge density and the effective membrane thickness were the parameters used in this equation (Bowen & Mukhtar, 1996). There are a few assumptions which were used for the mathematical derivation of the equation. They can be listed as:

1. Cylindrical pores of radius r_p and length Δx (with $\Delta x >> r_p$) are identical through the membrane.

2. Constant membrane charge density (X) through the membrane.

3. The Stokes radius r_s determine the size of neutral solutes and ions. r_s can be evaluated with the Stokes-Einstein equation by using diffusion coefficient (D_i).

$$rs = \frac{kT}{6\pi\eta Di} \tag{4.1}$$

4. Ion concentration (c_i), permeate volume flux (J_v), ion fluxes (J_i) and electric potential (ψ) are expressed according to averaged radially quantities.

5. Hagen-Poiseuille type parabolic profile was used to define the fully developed volume flux inside the pore (Labbez et al., 2002).

The Nernst-Planck equation can be written as (Bowen & Mukhtar, 1996; Labbez et al., 2002; Johan Schaep et al., 1999):

$$Ji = -D_{i,p}\frac{dc_i}{dx} - \frac{z_i c_i D_{i,p}}{RT} F \frac{d\Psi}{dx} + K_{i,c} c_i J_v \quad (4.2)$$

and

$$\text{Di,p} = K_{i,d} D_{i,\infty} \quad (4.3)$$

where J_i presents the flux of ion i. The terms on the right-hand side correspond to diffusion, electric field gradient and convection, respectively. Diffusivity of the ion I in the membrane is presented by hindered diffusivity $D_{i,p}$. The hindrance convection factor is presented by $K_{i,c}$. $K_{i,d}$ and $K_{i,c}$ are a function of the ratio of the solute radius to the pores radius (λ). These hindrance factors are related to hydrodynamic lag coefficient (G) and hydrodynamic enhanced drag (K^{-1}). A centerline approach and the finite-element technique were used to calculate enhanced lag and drag coefficients (Labbez et al., 2002; Johan Schaep et al., 1999):

$$K^{-1}(\lambda, 0) = 1.0 - 2.30\lambda + 1.154\lambda^2 + 0.224\lambda^3 \quad (4.4)$$

$$G(\lambda, 0) = 1.0 + 0.054\lambda - 0.988\lambda^2 + 0.441\lambda^3 \quad (4.5)$$

The hindrance factors can be written by using parabolic profile of the Hagen-Poiseuille type (Johan Schaep et al., 1999):

$$K_{i,d} = K^{-1}(\lambda, 0), \quad K_{i,c} = (2 - \phi)G(\lambda, 0) \quad (4.6)$$

where the steric term, ϕ, can be written as:

$$\phi = (1 - \lambda)^2 \quad (4.7)$$

The effective membrane charge density (X) can be assumed as constant and is written as (Bowen & Mukhtar, 1996),

$$\sum_{i=1}^{n} z_i c_i = -X (for\ 0 \leq x \geq \Delta x) \quad (4.8)$$

Electroneutrality in the bulk solution are defined as,

$$\sum_{i=1}^{n} z_i C_i = 0 \quad (4.9)$$

Overall electrical current is zero which passing through the membrane (Bowen & Mukhtar, 1996; Labbez et al., 2002; Johan Schaep et al., 1999),

$$I = \sum_{i=1}^{n} F z_i j_i = 0 \quad (4.10)$$

The electrical potential is not changing inside the membrane. It means every ion have the same electrical potential gradient. This situation provides advantage to obtain

the concentration and electrical potential gradient equations. The concentration gradient equation can be written by rearranging the Eq. 1.

$$\frac{dc_i}{dx} = \frac{J_v}{D_{i,p}}\left(K_{i,c}c_i - C_{i,p}\right) - \frac{z_i c_i}{RT} F \frac{d\Psi}{dx} \tag{4.11}$$

and

$$J_i = J_v C_{i,p} \tag{4.12}$$

where $C_{i,p}$ represents the concentration of ion i in the permeate side.

The electrical potential gradient can be expressed as (Bowen & Mukhtar, 1996; Labbez et al., 2002; Johan Schaep et al., 1999),

$$\frac{d\Psi}{dx} = \frac{\sum_{i=1}^{n} \frac{z_i J_v}{D_{i,p}}(K_{i,c}c_i - C_{i,p})}{\frac{F}{RT}\sum_{i=1}^{n} z_i^2 c_i} \tag{4.13}$$

The boundary conditions which were used to solve concentration and electrical potential gradient equations are given by (Bowen & Mukhtar, 1996),

$$x=0, \qquad C_i = C_{i,f} \tag{4.14}$$

$$x=\Delta x, \qquad C_i = C_{i,p} \tag{4.15}$$

where $C_{i,f}$ and $C_{i,p}$ represents the feed and permeate concentrations of ion i at the interfaces of the membrane, respectively.

Donnan equilibrium is used to determine the concentration at the interfaces which are feed and permeate sides. Donnan steric partitioning equation is given by (Bowen & Mukhtar, 1996; Labbez et al., 2002; Johan Schaep et al., 1999),

$$\frac{c_i}{C_i} = \phi \exp\left(\frac{z_i F}{RT} \Delta\psi_D\right) \tag{4.16}$$

Steric effects at the entrance of membrane are calculated by using the steric portioning term (ϕ). The real rejection is calculated from given equation in below (Bowen & Mukhtar, 1996; Labbez et al., 2002).

$$R=1-\frac{C_{i,p}}{C_{i,f}} \tag{4.17}$$

The Runge-Kutta-Gill numerical method can be used to solve all of the equations (Bowen & Mukhtar, 1996; Johan Schaep et al., 1999).

CHAPTER 5

EXPERIMENTAL

5.1. Materials

The materials used in membrane preparation and filtration experiments are listed in Table 5.1. All the chemicals were used as received without any further purification. Deionized water was used throughout this work.

Table 5.1. The used materials and characteristics.

Materials	**Characteristics**
0.5 µm alumina (Al_2O_3) 0.18 µm alumina (Al_2O_3)	99.8% purity, CT 3000 SG, Almatis 99.8% purity, AKP-50, Sumitomo
Boehmite (AlO(OH))	99.8 % purity, Disperal and P2, Sasol
Titanium (IV) isopropoxide	97% purity, Sigma Aldrich
Titanium (IV) butoxide	97% purity, Sigma Aldrich
Zirconium (IV) propoxide	70% purity, Sigma Aldrich
Polyvinyl Alcohol (PVA)	80% hydrolyzed, Sigma Aldrich
Ethanol	99.5% purity, Merck
1-Propanol	99% purity, Merck
Glycerol	99% purity, Panreac
Diethanolamine (DEA)	99.5% purity, Merck
Nitric acid (HNO_3)	65% purity, Merck
Dolapix CE 64	Eurokimya A.Ş.
Defoamer	Dağlar Kimya A.Ş.
Magnesium sulphate ($MgSO_4.7H_2O$)	99.5% purity, Merck
Sodium Sulphate (Na_2SO_4)	Anhydrous Riedel

5.2 Methods

5.2.1 Preparation of Support Materials

The most commonly used method for the preparation of membrane supports is extrusion. Commercial 5.2, 1.3 and 0.5 μm α-alumina (Al_2O_3) powder mixes along with organic/inorganic binders were used in paste preparation in this work. The tubular membrane supports were prepared by piston extrusion of the pastes in the Chemical Engineering Department laboratories of İzmir Institute of Technology. Tubular type membrane supports were heat treated at 1525^0C after room temperature drying. The dimensions of the tubular membrane supports were 200 mm in length with 16/25 mm inner/outer diameters.

5.2.2. Colloidal and Polymeric Sol-gel Processes

Ceramic membranes are generally prepared by sol-gel based methods due to the ease in sol/material structure/composition control and since they make room temperature processing possible. There are two different sol-gel routes in the literature: colloidal and polymeric sol-gel methods (Chen et al., 2015). Colloidal chemistry in aqueous media is the basis of colloidal sol-gel method. The polymeric sol-gel method is based on the dissolution of metal-organic precursors in organic solvents. Water is used as the solvent in colloidal sol-gel method. The use of water instead of organic solvents prevents harm to the environment. Water use is also more suitable for large-scale ceramic membrane production. A two-step process is usually used for colloidal sols which may be derived from oxide precursors. Firstly, hydrolyzed precursors are utilized to form condensed and hydroxylated precipitate. The precipitate is then dispersed to a stable sol with the help of peptization reaction by using acidic or basic electrolytes (Chen et al., 2015).

5.2.3 Preparation of the Membrane Interlayers by the Colloidal Sol-gel Process

The preparation and synthesis of membrane intermediate layers is outlined in this section. Support surface irregularities and imperfections can be eliminated by forming multiple intermediate layers through dip-coating method. MF (α-alumina), UF1 (boehmite and P2) and UF2 (titania hydrosol) layers were formed on tubular alumina supports by dip coating method using colloidal sol-gel derived sols.

5.2.3.1. MF Layer Preparation

In forming the MF layer, stable suspensions containing 7 wt.% α-alumina (0.5 μm), PVA, dispersant (dolapix) and defoamer were used. PVA was dissolved in water at 70°C, then cooled to room temperature and alumina was added. Dispersant and defoamer was added dropwise to this mixture under constant stirring. The prepared suspension was subjected to ultrasonic treatment for two hours to ensure the stability of particles and complete powder dispersion. The particle size and distribution of α-alumina suspensions were determined by dynamic light scattering (DLS Malvern Zetasizer 3000 HSA). Tubular ceramic membrane supports were coated with this suspension for 10 minutes and then dried at room temperature for 24 hours. The dried α-alumina-coated supports were heat treated at 1200 °C in a high temperature furnace (Carbolite CWF 1300). A furnace-controlled heating program (heating rate from room temperature to 110°C at 2°C / min, from 110°C to 1000°C at 2.7°C / min, from 1000°C to 1200°C at 2°C / min, soaked about 60 min at 1200°C cooled to room temperature) was applied to avoid breakage/cracking during heat treatment. The processing flowsheet of MF layer preparation is given in Figure 5.1. The second MF layer was prepared by using AKP-50 (0.18 μm α-alumina) sol with a similar procedure except a heat treatment application at 1000 ^{0}C.

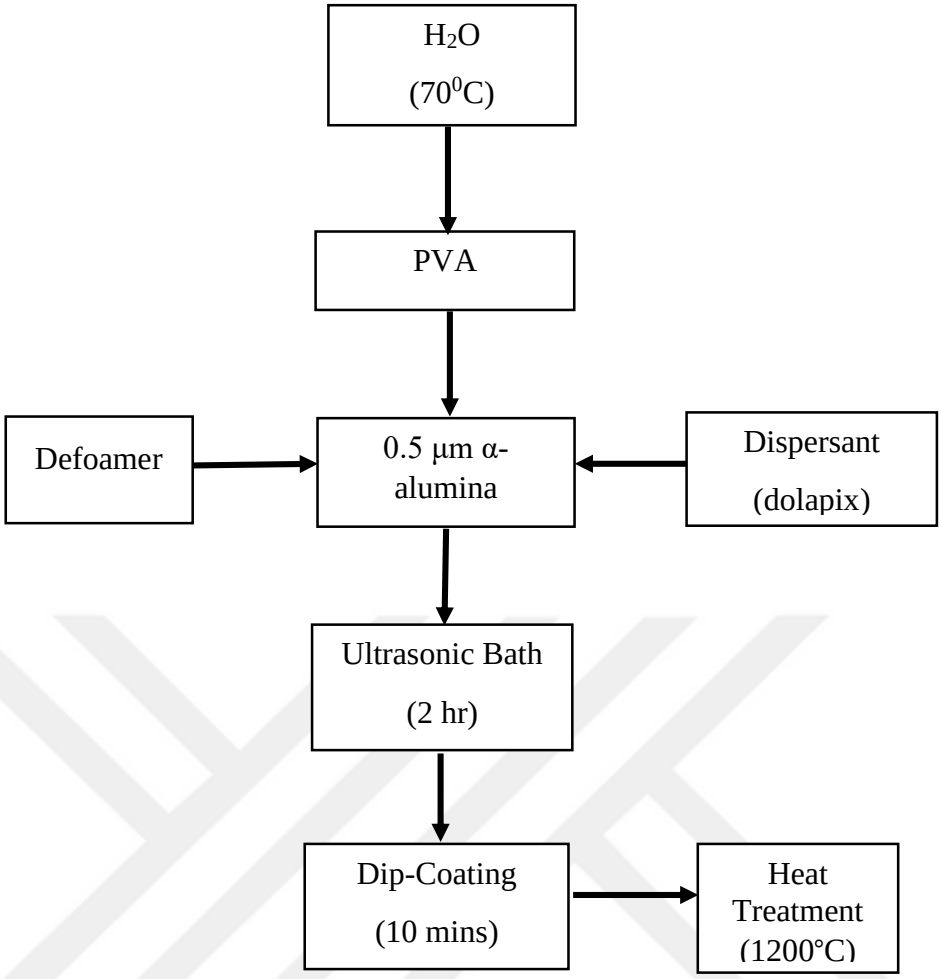

Figure 5.1. Flowsheet of MF layer preparation.

5.2.3.2. UF1 Layers Preparation

The UF1 layers were prepared by using 0.6 wt. % disperal (boehmite), 0.8 wt. % PVA and 3 ml HNO_3 (1 M). PVA was dissolved at 70^0C and cooled to room temperature in the initial step. Boehmite and HNO_3 were added and the suspension was stirred/ultrasonically treated for 20 minutes. This procedure was repeated 3 times to ensure that the boehmite particles were well dispersed. The particle size distribution of boehmite sols were determined by dynamic light scattering (DLS Malvern Zetasizer 3000 HSA). MF membranes were coated with this solution for 10 seconds and then dried at room temperature for 24 hours. The dried MF membranes were heat treated at 600^0C in a high temperature furnace (Carbolite CWF 1300). A furnace-controlled heating program (from room temperature to 200^0C at 2^0C/min, from 200^0C to 400^0C at

1^0C/min, from 400 to 600^0C at 2^0C/min heating rates and soaked about 1 hour at 600^0C) was applied for crack/defect free selective layer formation. The related processing flow diagram for UF-1 disperal (boehmite) layer preparation is given in Figure 5.2.

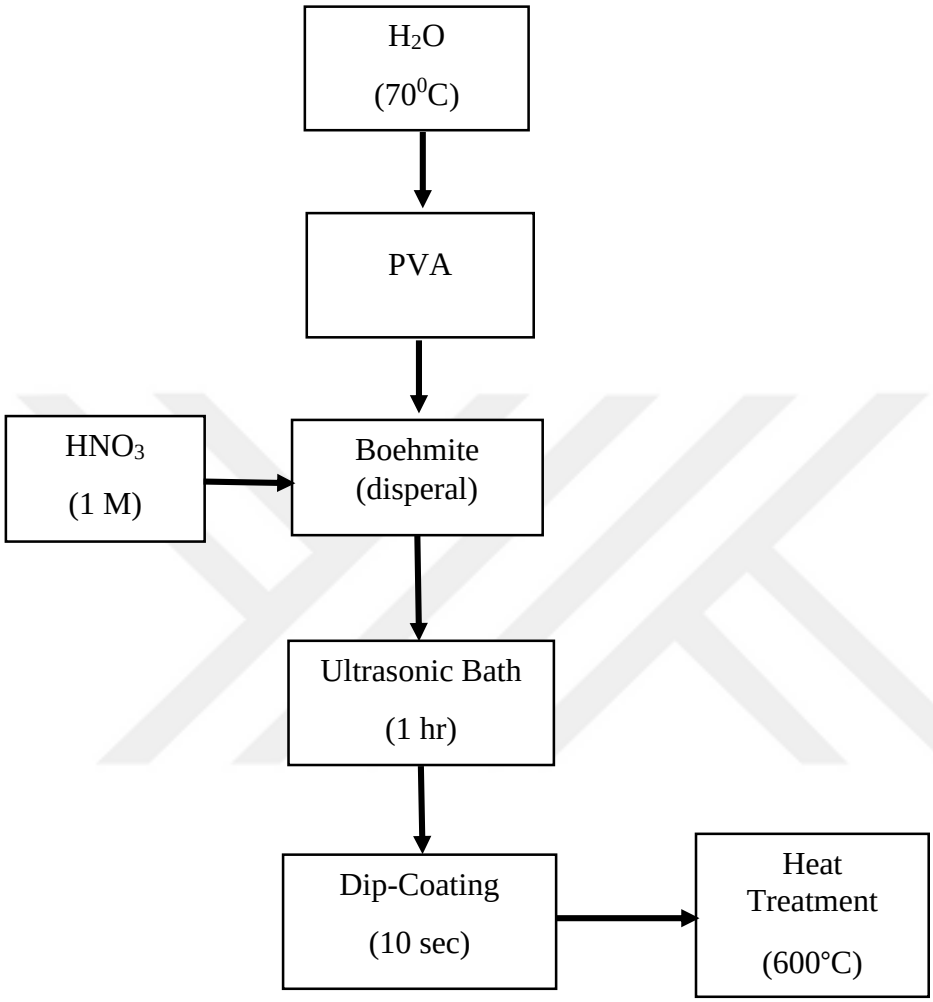

Figure 5.2. Schematic representation of UF-1 disperal (boehmite) layer preparation

Another boehmite (P2) sol which has no PVA addition is formed by adding 0.6 wt.% P2 boehmite powder followed by mechanical stirring for 20 min and 20 min ultrasonic treatment in water. This procedure was repeated 3 times to ensure that the P2 powder particles were well dispersed. The particle size distribution of boehmite sols were determined by dynamic light scattering (DLS Malvern Zetasizer 3000 HSA). MF membranes were coated with this solution for 10 seconds and then dried at room temperature for 24 hours. UF1 coated dried boehmite membranes were heat treated with the above heat treatment program at 600^0C in a high temperature oven (Carbolite CWF 1300).

5.2.3.3. UF2 Layer Preparation

The processing flow diagrams of the two TiO_2 hydrosols used in the UF2 layer formation are schematically illustrated in Figures 5.3 and 5.4. The sol particle sizes were controlled by varying the molar ratios of titanium tetraisopropoxide: diethanolamine: nitric acid: water: isopropanol (TTIP: DEA: HNO_3: H_2O: 2-propanol). UF1 coated membranes were coated with these sols for 10 seconds and then dried at room temperature for 24 hours. The dried titanium coated UF1 membranes were heat treated in a high temperature furnace (Carbolite CWF 1300) at 400^0C. The furnace was operated with a controlled heating program (heating from room temperature to 400^0C at 1^0C/min heating rate and soaked about 1 hour at 400^0C) for crack/defect free selective layer formation.

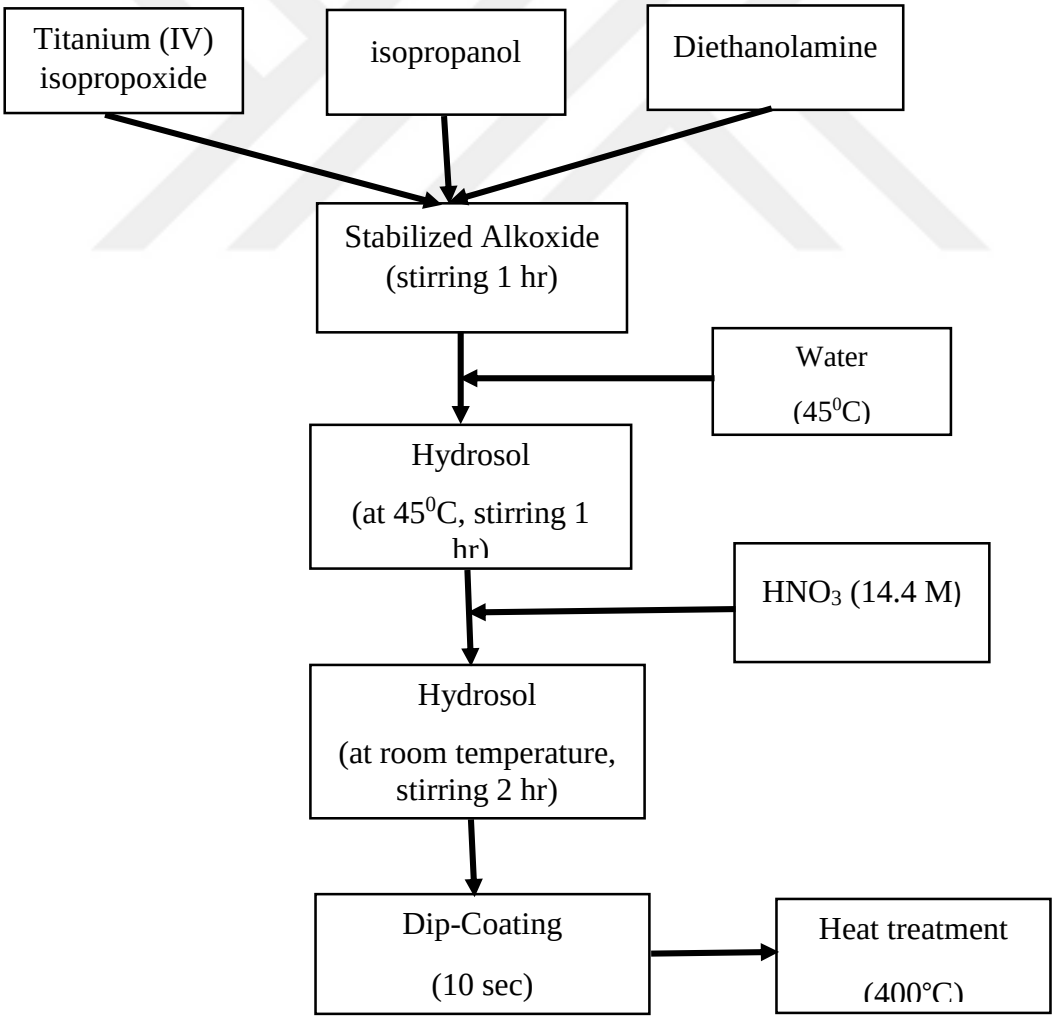

Figure 5.3. Preparation of colloidal TiO_2 (TTIP) hydrosols

The sol particle sizes were controlled by varying the molar ratio of titanium (IV) butoxide: glycerol: water: nitric acid (TTB:$C_3H_8O_3$: H_2O: HNO_3) in the second sol. UF1 coated membranes were coated with these solutions for 10 seconds and then dried at room temperature for 24 hours. The dried titania coated membranes were heat treated in a high temperature furnace (Carbolite CWF 1300) at 400^0C. The furnace was operated with a controlled heating program (heating from room temperature to 400^0C at 1^0C/min heating rate, soaked about 1 hour at 400^0C) for crack/defect free selective layer formation.

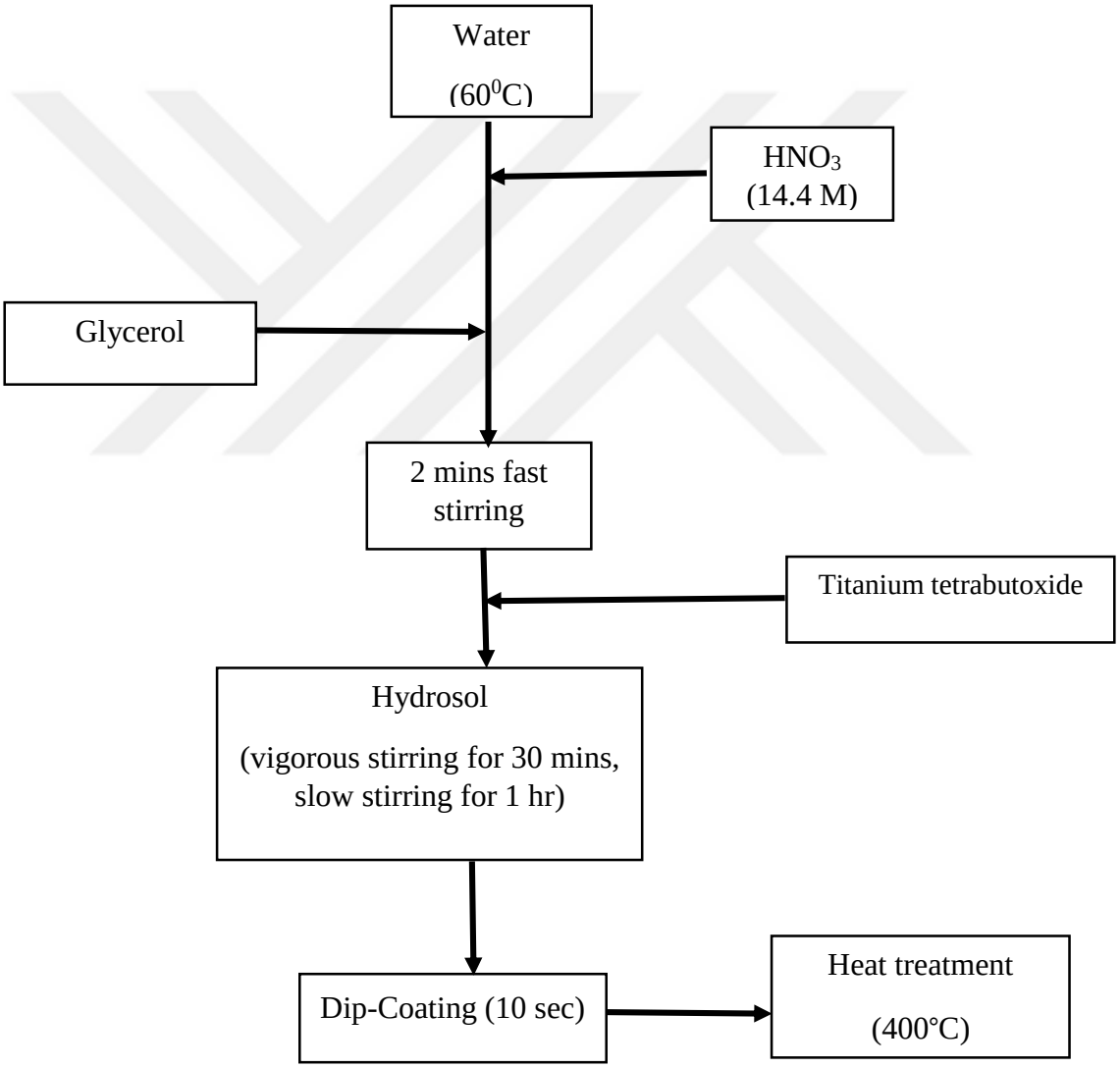

Figure 5.4. Preparation of colloidal TiO2 (TTB) hydrosols (titanium tetrabutoxide: glycerol: water: nitric acid=1:1:556:3.2).

5.2.4 Preparation of the Membrane Top Layer by the Polymeric Sol-gel Process

A thin separation top layer was synthesized as a final layer to form the multilayered asymmetric NF membrane structure. The thin top layer sol must contain species a few nanometers in size which were synthesized by using polymeric sol-gel technique.

5.2.4.1 NF Layer Preparation

NF selective layers were prepared by using as zirconia/titania mixed oxide and neodymium doped titania sols. These sols were prepared by starting with an alcoholic alkoxide solution as outlined in Figure 5.5.

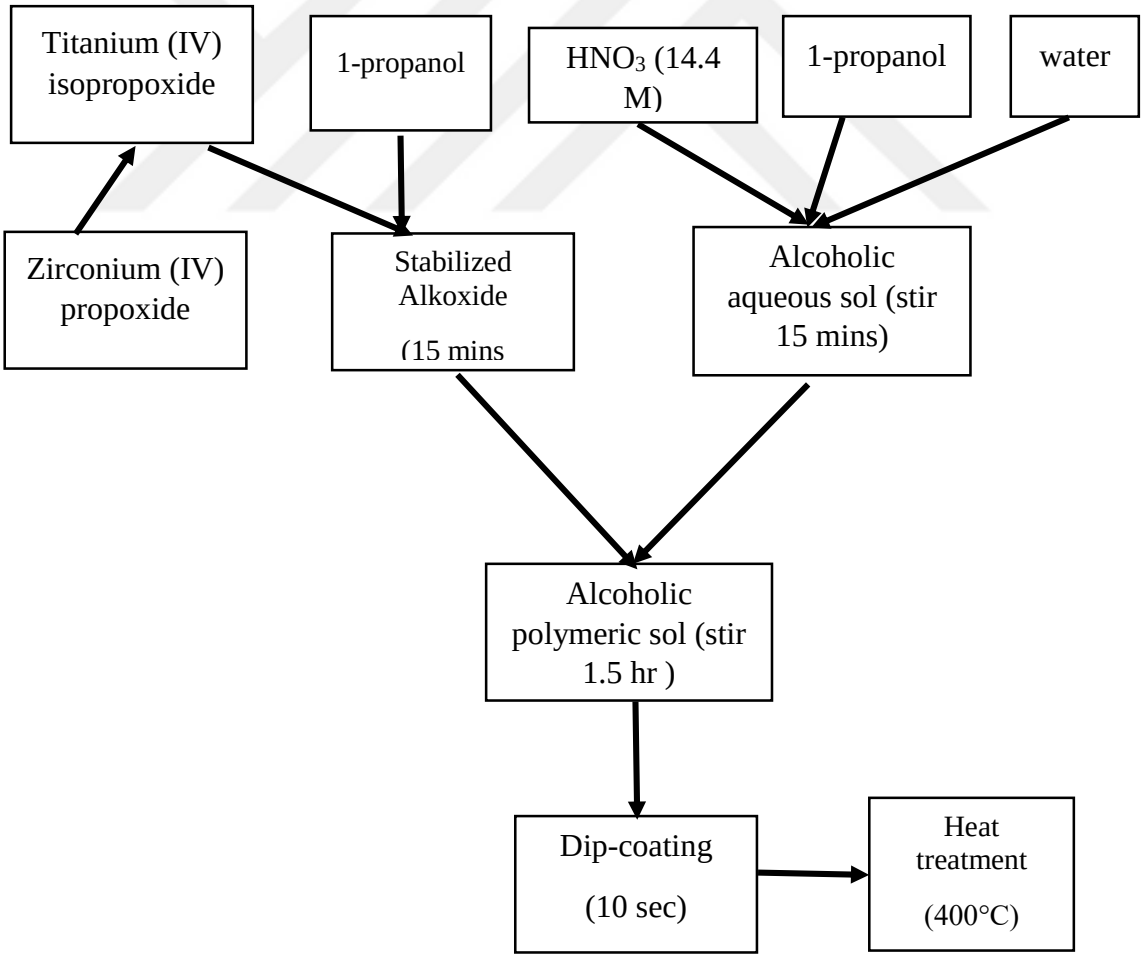

Figure 5.5. Preparation of titania/zirconia mixed oxide polymeric sols.

The first solution contains metal alkoxides and the second solution contains the acid catalyst, water and dopant (neodymium salt). Clear doped/mixed oxide polymeric sols were prepared by adding the water containing solution to the alcoholic metal alkoxide containing solution. The sol particle size distribution was determined by dynamic light scattering (DLS Malvern Zetasizer 3000 HSA) as a function of time. UF2-coated membranes were coated for 10 seconds with this sol and then dried at room temperature for 24 hours. The dried NF membranes were heat treated in a high temperature furnace at 400^0C. The furnace was operated with a controlled heating program (heating from room temperature to 400^0C at 1^0C/min heating rate, soaked about 1 hour at 400^0C) for crack/defect free selective layer formation.

5.3. Membrane Characterization

5.3.1. Structural Characterization

The particle sizes of the prepared intermediate layer and top layer sols were determined by using DLS Malvern Zetasizer 3000 HSA. A scanning electron microscope (SEM) (FEI QUANTA 250 FEG) was used to investigate the microstructure of the multilayer ceramic membrane, layer thicknesses, and morphology of the selective membrane layers.

5.4. Filtration Procedure

All filtration experiments were carried out on a laboratory scale cross-flow filtration set-up equipped with a tubular module. The filtration set-up is illustrated in Figure 5.6. The experiments were conducted at room temperature. Membranes with a length of 200 mm and an ID/OD of 16/25 mm were placed in the tubular module. Cross-flow velocity can be adjusted by the pressure pump controller. The maximum studied transmembrane pressure (TMP) was 4 bars. The tubular membrane module is made of stainless steel.

Figure 5.6. The membrane filtration system.

5.4.1. Pure Water Flux

Pure deionized water fluxes of the ceramic support, membranes with intermediate layers and top layers were achieved by using cross-flow filtration system under different transmembrane pressures at room temperature. The mass of the water was collected and weighed by using an electronic balance in a set time interval. Water flux was calculated from the following equation.

$$J=\frac{V}{A.t}$$

Where J is the permeate flux ($L/m^2.h$), V is the permeate volume (L, the weight determined during the set time interval divided by the water density), A is the effective membrane area (m^2) and t is the sampling time (h).

5.4.2. Desalination Experiments with Model Salts

Two model singles component electrolyte/salt solutions (Na_2SO_4 and $MgSO_4$) were used in salt retention experiments. Na_2SO_4 and $MgSO_4$ are called as mono-divalent salts. The salts used in the salt retention experiments were analytical grade and deionized water was used to prepare salt solutions. The fundamental experimental parameter was the solution pH. Transmembrane pressure was determined by using the arithmetic mean of the pressures at the inlet and at the outlet of the membrane module.

The pH was adjusted by adding HCl to the salt solution for acidification and NaOH for alkalization. The pH of the solutions was determined by using a METTLER Toledo Seven Compact S210 pH-meter. Laboratory-scale cross-flow system was used for the filtration experiments. The conductivities and the ion concentrations of the collected feed and permeate samples at set time intervals were determined and percent salt retentions were determined by using the ion concentrations with the following equation:

$$R(\%) = (1 - \frac{C_p}{C_f}) \times 100$$

C_p is the ion concentration in permeate and C_f is the ion concentration in the feed. Mg^{+2} and $SO4^{-2}$ ion concentrations were determined by using the methods outlined below.

5.5. Ion Determination Techniques

5.5.1. SO_4^{-2} Ion Determination

The SO_4^{-2} ion concentration determination scheme is shown in Figure 5.7.

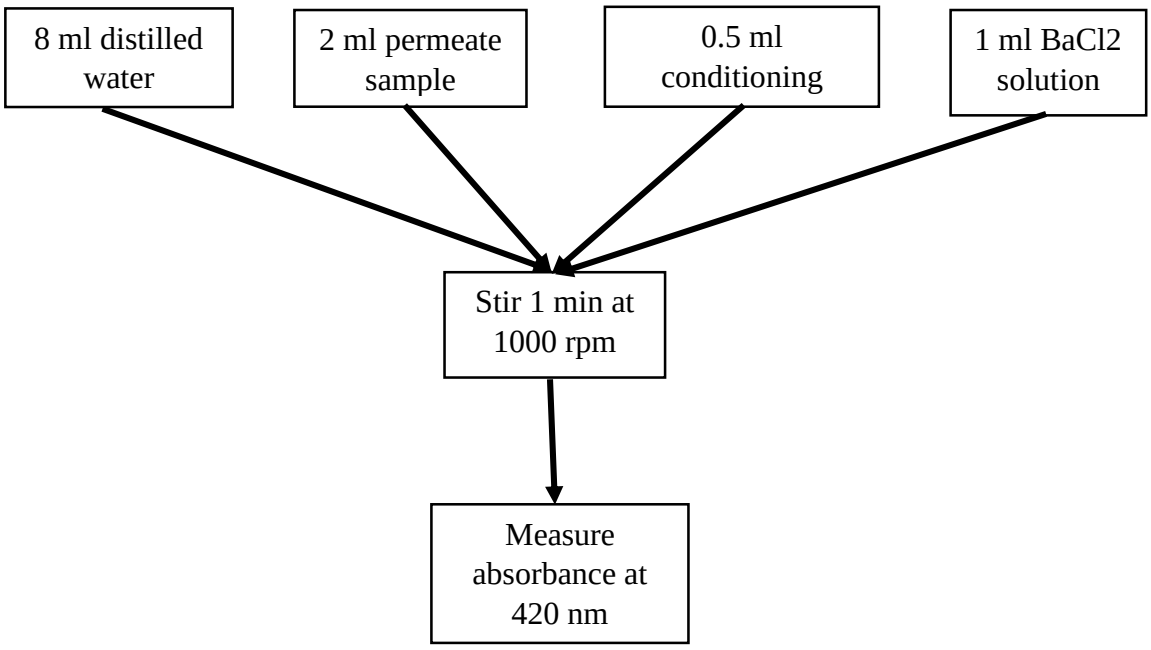

Figure 5.7. The SO_4^{-2} ion concentration determination scheme.

2 ml of permeate sample and 8 ml of deioinized water were combined and 0.5 ml of conditioning reagent was added to this combined solution in a schott bottle and stirred at 1000 rpm. 1 ml of $BaCl_2$ solution was added to the stirred solution and the stirring was conducted for 60 seconds. The suspension was poured into a cuvette and the turbidity was measured in 30 s intervals until the turbidity value was stable. A spectrophotometer (Hach Lange DR 3900) was used for measuring the turbidity at 420 nm wavelength. The maximum obtained value was recorded. The SO_4^{-2} ion concentrations were determined by using a calibration curve plotted previously and given in Figure 5.8 (absorbance vs. SO_4^{-2} ion concentration in mg/L).

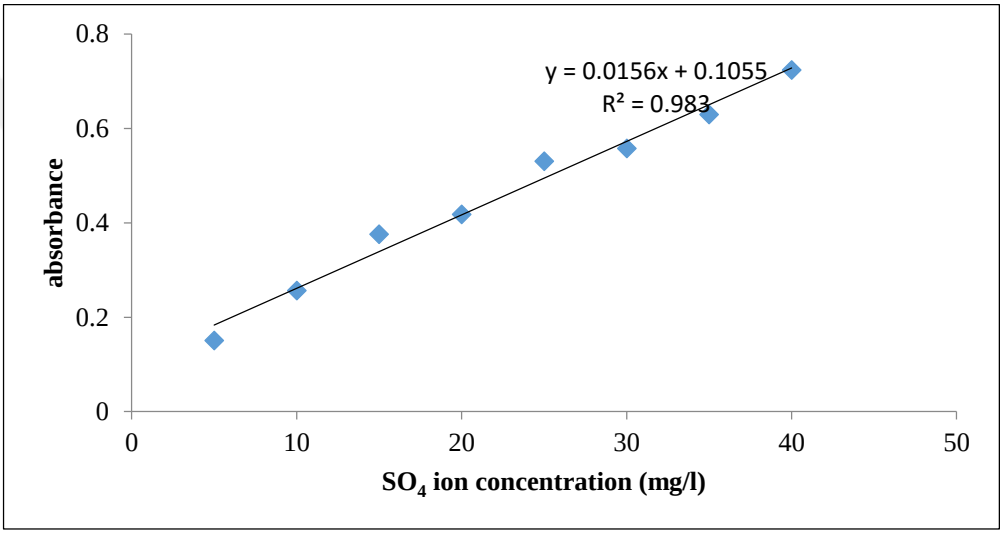

Figure 5.8. Absorbance vs. SO_4^{-2} ion concentration (mg/L) calibration curve.

5.5.2. Mg^{+2} Ion Determination

Figure 5.9 shows the Mg^{+2} ion concentration determination scheme. 10 ml of ethanolamine, 3 ml of pH=10 buffer solution and 3 to 4 drops of eriochrome black T indicator were added to 50 ml of permeate sample in a volumetric flask. This solution was titrated with 0.01 M EDTA until the color changes from light pink to light blue. EDTA consumptiom was recorded and Mg^{+2} ion concentration was calculated in mg/L.

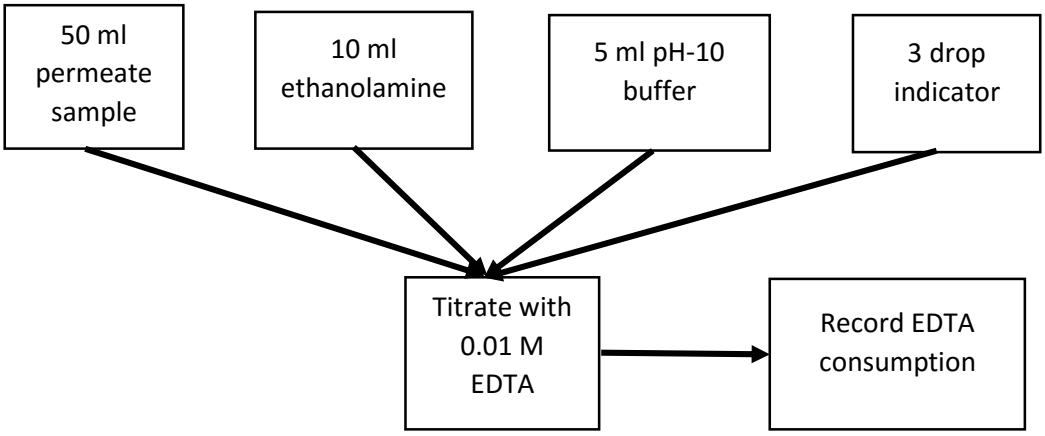

Figure 5.9. Mg^{+2} ion concentration determination scheme.

CHAPTER 6

RESULTS AND DISCUSSION

6.1. Preparation of Support Materials

The extrusion method was used to produce membrane supports. The materials of the membrane support are commercial 5.2 μm, 1.3 μm and 0.5 μm α-alumina (Al_2O_3) powders. Figure 6.1 shows the tubular alumina ceramic membrane supports after shaping and heat treatment processing. The dimensions of tubular membrane support were 200 mm in length and inner and outer diameters are 16 and 25 mm, respectively.

Figure 6.1. Tubular alumina ceramic membrane supports.

6.2. Preparation of Selective Membrane Layers

The intermediate layers and thin top layers were formed by using dip-coating method on the tubular ceramic membrane supports. The purposes of multiple layer structure are reducing the rough pore structure of the tubular support, eliminating

surface irregularities and imperfections. MF (α-alumina and AKP-50), UF1 (disperal and P2) and UF2 (titania hydrosol) layers are called as intermediate layers. They were colloidal sol-gel derived. A thin top layer was nanometer-sized and polymeric sol-gel derived. The final layer is called as NF (titania/zirconia).

6.2.1. Characterization of Particle Sizes of Selective Membrane Layer Sols

The stable MF colloidal sol was formed by using 0.5 µm α-alumina powder. Figure 6.2 shows the volume based particle size distribution of the MF colloidal sol. The average particle size of the α-alumina sol was determined as 522 nm.

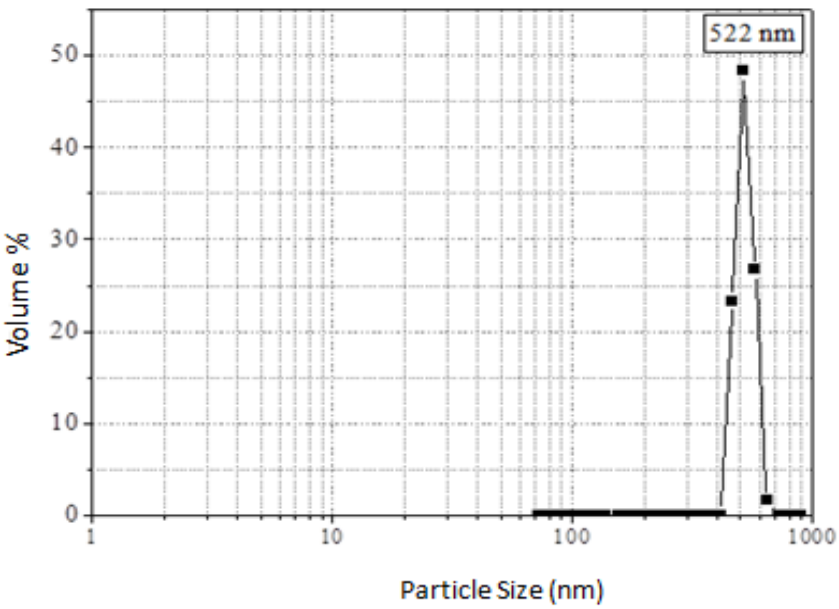

Figure 6.2 The volume based particle size distribution of the 0.5 µm α-alumina colloidal sol (wt 7% α-alumina, 0.8% PVA).

The second MF layer was formed by using AKP-50 powder colloidal suspension. This layer was located between MF and UF-1 layers. Figure 6.3 shows the volume based particle size distribution of the AKP-50 colloidal sol. The average particle size of the AKP-50 sol was 175 nm.

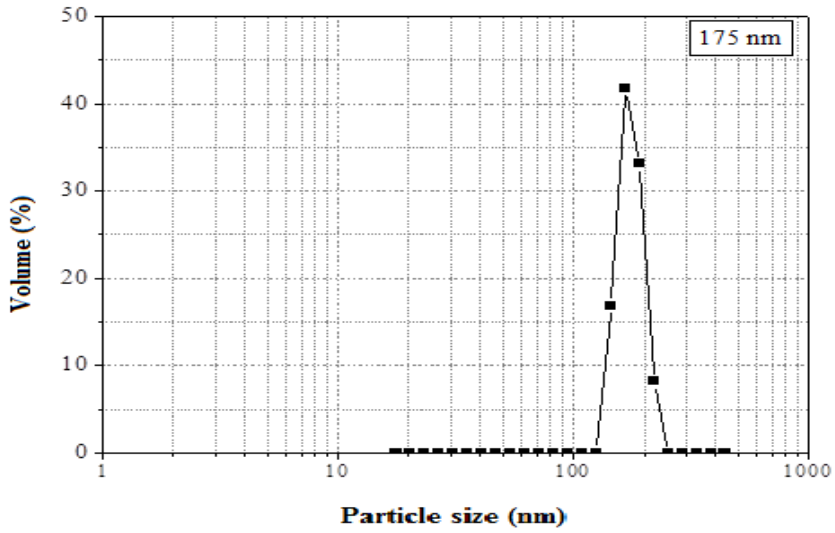

Figure 6.3 Volume based particle size distribution of the AKP-50 colloidal sol (wt 7% AKP-50)

The first UF-1 layer was formed by using boehmite (disperal) powder sol. This layer was located between AKP-50 and P2 layers. Figure 6.4 shows the volume based particle size distribution of the boehmite colloidal sol. The average particle size of the boehmite sol was 42 nm.

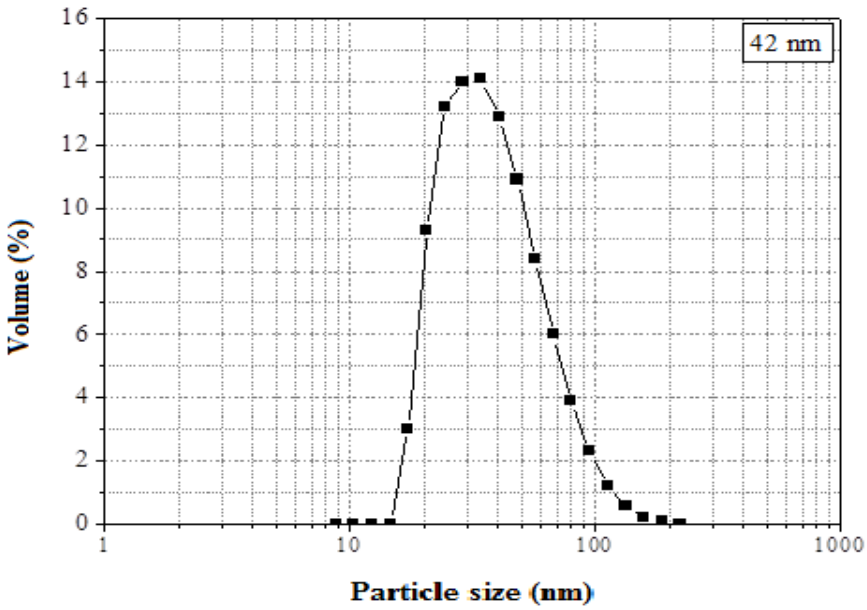

Figure 6.4 Volume based particle size distribution of disperal (boehmite) colloidal sol (0.6 wt % boehmite and 0.8 wt % PVA)

The second UF-1 layer was prepared by using P2 powder sol. This layer was located in between the boehmite and UF-2 layers. Figure 6.5 shows the volume based particle size distribution of the P2 colloidal sol. The average particle size of the P2 sol was 16 nm.

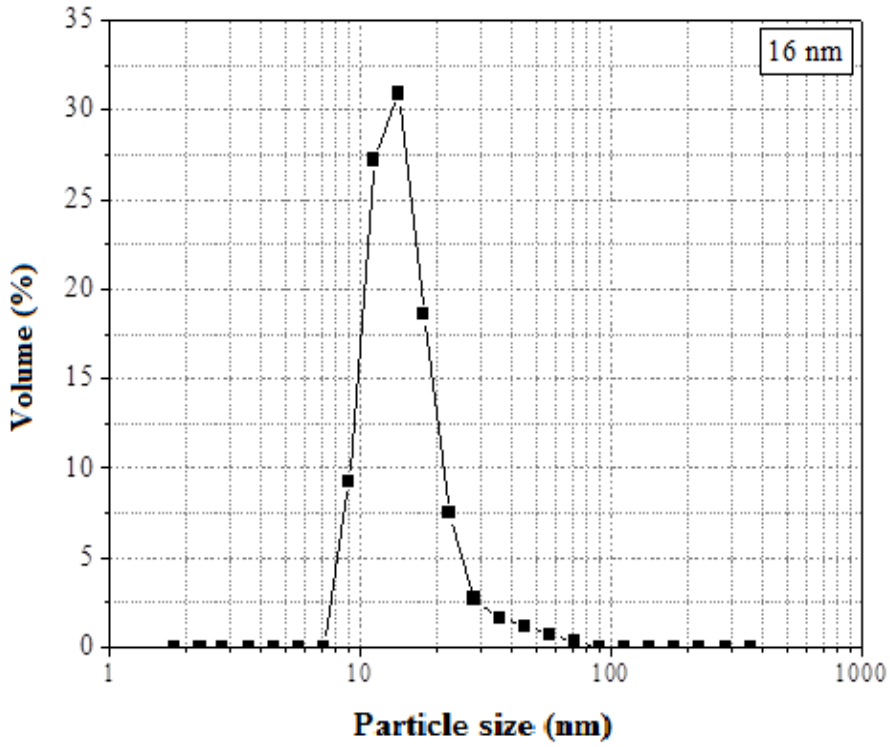

Figure 6.5. The volume based average particle size distribution of the P2 (boehmite) colloidal sol (0.6 wt % P2)

The first UF-2 layer was consolidated by using titanium tetraisopropoxide (TTIP) hydrosol in between P2 and NF layers. Figure 6.6 shows the volume based particle size distribution of the TTIP hydrosol. The average particle size of the TTIP hydrosol was 14 nm.

The second UF-2 layer was consolidated by using titanium tetrabutoxide (TTB) hydrosol in between TTIP hydrosol and NF layers. Figure 6.7 shows the volume based particle size distribution of the TTB hydrosol. The average particle size of the TTB hydrosol is 4.9 nm.

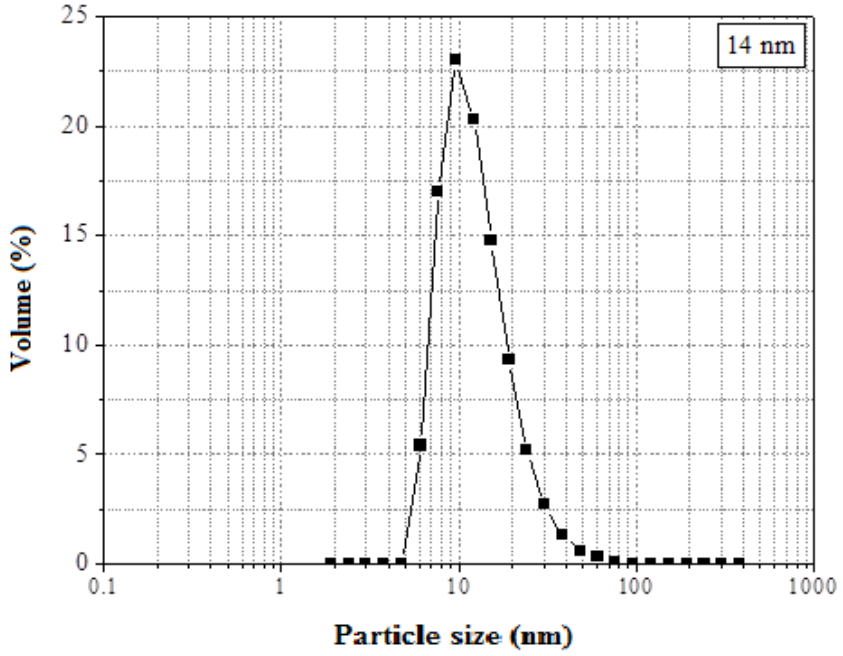

Figure 6.6. The volume based average particle size distribution of the TTIP hydrosol (TTIP: DEA: HNO_3:H_2O:2-Propanol=1:0.8:2.4:1000:10)

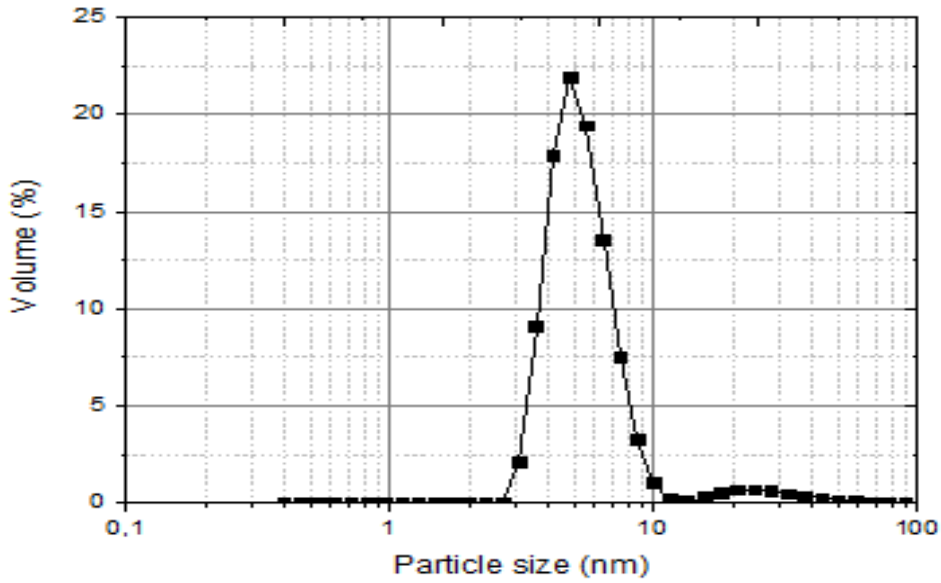

Figure 6.7. The volume based average particle size distribution of the TTB hydrosol (TTB: Glycerol: H_2O: HNO_3= 1:1:556:3.2).

The NF layer was consolidated by using titanium tetraisopropoxide (TTIP)/ zirconium tetrapropoxide (ZTP) mixed-oxide polymeric sol on the TTB hydrosol layer.

Figure 6.8 shows the volume based particle size distribution of the titanium tetraisopropoxide (TTIP)/ zirconium tetrapropoxide (ZTP) mixed-oxide polymeric sol. The average particle size of the polymeric sol was 3.6 nm.

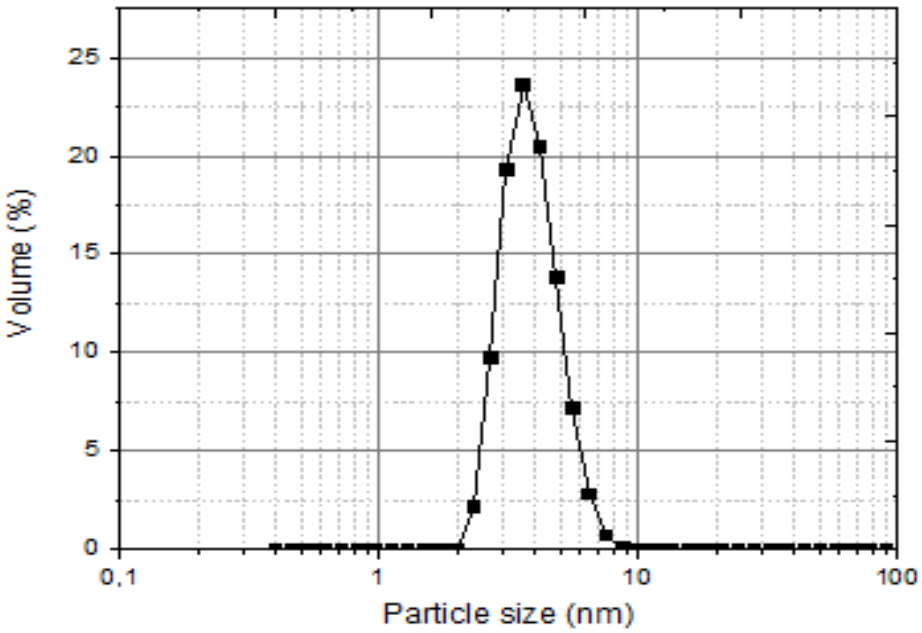

Figure 6.8. The volume based average particle size distribution of the titanium tetraisopropoxide (TTIP)/zirconium tetrapropoxide (ZTP) mixed-oxide polymeric sol

6.2.2. Characterization of Membrane Layers with Scanning Electron Microscope

The tubular asymmetric ceramic membrane structure was obtained by applying the different MF, UF and NF layers on the surface of α-alumina tubular support. The morphology of the microstructure for the different membrane layer surfaces and the cross-section of asymmetric structures were analyzed with scanning electron microscopy (SEM). SEM image in Figure 6.9 shows the surface and cross-sectional areas of 0.5 μm α-alumina MF layer. The texture of the elaborated membrane surface can be seen from this figure. Uniform membrane was formed on the ceramic support. Defect free, homogeneous and smooth MF layer was obtained. The organic additives are the important factors in obtaining defect free membrane with desired pore sizes. PVA was used as a controller for drying. Furthermore, from the cross-section of the

SEM images it is apparent that the thickness of the microfiltration membrane layer was about 40-50 μm.

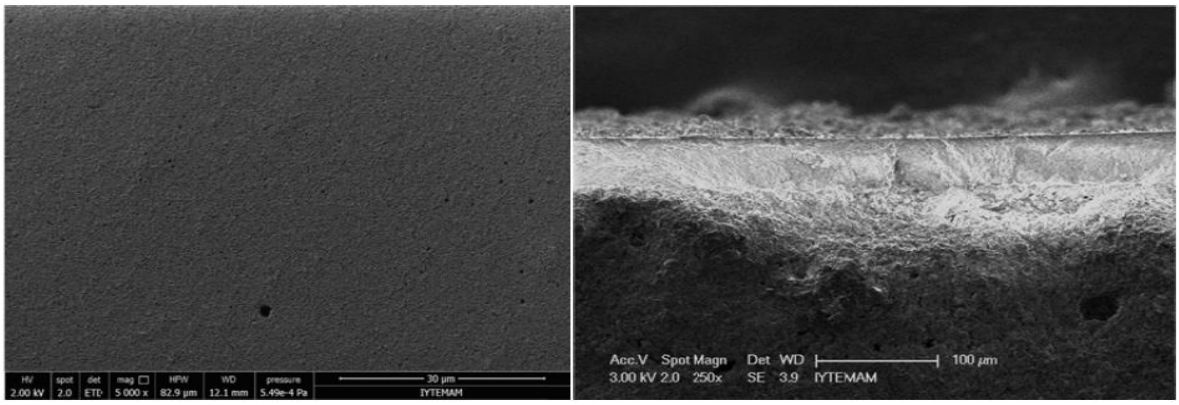

a b

Figure 6.9. SEM micrograph of the surface (a) and cross-sectional area of microfiltration layer (b)

Boehmite and P2 colloidal sols were applied on the MF coated tubular ceramic membrane. These two layers constitute the UF-1 layers. Figure 6.10 shows the SEM images of P2 membrane layer at different magnifications. Membrane layer had no visible defects and pores as shown in the figure where the presence of uniform and separate membrane layers can be easily seen. Penetration of the sol particles into the lower layer pore structures was also not observed.

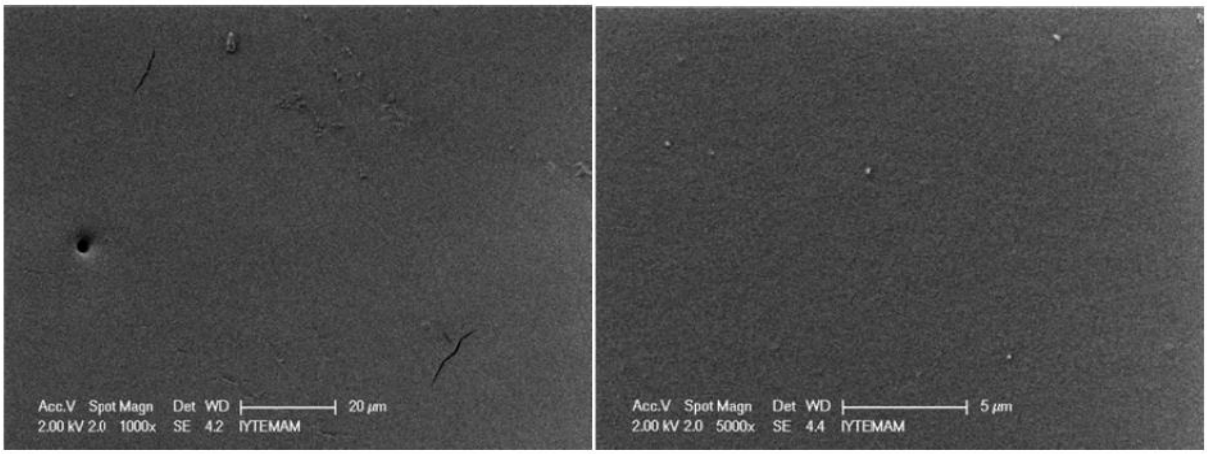

Figure 6.10. SEM micrograph of the surface of UF-1 layer.

SEM images of a TTIP top layer coated on a mesoporous P2 layer after firing at 600 ^{0}C is given in Figure 6.11 where a typical multilayer membrane structure can also be seen. A flat and smooth TTIP top layer clearly formed. Cross-section of multilayer membrane structure shows the macroporous α-alumina (Al_2O_3) support, mesoporous interlayers and microporous top layer. Discrete and uniform membrane layer were formed. No obvious penetration of the top layer sol particles into the intermediate layer pores was observed. The The total UF-1 layer thickness was estimated as 3.59 μm. and an average thickness of UF-2 layer was determined as 733 nm by using these SEM pictures.

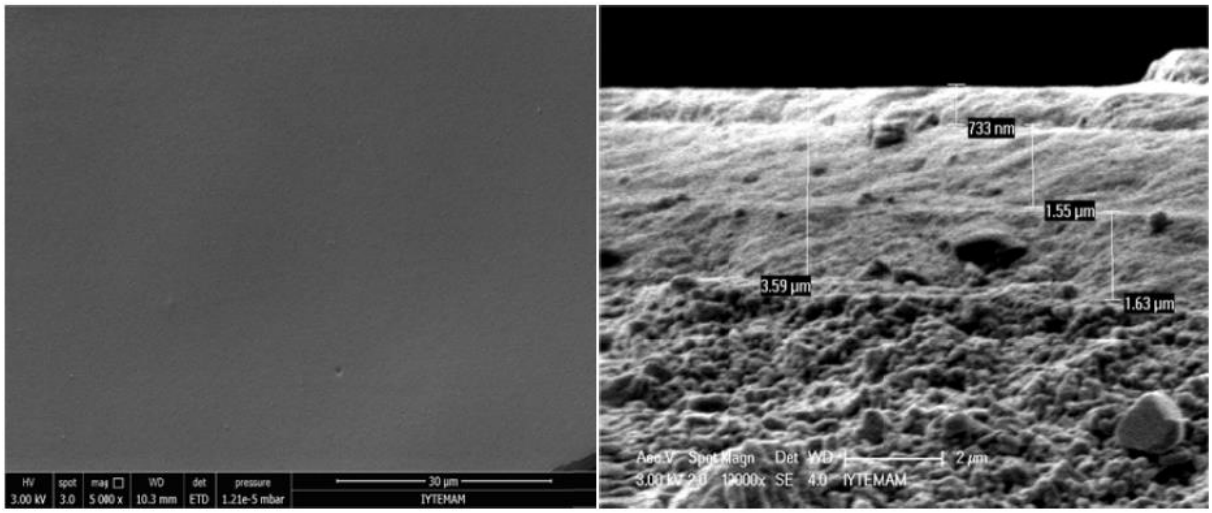

Figure 6.11. SEM micrograph of the surface and cross-sectional areas of TTIP (UF-2) layer.

6.3. Membrane Performance

6.3.1. Pure Water Flux

The variation of the pure water fluxes of all the membranes [support, MF (α-alumina and AKP-50), UF-1 (disperal and P2), UF-2 (TTIP and TTB) and NF (titania/zirconia)] used in this work as a function of time at TMP 2 for 70 minutes are presented in Figures 6.12 and 6.13. The clean water flux decreased from MF towards NF coated membrane which was expected due to the decrease in pore sizes of the successive selective layers. The macroporous support has the highest clean water flux of about 1800 L/m^{2}h. The three layers coated NF membrane has the lowest clean water

flux of 29 L/m^{2}h. Clean water fluxes of all the membranes were stable and time independent.

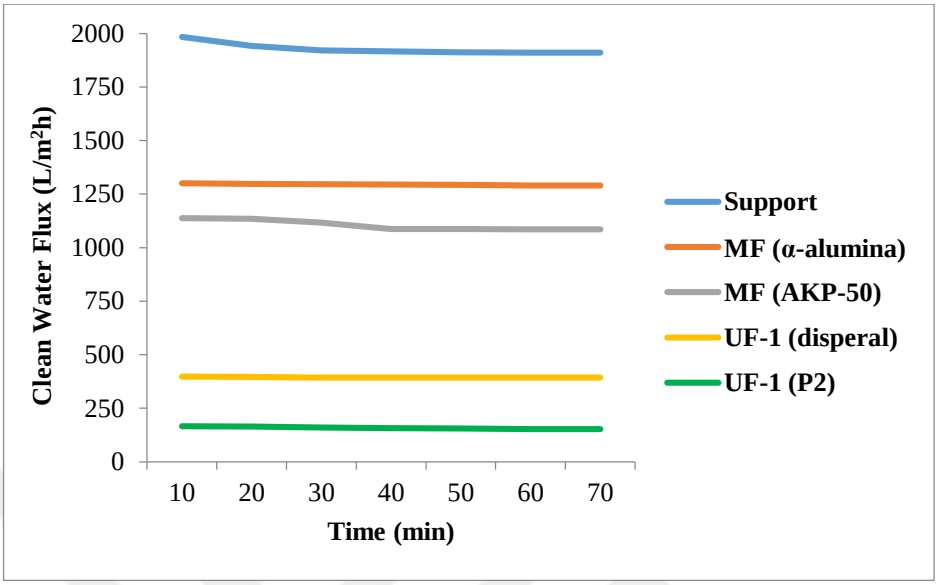

6.12. Clean water flux as a function of time at TMP 2 (support, α-alumina, AKP-50, boehmite and P2)

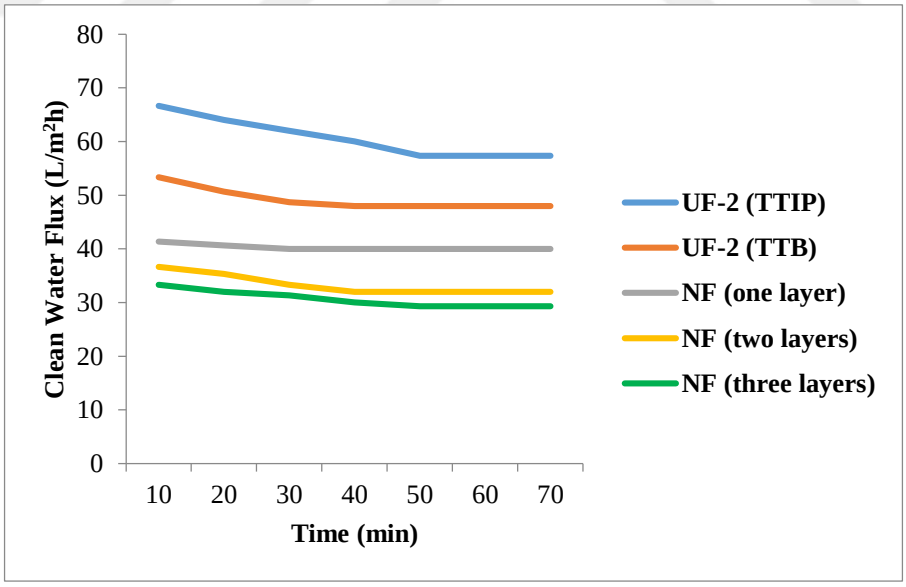

6.13. Clean water flux as a function of time at TMP 2 (TTIP, TTB, NF (one, two and three layer))

6.3.2. Salt Retention for Model Salts

Textile dyeing waters contain significant amounts of various salts. Conductivity is 8-18 mS/cm for the textile wastewaters studied within the scope of the TUBİTAK project conducted in İYTE ChE Laboratories. In order to use these waters again, it is necessary to lower the conductivity value to below 1 mS/cm using membranes. Desalination studies are predominantly carried out using NF / RO membranes today. Significant concentrations of Na^{+}, Cl^{-}, SO_4^{2-}, Mg^{+2}, and other ions are also present in these wastewaters. Desalting process was in this context investigated by preparing two model salt solutions (Na_2SO_4 and $MgSO_4$) containing the Mg^{+2} and SO_4^{-2} ions. Studies were carried out to determine the salt retention capacities of 5 different membranes with UF and NF selective layers using selected model salt solutions and textile wastewaters. Percent salt retention over time was determined by using ion concentrations in permeate and retentate streams in these experiments. Salt retention experiments were carried out by changing the pH of 10^{-3} M $MgSO_4$ and Na_2SO_4 salt solutions. The Mg^{2+} content was determined by titration with 0.01 M EDTA and the SO_4^{-2} content was determined by spectrophotometer at 420 nm wave length. Various radii of ions present in these solutions as stated in the literature are given in Table 6.1 nm where hydrated radius is the largest for all ions. The commonly reported isoelectric points of membrane layer materials are also given in Table 6.2.

Table 6.1. Properties of related cations and anions.

Ion	**Stokes radius (nm)**	**Ionic/Pauling radius (nm)**	**Hydrated radius (nm)**
Mg^{2+}	0.341	0.065	0.428
Na^{+}	0.184	0.107	0.358
Cl^{-}	0.121	0.181	0.332
SO_4^{-2}	0.231	0.245	0.300

Table 6.2. Isoelectric Point (IEP) of Membrane Layer Materials

Material	**IEP**
α-alumina	8 - 9
γ-alumina	7 - 8
Titania (TiO_2)	3.9 - 8.2
Zirconia (ZrO_2)	4- 11

6.3.2.1. Na_2SO_4

The permeate flux change of 10^{-3} M Na_2SO_4 solution over time at different pH levels by using MF (double layer) + AKP-50 membrane is given in Figure 6.14. It has been observed that the flux decreases from acidic to basic environment and this may be due to the slight increase in the salt solution viscosity since a considerable quantity of NaOH was added to achieve high pH values. The highest flux was found at pH 3.36 and the lowest flux at pH 12.03. The permeate fluxes were nearly the same with the pure water fluxes of AKP-50 membrane.

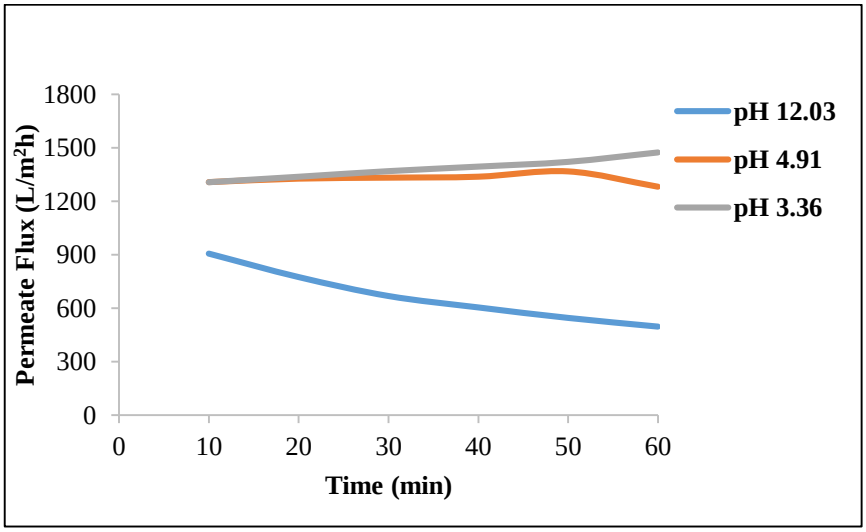

Figure 6.14. Permeate flux as a function of time at different pH values of 10^{-3} M Na_2SO_4 salt solution using MF (double layer) +AKP-50 membrane.

The SO_4^{2-} ion retention as a function of pH with MF (double layer) + AKP-50 membrane filtration is given in Figure 6.15. Retention is minimal at a pH around 8. There is no attraction or repulsion between the membrane surface and ionic species in salt solution at this pH. Membrane carries small charges on the surface since this pH may be very close to the isoelectric point (IEP) of the α-alumina surface. Salt retention can be explained with a positive membrane charge which repels Na^+ ions at a pH<8. An equivalent number of SO_4^{2-} ions must be retained which results in salt retention to satisfy charge neutrality. At a pH>8, the membrane exhibits a negative charge which causes SO_4^{2-} ion repulsion leading to high retention. The retention correlates well with the zeta potential of the membrane. The higher retention at acidic pH may most likely be due to a higher absolute value of the zeta potential. A retention drop was observed at a pH around 12 with the highest NaOH addition which can be explained by the reduction in the thickness of the double layer formed in the pores due to a higher ionic strength in contact with a salt solution. The thickness of the double layer decreases resulting in a lower retention with increasing base concentration. The highest ion retention was observed as 31.5 % at pH=3.36.

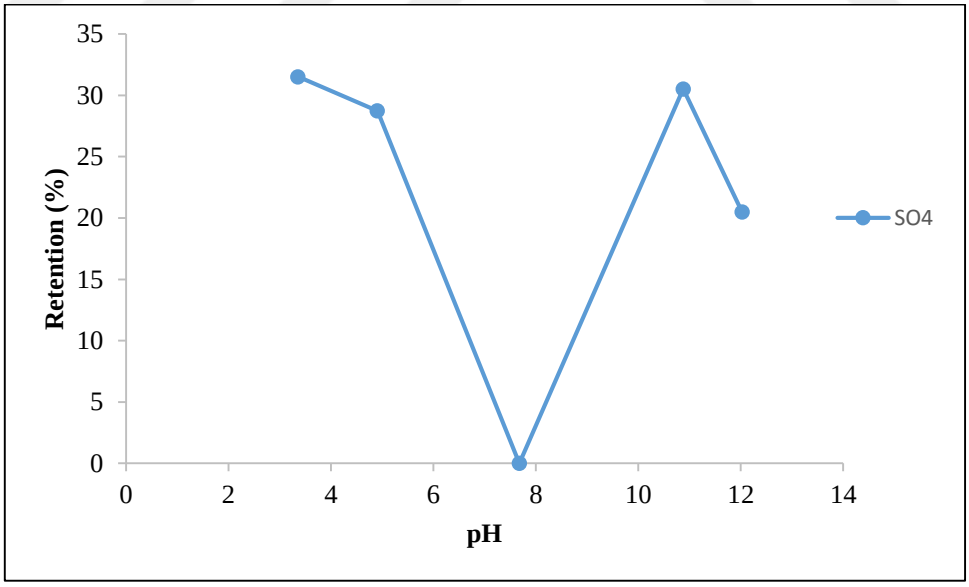

Figure 6.15. Salt retention vs. pH for 10^{-3} M Na_2SO_4 salt solution using MF(double layer) +AKP-50 membrane

Figure 6.16 shows the permeate flux change of 10^{-3} M Na_2SO_4 solution over time at different pH values in the MF + boehmite + P2 (400 ^{0}C) membrane filtration. It has been observed that the flux decreases from basic to acidic environment. The highest flux was found at pH 10.70 and the lowest flux at pH 3.21.

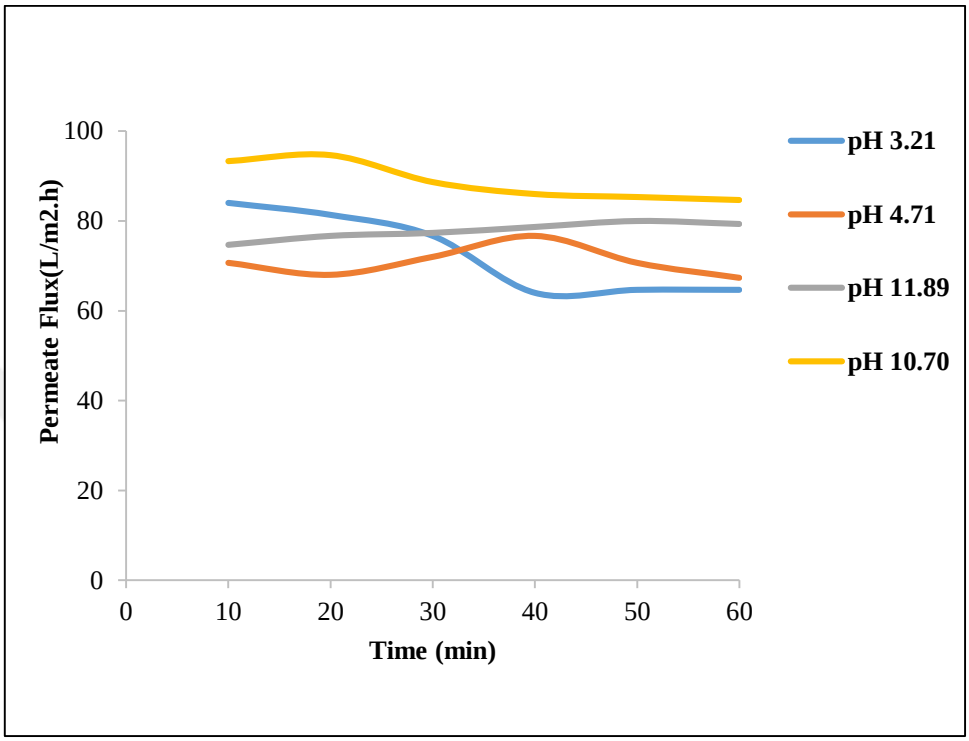

Figure 6.16. Permeate flux as a function of time at different pH values of 10^{-3} M Na_2SO_4 salt solution using MF + boehmite + P2 (400 ^{0}C) membrane.

In Figure 6.17, SO_4^{2-} ion retention as a function of pH with MF + boehmite + P2 (400 ^{0}C) membrane is given. Retention is minimal at pH around 7. This means that the surface has almost no charge at this pH. This pH level may most likely be close to the membrane selective layer oxide IEP value given in Table 6.2. The observed salt retention can be explained as a result of positively charged membrane surface when the solution pH is smaller than 7. Na^+ ions are repelled and the equal amount of SO_4^{2-} ions are retained by positively charged ions. SO_4^{2-} ion repulsion was observed due to the negative surface charge above pH=7. The highest ion retention was observed as 48.4 % at pH 10.70.

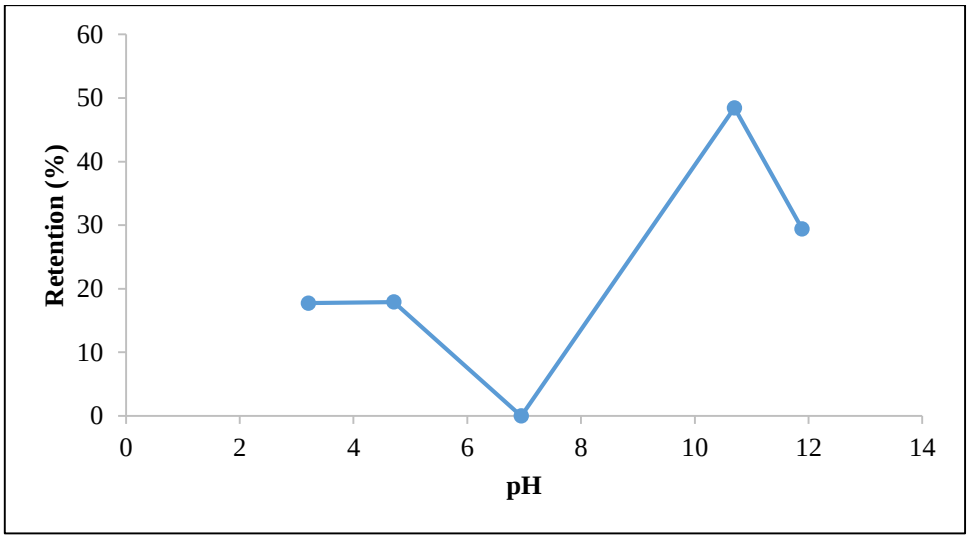

Figure 6.17. Salt retention vs. pH for 10^{-3} M Na_2SO_4 salt solution using MF + boehmite + P2 (400 ^{0}C) membrane.

The permeate flux change of 10^{-3} M Na_2SO_4 solution over time at different pH values with using MF + boehmite + P2 (400 ^{0}C) + Ti/Zr polymeric (double layer) membran is shown in Figure 6.18. Permeate flux figure illustrates that there is no trend in fluxes. Permeate fluxes were higher than the pure water fluxes of this membrane. Instantaneous pressure changes may be the reason. The highest flux was found at pH 10.30 and the lowest flux at pH 2.34.

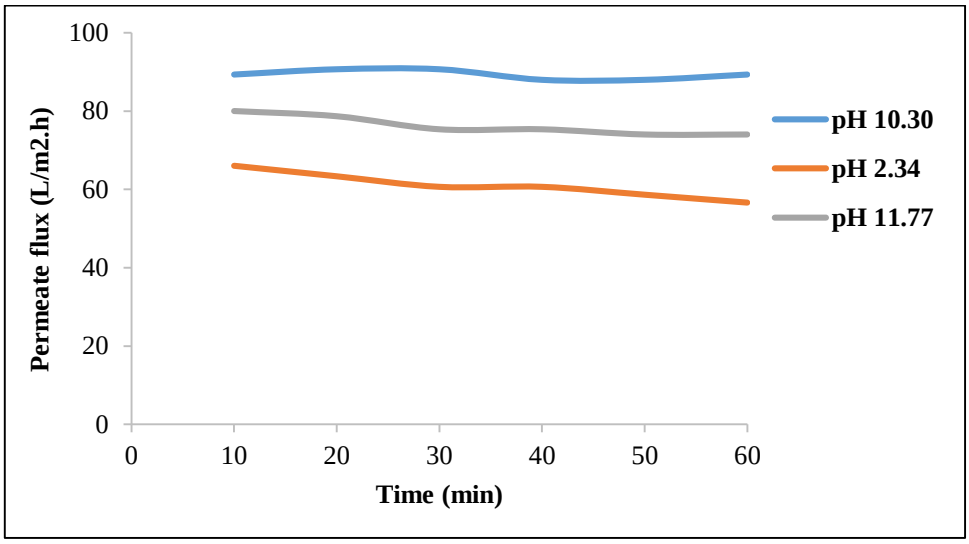

Figure 6.18 Permeate flux as a function of time at different pH values of 10^{-3} M Na_2SO_4 salt solution using MF + boehmite + P2 (400 ^{0}C) + Ti/Zr polymeric (double layer) membrane

In Figure 6.19, SO_4^{2-} ion retention as a function of pH with MF + boehmite + P2 (400 ^{0}C) + Ti/Zr polymeric (double layer) membrane is given. The lowest retention values were observed at pH 4 and pH 8. There is no electrostatic attraction or repulsion between membrane surface and ions in salt solution from pH 4 to pH 8. The highest ion retention was observed as 43 % at pH 2.34. The reason is that positively charged membrane surface repels the Na^+ ions. An equivalent number of SO_4^{2-} ions are retained to maintain the charge uniformity. When pH is higher than 8, negatively charged membrane surface repels the SO_4^{2-} ions.

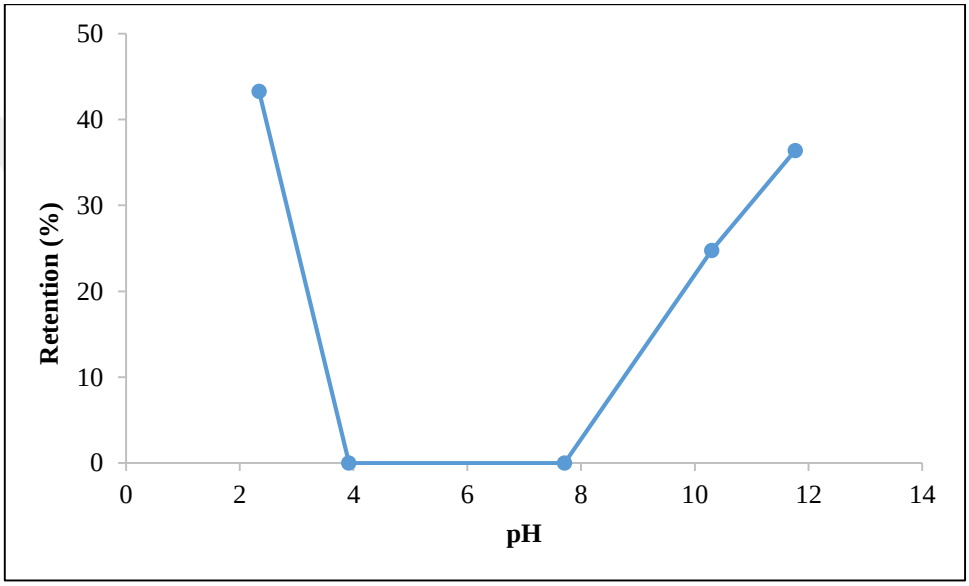

Figure 6.19. Salt retention vs. pH for 10^{-3} M Na_2SO_4 salt solution using MF + boehmite + P2 (400 ^{0}C) + Ti/Zr polymeric (double layer) membrane

Figure 6.20 shows the permeate flux change of 10^{-3} M Na_2SO_4 solution over time at different pH values with using MF + boehmite + P2 (600 ^{0}C) + TTIP hydrosol + Ti/Zr polymeric (double layer) membrane. It has been observed that the flux decreases from acidic to basic environment. The slight increasing in viscosity due to adding high amount of NaOH base may be the reason of this flux decrease. The highest flux was found at pH 2.45 and the lowest flux at pH 11.77.

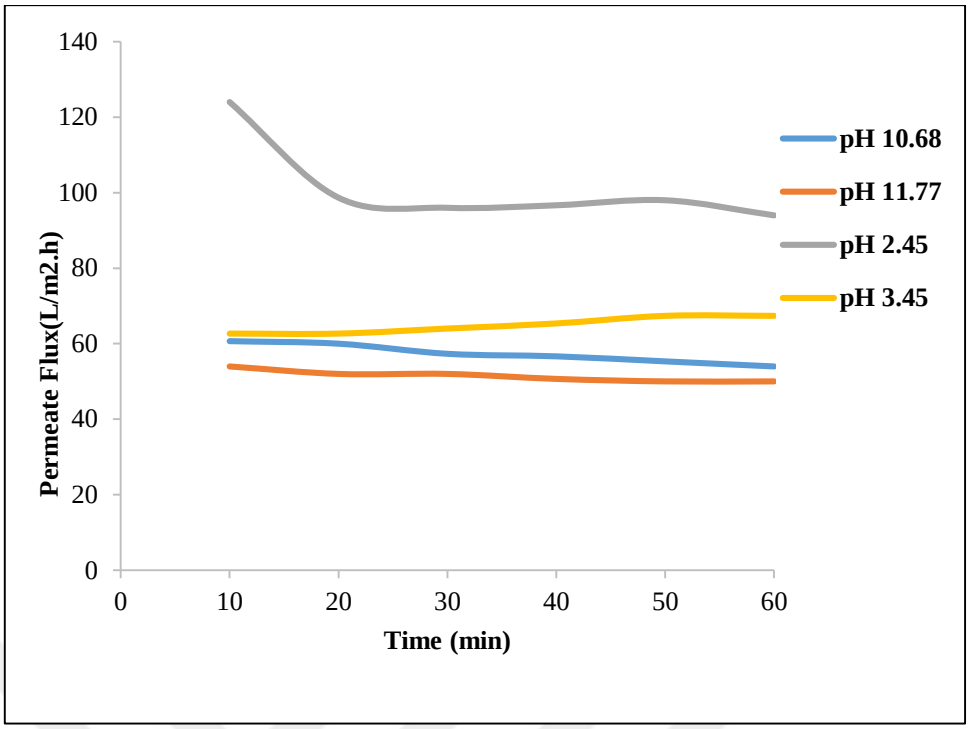

Figure 6.20. Permeate flux as a function of time at different pH values of 10^{-3} M Na_2SO_4 salt solution using MF + boehmite + P2 (600 ^{0}C) + TTIP hydrosol + Ti/Zr polymeric (double layer) membrane

In Figure 6.21, SO_4^{2-} ion retention as a function of pH with MF + boehmite + P2 (600 ^{0}C) + TTIP hydrosol + Ti/Zr polymeric (double layer) membrane is given. At pH around 7, retention is minimal due to weak electrostatic attraction and repulsion. This point makes an agreement with IEP of titanium in the literature values. At low pH region, Na^+ ions repulsion is caused by the positively charged membrane surface. Therefore, SO_4^{2-} ion retention is fairly high. At high pH region, the negatively charged membrane surface repels the SO_4^{2-} ions which results in salt retention. The retention in the acidic region is higher than the basic region due to the higher absolute surface charge of the membrane at the acidic region. The highest ion retention was observed as 80 % at pH 2.45.

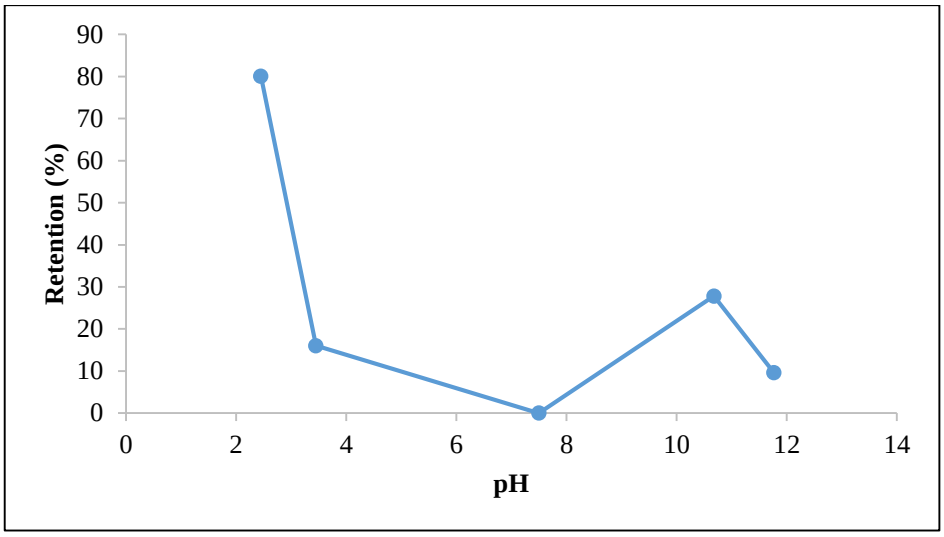

Figure 6.21. Salt retention vs. pH for 10^{-3} M Na_2SO_4 salt solution using MF + boehmite + P2 (600 ^{0}C) + TTIP hydrosol + Ti/Zr polymeric (double layer) membrane

Figure 6.22 shows the permeate flux change of 10^{-3} M Na_2SO_4 solution over time at different pH values with using MF + boehmite + P2 (400 ^{0}C) + Ti/Zr polymeric (triple layer) membrane. It has been observed that the flux decreases from acidic to basic environment. The highest flux was found at pH 2.04 and the lowest flux at pH 11.87.

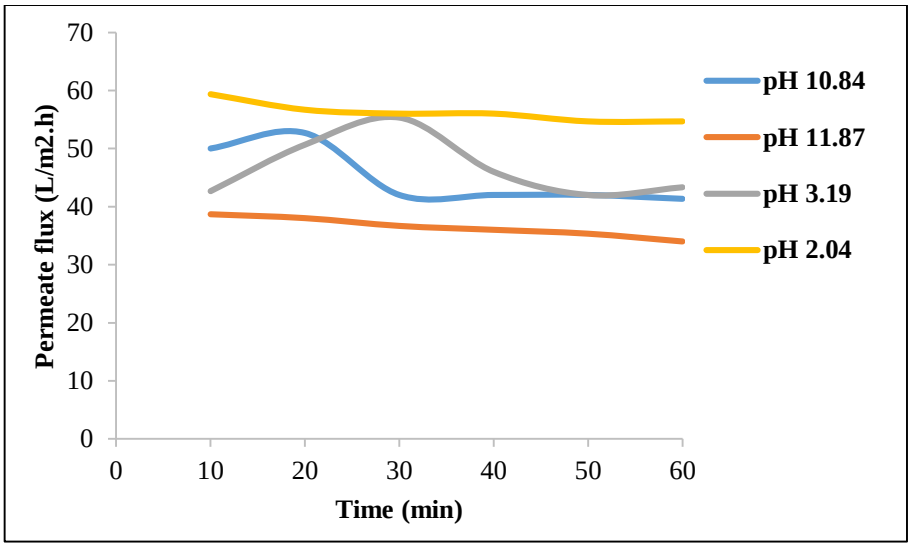

Figure 6.22. Permeate flux as a function of time at different pH values of 10^{-3} M Na_2SO_4 salt solution using MF + boehmite + P2 (400 ^{0}C) + Ti/Zr polymeric (triple layer) membrane

In Figure 6.23, SO_4^{2-} ion retention as a function of pH with MF + boehmite + P2 (400 ^{0}C) + Ti/Zr polymeric (triple layer) membrane is given. At the neutral pH, the membrane is uncharged and ion transport is only hindered by the size of the ions, so that salt retention is very low. At low pH, Na^+ ions are repelled by the positively charged membrane surface and yield SO_4^{2-} ion retention. At the high pH region, increase in SO_4^{2-} ion retention occurs, because again the charge increases. The highest ion retention was observed as 86.6 % at pH 10.84.

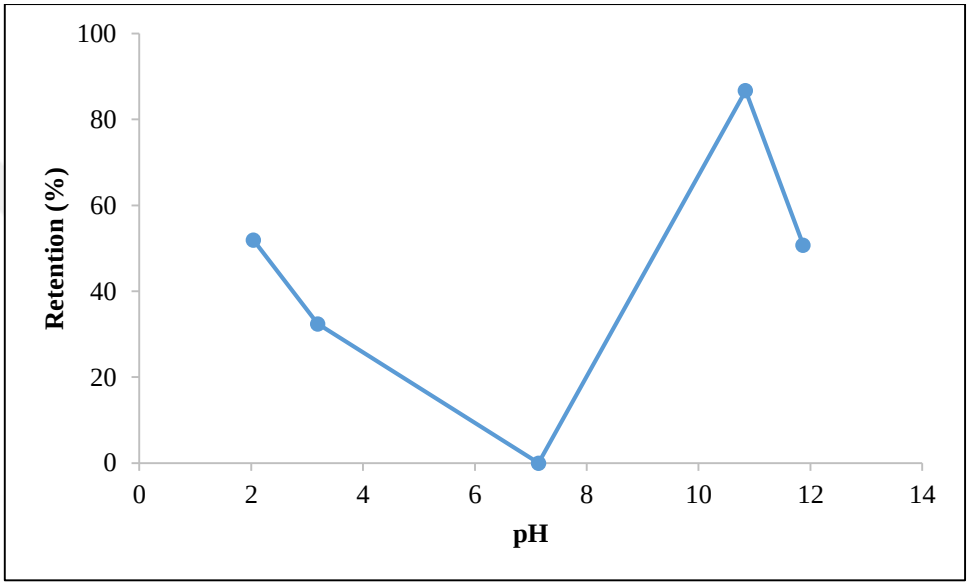

Figure 6.23. Salt retention vs. pH for 10^{-3} M Na_2SO_4 salt solution using MF + boehmite + P2 (400 ^{0}C) + Ti/Zr polymeric (triple layer) membrane

6.3.2.2. MgSO4

The other used salt was $MgSO_4$. Retention experiments were performed with the same membranes which were used in Na_2SO_4 salt retention experiments, except the last membrane since the membrane was broken during the experiment due to a sudden pressure increase.

Figure 6.24 shows the permeate flux change of 10^{-3} M $MgSO_4$ solution over time at different pH values by using MF (double layer) + AKP-50 membrane. Permeate flux decreases from acidic to basic pH. The reason may be a slight viscosity increase in salt solution since a large quantity of NaOH base was added to achieve high pH values. There were some fluctuations in fluxes most likely due to instantaneous pressure

changes. The highest flux was found at pH 2.18 and the lowest flux at pH 11.82. The permeate fluxes were nearly the same with the pure water fluxes of the AKP-50 membrane.

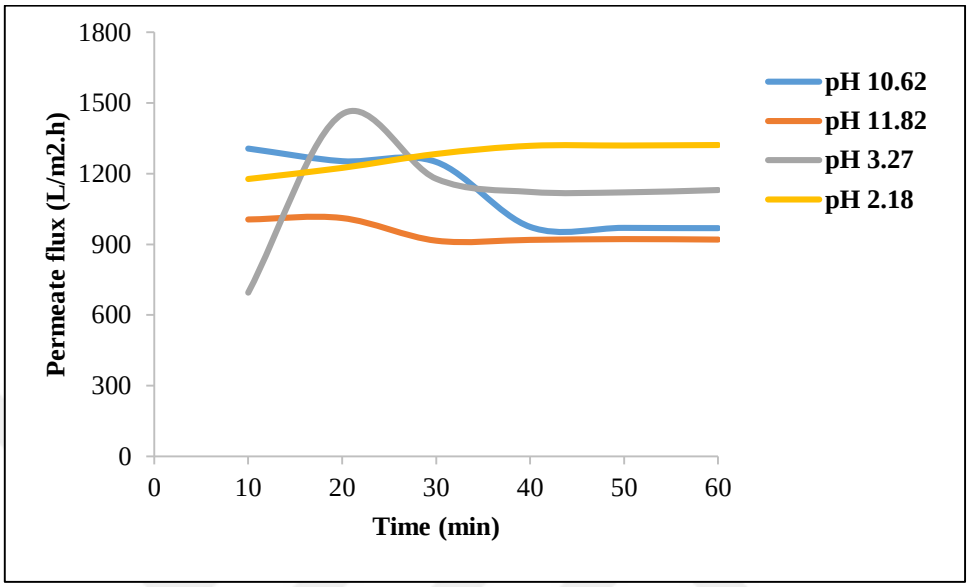

Figure 6.24. Permeate flux as a function of time at different pH values of 10^{-3} M $MgSO_4$ salt solution using MF (double layer) +AKP-50 membrane.

SO_4^{2-} and Mg^{+2} ion retentions as a function of pH with MF (double layer) + AKP-50 membrane is given in Figure 6.25. The Mg^{+2} ion retention in general was higher than the SO_4^{2-} ion retention at all pH values. This could be explained by the electrostatic interaction or Donnan exclusion mechanism together with size exclusion mechanism. Retention may be dominated by the hydrated radius for ions with similar valences. The ion with a larger hydrated radius always had a higher retention. The hydrated radii of different ions were listed in the experimental section previously. The Mg^{+2}ion have a higher hydrated radius than the SO_4^{2-} ion. Retentions are minimal at a pH around 8. The attraction or repulsion between the membrane surface and the ionic species in salt solution at this pH may be at a minimum level. Membrane surface charge close to the IEP may be at a very low level. The retention correlates well with the zeta potential of the membrane. The higher retention at acidic pH is consistent with the probable higher absolute value of the zeta potential. The highest Mg^{+2} ion retention was observed as 84.4 % at pH 11.82. The highest SO_4^{2-} ion retention was observed as 41.1 % at pH 2.18.

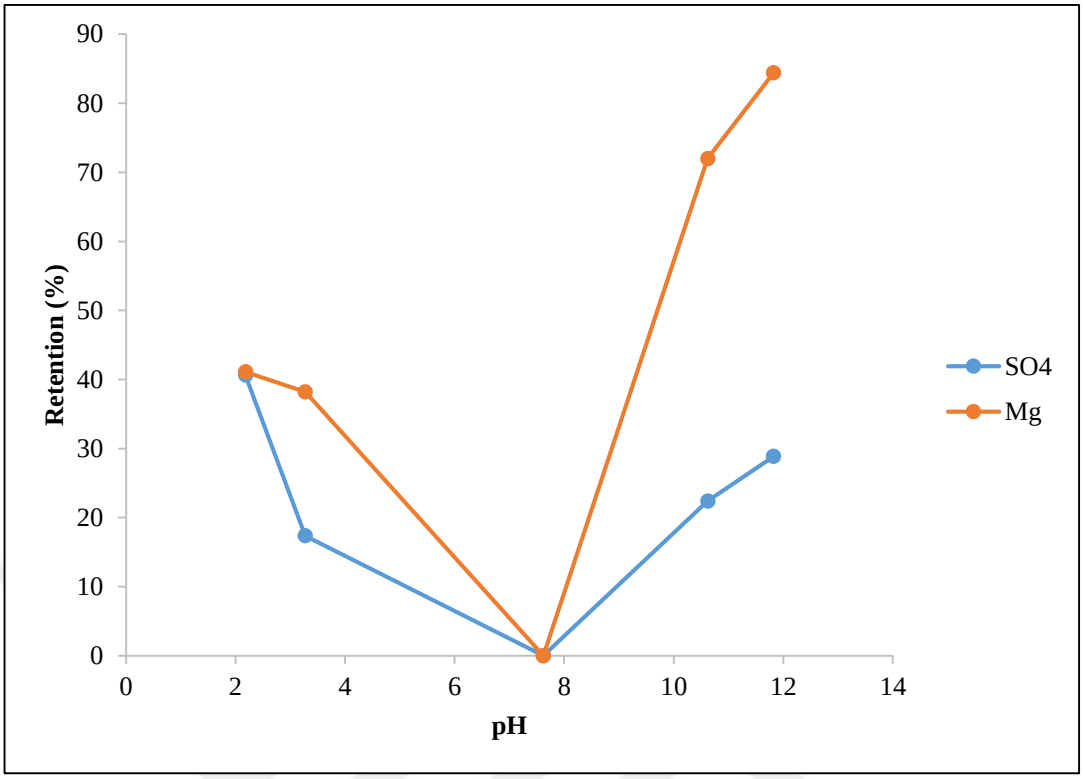

Figure 6.25. Salt retention vs. pH for 10^{-3} M $MgSO_4$ salt solution using MF (double layer) +AKP-50 membrane

Figure 6.26 shows the permeate flux change of 10^{-3} M $MgSO_4$ solution over time at different pH values by using MF + boehmite + P2 (400 ^{0}C) membrane. There is decreasing permeate flux trend from acidic to basic pH. The permeate fluxes are similar with the pure water fluxes of this membrane. The highest flux was found at pH 3.59 and the lowest flux at pH 11.72.

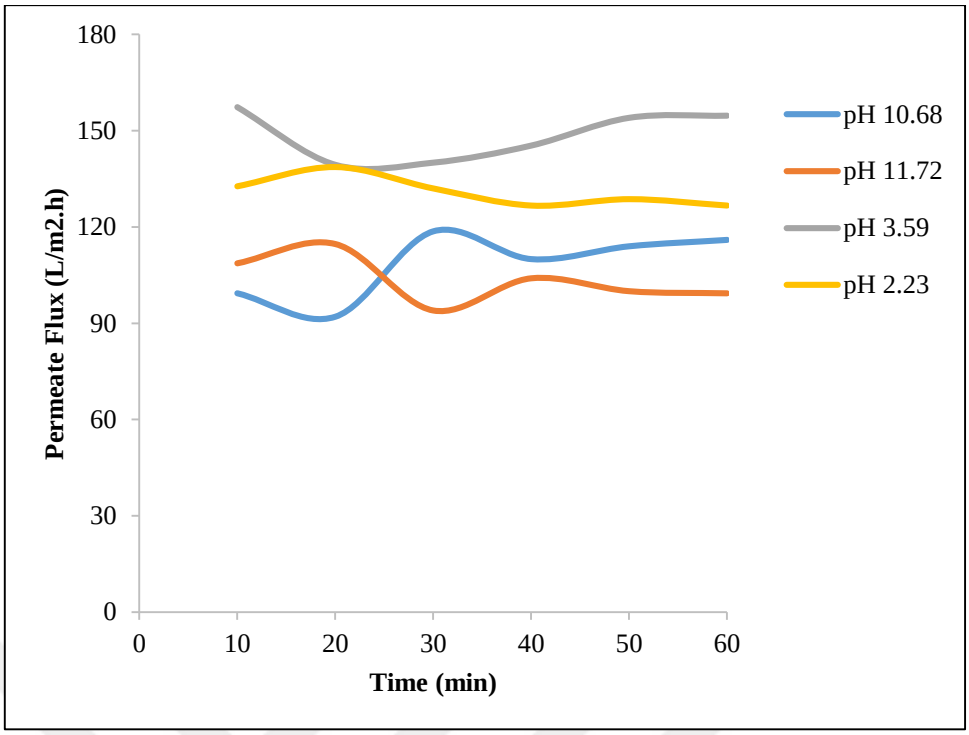

Figure 6.26. Permeate flux as a function of time at different pH values of 10-3 M MgSO4 salt solution using MF + boehmite + P2 (400 0C) membrane

SO_4^{2-} and Mg^{+2} ion retentions as a function of pH with MF + boehmite + P2 (400 ^{0}C) membrane is given in Figure 6.27. Again, retention of Mg^{+2} ions is higher than the retention of SO_4^{2-} ions at all pH values due to the bigger hydrated radius of Mg^{+2} ion. There is no ion retention at pH around 9. It means that IEP of this membrane is at pH 9. This value is close to the literature value. The highest Mg^{+2} ion retention was observed as 94.4 % at pH 10.68. The highest SO_4^{2-} ion retention was observed as 43.7 % at pH 11.72.

Figure 6.28 shows the permeate flux change of 10^{-3} M $MgSO_4$ solution over time at different pH values with using MF + boehmite + P2 (400 ^{0}C) + Ti/Zr polymeric (double layer) membrane. There is decreasing permeate flux trend from acidic to basic region. There is big difference between fluxes at acidic region and fluxes at basic region. Adding high amounts of NaOH may most likely be the reason as was previously discussed. The highest flux was determined at pH 2.26 and the lowest flux at pH 10.85.

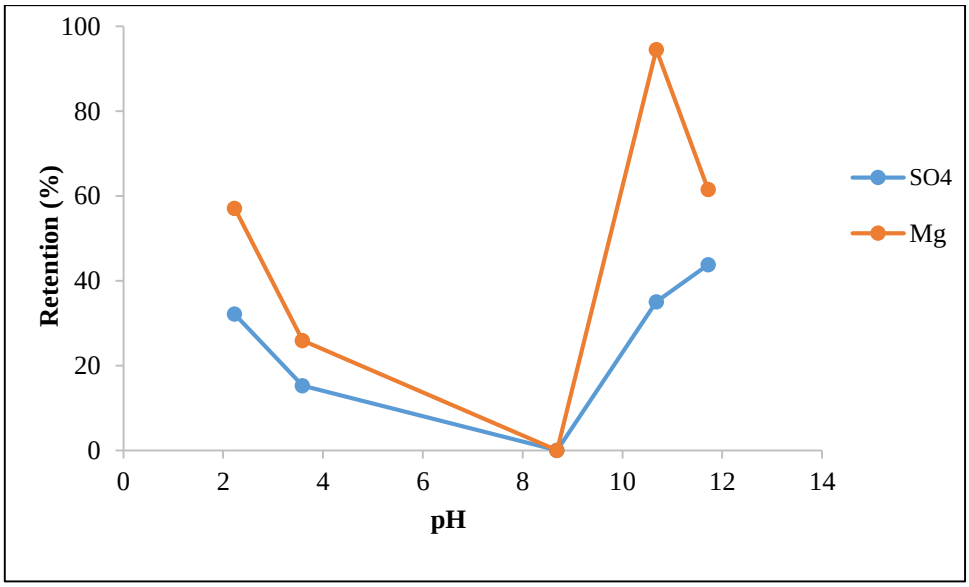

Figure 6.27. Salt retention vs pH for 10^{-3} M $MgSO_4$ salt solution using MF + boehmite + P2 (400 ^{0}C) membrane.

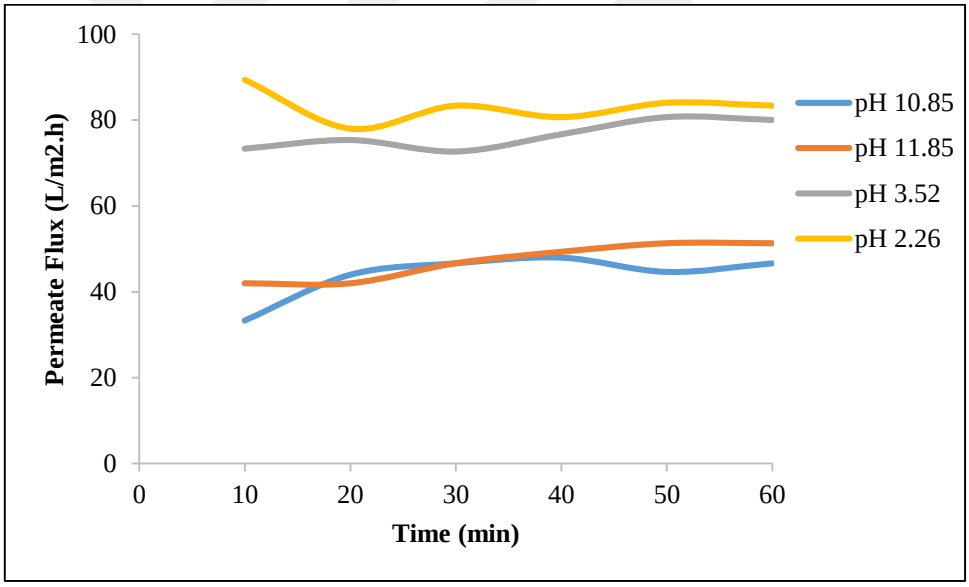

Figure 6.28. Permeate flux as a function of time at different pH values of 10^{-3} M $MgSO_4$ salt solution using MF + boehmite + P2 (400 ^{0}C) + Ti/Zr polymeric (double layer) membrane.

SO_4^{2-} and Mg^{+2} ion retentions as a function of pH with MF + boehmite + P2 (400 ^{0}C) + Ti/Zr polymeric (double layer) membrane is given in Figure 6.29. Mg^{+2} ion retention similar to the previous membranes were higher than SO_4^{2-} ion retention at all pH values due to the bigger hydrated radius of Mg^{+2} ion. The lowest retentions were observed at pH around 7. Positive and negative membrane surface charges are most

likely responsible from Mg^{+2} and SO_4^{2-} ion retentions.The highest Mg^{+2} ion retention was observed as 83.3 % at pH 10.85. The highest SO_4^{2-} ion retention was observed as 84.2 % at pH 2.26.

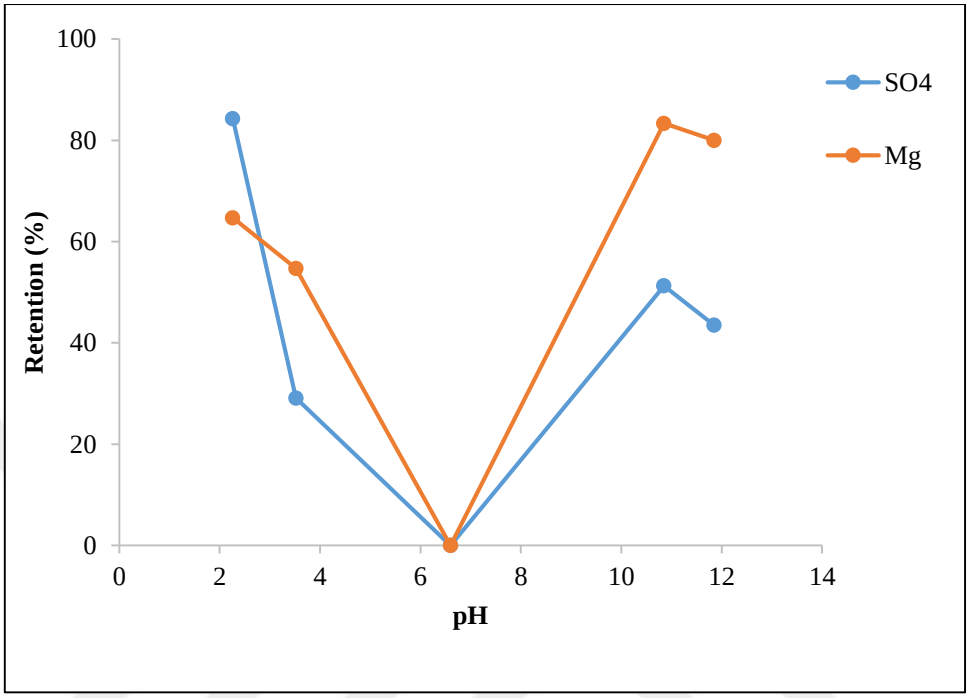

Figure 6.29. Salt retention vs pH for 10^{-3} M $MgSO_4$ salt solution using MF + boehmite + P2 (400 ^{0}C) + Ti/Zr polymeric (double layer) membrane.

Figure 6.30 shows the permeate flux change of 10^{-3} M $MgSO_4$ solution over time at different pH values with using MF + boehmite + P2 (600 ^{0}C) + TTIP hydrosol + Ti/Zr polymeric (double layer) membrane. There is no trend in permeate fluxes. Permeate fluxes are higher than pure water fluxes of this membrane. Pressure changes cause this difference. The highest flux was found at pH=3.22 and the lowest flux at pH=11.86.

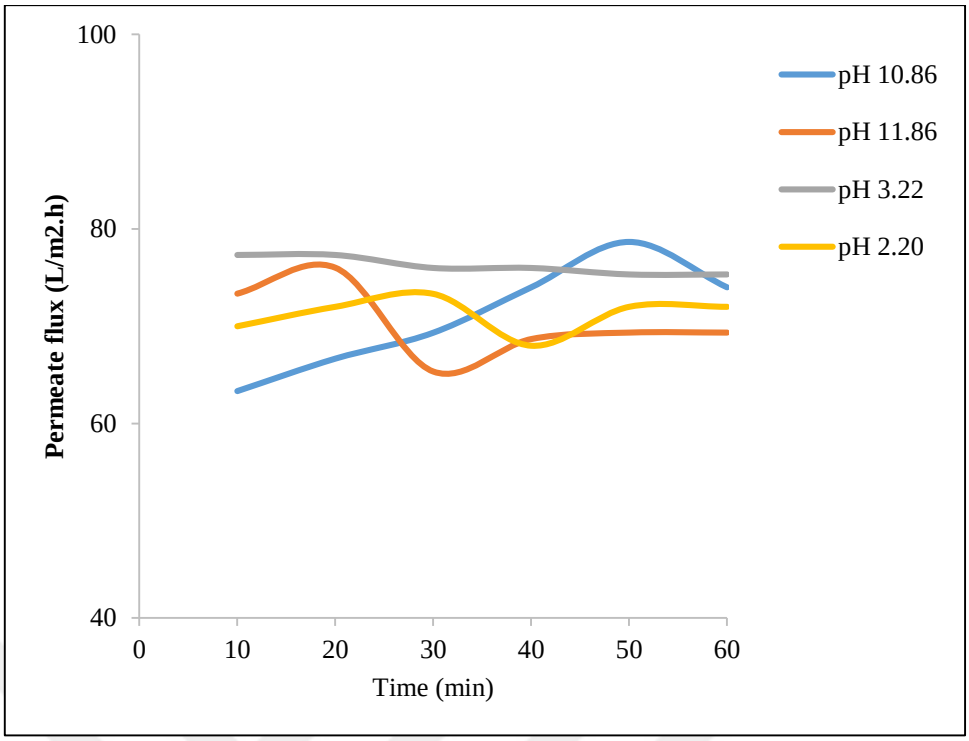

Figure 6.30. Permeate flux as a function of time at different pH values of 10^{-3} M $MgSO_4$ salt solution using MF + boehmite + P2 (600 ^{0}C) + TTIP hydrosol + Ti/Zr polymeric (double layer) membrane.

The SO_4^{2-} and Mg^{2+} ion retentions as a function of pH with MF + boehmite + P2 (600 ^{0}C) + TTIP hydrosol + Ti/Zr polymeric (double layer) membrane is given in Figure 6.31. Again, retention of Mg^{2+} ions is higher than the retention of SO_4^{2-} ions at all pH values due to the bigger hydrated radius of Mg^{2+}ion. The lowest retentions were observed at pH around 6. Positive and negative membrane surface charges are responsible from Mg^{2+} and SO_4^{2-} ion retentions, also. The SO_4^{2-} ion retention was high at basic pH while rejection decreased in the acidic region. Because absolute surface charge value is higher in basic region. The opposite is true for Mg^{2+} ion. The highest Mg^{2+} ion retention was observed as 91.3 % at pH 11.85. The highest SO_4^{2-} ion retention was observed as 95.1 % at pH 2.20.

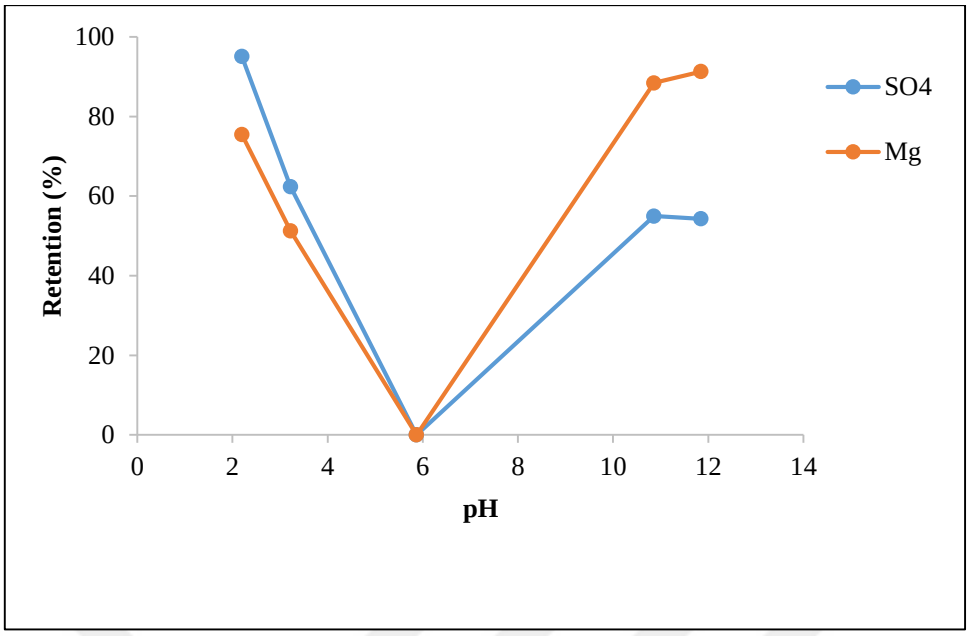

Figure 6.31. Salt retention vs pH for 10^{-3} M $MgSO_4$ salt solution using MF + boehmite + P2 (600 ^{0}C) + TTIP hydrosol + Ti/Zr polymeric (double layer) membrane.

CHAPTER 7

CONCLUSIONS

Water management in industrial installations must include recycle/reuse opportunities to meet the ever-increasing water demand which also would contribute to global water conservation. In water intensive industries such as textile industry, water management must approach for economization and rationalization of the use of water resources. In the textile industry, high salinity waste streams are a challenge urging for the recovery and purification of dyes and salts (e.g., NaCl), requiring a treatment going beyond the classical filtration by e.g., nanofiltration and reverse osmosis to produce pure water. As more stringent regulations and increasing costs of water is becoming a huge burden for textile industries, membrane processes emerge as the technology-of-choice to provide recyclable water through the treatment of effluents. The application of membrane separation processes does provide the industries with a technology to meet water quality limits and produce reusable water. Membrane processes, especially nanofiltration (NF) and reverse osmosis (RO) with polymeric membranes, are being increasingly used in the treatment and reuse of coloured wastewater. However, the limitation in polymeric membrane operation occurs when the chemical, thermal or mechanical stability of the membrane is exceeded by the solution to be treated. Ceramic membranes may be economically more favourable than polymeric membranes due to extremely high chemical and physical stability, possibility of regeneration and long life. Amphoteric nanofiltration membranes with pore size around a nanometer, the interactions between the membrane material and the ions in solution become stronger. This allows the separation of ionic and molecular species by using these NF membranes.

Tubular membrane supports were prepared from commercial α-alumina (Al_2O_3) powders by extrusion. The extruded supports were heat treated at 1525 ^{0}C. The dimensions of tubular membrane support were 200 mm in length and ID/OD of 16/25 mm. The asymmetric membranes used in this thesis were formed from multiple intermediate layers and thin top layers by using dip-coating method on tubular ceramic membrane supports. The purposes of multiple layer structure were the reduction of the

tubular support surface roughness/pore structure and elimination of irregularities/imperfections. MF (α-alumina and AKP-50), UF1 (disperal and P2) and UF2 (titania hydrosol) layers were called as intermediate layers. They were colloidal sol-gel derived. The final thin top layer was prepared by using nanometer-sized polymeric titania/zirconia mixed-oxide sol and this asymmetric structure was called as the NF membrane. The average DLS particle sizes of the prepared interlayer and top layer (α-alumina, AKP-50, disperal (boehmite), P2 (boehmite), TTIP hydrosol, TTB hydrosol and polymeric) sols were determined as 522 nm, 175 nm, 42 nm, 16 nm, 14 nm, 4.9 nm and 3.6 nm, respectively.

Salt retention experiments were conducted at room temperature by using a laboratory scale cross-flow filtration set-up equipped with a tubular module. Pure water flux values of ceramic support, intermediate layers and top layers were determined at TMP=4. The macroporous support had the highest clean water flux around 1800 L/m^2h. The three layers coated NF membrane had the lowest clean water flux around 29 L/m^2h.

Desalting process was started by preparing two model salt solutions (Na_2SO_4 and $MgSO_4$) with 10^{-3} M Mg^{+2} and SO_4^{-2} ion concentration. Studies were carried out to determine the salt retention capacities of 5 different membranes containing UF and NF selective layers using selected model salt solutions. For these experiments, percent retention over time was determined by using ion concentrations of permeate and retentate streams. Salt retention experiments were carried out by changing the pH of the 10^{-3} M $MgSO_4$ and Na_2SO_4 salt solutions. The Mg^{2+} content was determined by titration with 0.01 M EDTA and the SO_4^{-2} content was determined by spectrophotometer at 420 nm wave length.

The highest SO_4^{-2} and Mg^{+2} ion retentions were obtained with using MF+disperel (boehmite)+P2 (600 ^{0}C)+TTIP hydrosol+Ti/Zr polymeric (double layer) membrane as 95% and 91%, respectively. The retention close to the IEP of the layer phases was almost close to zero. The relatively high retentions determined in this work at high and low pH levels were conluded to be due to the electrical attrations/repulsions between the charged surfaces and the ions present in the solutions. The Mg^{+2} retention was higher than the SO_4^{-2} ion retention for most of the pH levels of the $MgSO_4$ salt solutions.

REFERENCES

Al-Zoubi, H., & Omar, W. (2009). Rejection of salt mixtures from high saline by nanofiltration membranes. *Korean Journal of Chemical Engineering, 26*(3), 799-805.

Alamiyounssi, S., Larbot, A., Persin, M., Sarrazin, J., & Cot, L. (1995). Rejection of mineral salts on a gamma-alumina nanofiltration membrane application to environmental process. *Journal of Membrane Science, 102*, 123-129. doi:10.1016/0376-7388(94)00302-f

Alcaina-Miranda, M. I., Barredo-Damas, S., Bes-Pia, A., Iborra-Clar, M. I., Iborra-Clar, A., & Mendoza-Roca, J. A. (2009). Nanofiltration as a final step towards textile wastewater reclamation. *Desalination, 240*(1-3), 290-297. doi:10.1016/j.desal.2008.02.028

Alventosa-deLara, E., Barredo-Damas, S., Zuriaga-Agustí, E., Alcaina-Miranda, M. I., & Iborra-Clar, M. I. (2014). Ultrafiltration ceramic membrane performance during the treatment of model solutions containing dye and salt. *Separation and Purification Technology, 129*, 96-105. doi:10.1016/j.seppur.2014.04.001

Bandini, S., & Vezzani, D. (2003). Nanofiltration modeling: the role of dielectric exclusion in membrane characterization. *Chemical Engineering Science, 58*(15), 3303-3326. doi:10.1016/s0009-2509(03)00212-4

Bargeman, G., Westerink, J. B., Guerra Miguez, O., & Wessling, M. (2014). The effect of NaCl and glucose concentration on retentions for nanofiltration membranes processing concentrated solutions. *Separation and Purification Technology, 134*, 46-57. doi:10.1016/j.seppur.2014.07.025

Barredo-Damas, S., Alcaina-Miranda, M. I., Bes-Piá, A., Iborra-Clar, M. I., Iborra-Clar, A., & Mendoza-Roca, J. A. (2010). Ceramic membrane behavior in textile wastewater ultrafiltration. *Desalination, 250*(2), 623-628. doi:http://dx.doi.org/10.1016/j.desal.2009.09.037

Barredo-Damas, S., Alcaina-Miranda, M. I., Iborra-Clar, M. I., & Mendoza-Roca, J. A. (2012). Application of tubular ceramic ultrafiltration membranes for the treatment of integrated textile wastewaters. *Chemical Engineering Journal, 192*, 211-218. doi:10.1016/j.cej.2012.03.079

Baticle, P., Kiefer, C., Lakhchaf, N., Larbot, A., Leclerc, O., Persin, M., & Sarrazin, J. (1997). Salt filtration on gamma alumina nanofiltration membranes fired at two different temperatures. *Journal of Membrane Science, 135*(1), 1-8. doi:10.1016/s0376-7388(97)00114-2

Bayati, B., Bayat, Y., Charchi, N., Ejtemaei, M., Babaluo, A. A., Haghighi, M., & Drioli, E. (2013). Preparation of Crack-Free Nanocomposite Ceramic Membrane

Intermediate Layers on α-alumina Tubular Supports. *Separation Science and Technology, 48*(13), 1930-1940. doi:10.1080/01496395.2013.786728

Blanc, P., Larbot, A., Palmeri, J., Lopez, M., & Cot, L. (1998). Hafnia ceramic nanofiltration membranes. Part I: Preparation and characterization. *Journal of Membrane Science, 149*(2), 151-161. doi:10.1016/s0376-7388(98)00154-9

Boncukoğlu, B. K. R. (2013). *Boyar Madde İçeren Atıksular için Deşarj Renk Standardının Belirlenmesi ve Arıtım Teknolojilerinin Araştırılması*.

Bowen, W. R., & Mukhtar, H. (1996). Characterisation and prediction of separation performance of nanofiltration membranes. *Journal of Membrane Science, 112*, 263-274.

Capar, G., Yetis, U., & Yilmaz, L. (2007). The most effective pre-treatment to nanofiltration for the recovery of print dyeing wastewaters. *Desalination, 212*(1–3), 103-113. doi:http://dx.doi.org/10.1016/j.desal.2006.09.020

Chen, X., Zhang, W., Lin, Y., Cai, Y., Qiu, M., & Fan, Y. (2015). Preparation of high-flux γ-alumina nanofiltration membranes by using a modified sol–gel method. *Microporous and Mesoporous Materials, 214*, 195-203. doi:10.1016/j.micromeso.2015.04.027

Cheremisinoff, N. P. (2002). *Handbook of Water and Wastewater Treatment Technologies.* (Ph.D.), Clarkson College of Technology, Washington, D. C.

Chevereau, E., Zouaoui, N., Limousy, L., Dutournié, P., Déon, S., & Bourseau, P. (2010). Surface properties of ceramic ultrafiltration TiO2 membranes: Effects of surface equilibriums on salt retention. *Desalination, 255*(1-3), 1-8. doi:10.1016/j.desal.2009.12.007

Combe, C., Guizard, C., Aimar, P., & Sanchez, V. (1997). Experimental determination of four characteristics used to predict the retention of a ceramic nanofiltration membrane. *Journal of Membrane Science, 129*(2), 147-160. doi:10.1016/s0376-7388(96)00290-6

Condom, S., Larbot, A., Alami Younssi, S., & Persin, M. (2004). Use of ultra- and nanofiltration ceramic membranes for desalination. *Desalination, 168*, 207-213. doi:10.1016/j.desal.2004.06.189

de Lint, W. B. S., & Benes, N. E. (2005). Separation properties of γ-alumina nanofiltration membranes compared to charge regulation model predictions. *Journal of Membrane Science, 248*(1-2), 149-159. doi:10.1016/j.memsci.2004.08.026

De´on, S. b., Dutournie´, P., & Bourseau, P. (2007). Transfer of Monovalent Salts through Nanofiltration Membranes: A Model

Combining Transport through Pores and the Polarization Layer. *Ind. Eng. Chem. Res., 46*, 6752-6761.

Fersi, C., Gzara, L., & Dhahbi, M. (2005). Treatment of textile effluents by membrane technologies. *Desalination, 185*(1-3), 399-409. doi:10.1016/j.desal.2005.03.087

Friedrich, J. P. H. (2003). *Membrane Technology for Waste Water Treatment*.

Hajarat, R. A. (2010). *The use of nanofiltration membrane in desalinating brackish water.* (Doctor of Philosophy), University of Manchester.

Hilal, N., Al-Zoubi, H., Mohammad, A. W., & Darwish, N. A. (2005). Nanofiltration of highly concentrated salt solutions up to seawater salinity. *Desalination, 184*(1-3), 315-326. doi:10.1016/j.desal.2005.02.062

Jonathan, H. K. O. (2012). *Analysis of Membrane Alternatives suitable for Kvarnagården Water Treatment Plant An Evaluation of Hollow Fiber Nanofiltration Membranes.* (Master of Science), Chalmers University of Technology.

Khalili, M., Sabbaghi, S., & Zerafat, M. M. (2015). Preparation of ceramic γ-Al2O3-TiO2 nanofiltration membranes for desalination. *Chemical Papers, 69 (2)*, 309-315. doi:10.1515

Labbez, C., Fievet, P., Szymczyk, A., Vidonne, A., Foissy, A., & Pagetti, J. (2002). Analysis of the salt retention of a titania membrane using the "DSPM" model: effect of pH, salt concentration and nature. *Journal of Membrane Science, 208*(1-2), 315-329. doi:10.1016/s0376-7388(02)00310-1

Lee, K. P. (2013). *Fabrication and Applications of Nanoporous Alumina Membranes.* (Ph.D.), University of Bath.

Lin, J., Ye, W., Zeng, H., Yang, H., Shen, J., Darvishmanesh, S., . . . Van der Bruggen, B. (2015). Fractionation of direct dyes and salts in aqueous solution using loose nanofiltration membranes. *Journal of Membrane Science, 477*, 183-193. doi:10.1016/j.memsci.2014.12.008

Luo, J., & Wan, Y. (2013). Effects of pH and salt on nanofiltration—a critical review. *Journal of Membrane Science, 438*, 18-28. doi:10.1016/j.memsci.2013.03.029

Majewska-Nowak, K., & Kawiecka-Skowron, J. (2011). Ceramic membrane behaviour in anionic dye removal by ultrafiltration. *Desalination and Water Treatment, 34*(1-3), 367-373. doi:10.5004/dwt.2011.2806

Mazzoni, C., Orlandini, F., & Bandini, S. (2009). Role of electrolyte type on TiO2–ZrO2 nanofiltration membranes performances. *Desalination, 240*(1-3), 227-235. doi:10.1016/j.desal.2007.11.074

Meyn, T. (2011). *NOM Removal in Drinking Water Treatment Using Dead- End Ceramic Microfiltration.* (Ph.D.), Norwegian University of Science and Technology.

Peeters, J. M. M., Boom, J. P., Mulder, M. H. V., & Strathmann, H. (1998). Retention measurements of nanofiltration membranes with electrolyte solutions. *Journal of Membrane Science, 145*(2), 199-209. doi:10.1016/s0376-7388(98)00079-9

Perez-Moreno, V., Bonilla-Suarez, C. B., Fortanell-Trejo, M., & Pedraza-Aboytes, G. (2012). Seawater Desalination Using Modified Ceramic Membranes. *Industrial & Engineering Chemistry Research, 51*(17), 5900-5904. doi:10.1021/ie2009313

Perez-Moreno, V., Bonilla-Suarez, C. B., & Rodriguez-Munoz, M. E. (2013). Seawater desalination in Mexican Pacific coast by a new technology: use and perspectives. *Desalination and Water Treatment, 51*(1-3), 175-183. doi:10.1080/19443994.2012.714734

Puhlfürß, P., Voigt, A., Weber, R., & Morbé, M. (2000). Microporous TiO2 membranes with a cut off <500 Da. *Journal of Membrane Science, 174*, 123-133.

Ren, C., Fang, H., Gu, J., Winnubst, L., & Chen, C. (2015). Preparation and characterization of hydrophobic alumina planar membranes for water desalination. *Journal of the European Ceramic Society, 35*(2), 723-730. doi:10.1016/j.jeurceramsoc.2014.07.012

Samueldelint, W., Zivkovic, T., Benes, N., Bouwmeester, H., & Blank, D. (2006). Electrolyte retention of supported bi-layered nanofiltration membranes. *Journal of Membrane Science, 277*(1-2), 18-27. doi:10.1016/j.memsci.2005.10.004

Sarkar, S., Bandyopadhyay, S., Larbot, A., & Cerneaux, S. (2012). New clay-alumina porous capillary supports for filtration application. *Journal of Membrane Science, 392*, 130-136. doi:10.1016/j.memsci.2011.12.010

Sarkar, S., Ghosh, S., Banerjee, P., Larbot, A., Cerneaux, S., Bandyopadhyay, S., & Bhattacharjee, C. (2014). Preparation and Characterization of Single Layer Ultra Filtration Alumina Membrane Directly over Porous Clay-Alumina Tubular and Capillary Support for Textile Effluent Treatment. *Transactions of the Indian Ceramic Society, 73*(3), 197-204. doi:10.1080/0371750x.2014.882246

Schaep, J., Bruggen, B. V. d., Vandecasteele, C., & Wilms, D. (1998). Influence of ion size and charge in nanofiltration. *Separation and Purification Technology, 14*, 155-162.

Schaep, J., Vandecasteele, C., Mohammad, A. W., & Bowen, W. R. (1999). Analysis of the Salt Retention of Nanofiltration Membranes Using the Donnan–Steric Partitioning Pore Model. *Separation Science and Technology, 34*(15), 3009-3030. doi:10.1081/ss-100100819

Schaep, J., Vandecasteele, C., Peeters, B., Luyten, J., Dotremont, C., & Roels, D. (1999). Characteristics and retention properties of a mesoporous gamma-Al2O3 membrane for nanofiltration. *Journal of Membrane Science, 163*(2), 229-237. doi:10.1016/s0376-7388(99)00163-5

Skluzacek, J. M., Isabel Tejedor, M., & Anderson, M. A. (2006). An iron-modified silica nanofiltration membrane: Effect of solution composition on salt rejection. *Microporous and Mesoporous Materials, 94*(1-3), 288-294. doi:10.1016/j.micromeso.2006.03.043

Sondhi R., B. R., Jung G. (2003). Applications and benefits of ceramic membranes. *Membrane Technology*.

Strathmann, H. (2000). *Introduction to Membrane Science and Technology*.

Tang, C., & Chen, V. (2002). Nanofiltration of textile wastewater for water reuse. *Desalination, 143*(1), 11-20. doi:http://dx.doi.org/10.1016/S0011-9164(02)00216-3

Tsuru, T., Hironaka, D., Yoshioka, T., & Asaeda, M. (2001). Titania membranes for liquid phase separation: effect of surface charge on flux. *Separation and Purification Technology, 25*(1-3), 307-314. doi:10.1016/s1383-5866(01)00057-0

Uzal, N., Yilmaz, L., & Yetis, U. (2009). Microfiltration/ultrafiltration as pretreatment for reclamation of rinsing waters of indigo dyeing. *Desalination, 240*(1-3), 198-208. doi:10.1016/j.desal.2007.10.092

Vacassy, R., Guizard, C., Thoraval, V., & Cot, L. (1997). Synthesis and characterization of microporous zirconia powders: Application in nanofilters and nanofiltration characteristics. *Journal of Membrane Science, 132*, 109-118.

Van Gestel, T., Vandecasteele, C., Buekenhoudt, A., Dotremont, C., Luyten, J., Leysen, R., . . . Maes, G. (2002a). Alumina and titania multilayer membranes for nanofiltration: preparation, characterization and chemical stability. *Journal of Membrane Science, 207*(1), 73-89. doi:10.1016/s0376-7388(02)00053-4

Van Gestel, T., Vandecasteele, C., Buekenhoudt, A., Dotremont, C., Luyten, J., Leysen, R., . . . Maes, G. (2002b). Salt retention in nanofiltration with multilayer ceramic TiO2 membranes. *Journal of Membrane Science, 209*(2), 379-389. doi:10.1016/s0376-7388(02)00311-3

Wang, Z., Wei, Y.-M., Xu, Z.-L., Cao, Y., Dong, Z.-Q., & Shi, X.-L. (2016). Preparation, characterization and solvent resistance of γ-Al2O3/α-Al2O3 inorganic hollow fiber nanofiltration membrane. *Journal of Membrane Science, 503*, 69-80. doi:10.1016/j.memsci.2015.12.039

Weber, R., Chmiel, H., & Mavrov, V. (2003). Characteristics and application of new ceramic nanofiltration membranes. *Desalination, 157*(1-3), 113-125. doi:10.1016/s0011-9164(03)00390-4

Yelken, G. (2000). *Preparation and Characterization of Inorganic Membranes by using Sol-GelTechniques.* (Master of Science), izmir Institute of Technology.

Zaiter, K., Belouatek, A., Chougui, A., Asli, B., & Szymczyk, A. (2013). Color, COD, and salt retention by inorganic membrane. *Desalination and Water Treatment, 53*(1), 66-72. doi:10.1080/19443994.2013.838525